Cape Peninsula
University of Technology

LAMINAR FLOW IN A CHANNEL FILLED WITH SATURATED POROUS MEDIA

By

LAZARUS RUNDORA

(Student Number: 210266430)

BSc (Hons), MSc (UZ)

Thesis submitted in fulfilment of the requirements for the degree

Doctor of Technology: Mechanical Engineering

Cape Peninsula University of Technology

Supervisor: Professor O.D. Makinde

Senior Professor & Director, Institute for Advanced Research in

Mathematical Modelling and Computations

Cape Peninsula University of Technology, South Africa

Year 2013

DECLARATION

I, Lazarus Rundora, declare that the contents of this thesis represent my own unbiased work, and that the thesis has not previously been submitted for academic examination towards any qualification. Furthermore, it represents my own opinions and not necessarily those of the Cape Peninsula University of Technology.

Signed **Date**

ACKNOWLEDGEMENTS

- My Supervisor, Professor Oluwole D Makinde, I have gained useful and life-changing knowledge from you. Your readiness to assist and to share your wide knowledge is beyond human imagination. Thank you and may the Lord continue to reward you.
- Dr Tirivanhu Chinyoka, collaborating with you has assisted me a lot more than you can imagine. Thank you for the guidance that you provided me.
- My wife, Rosebud and children: Laura, Nicola, Tashinga and Ashlynn, I will forever cherish your daily company and patience. If it were not for all of you, it may not have been possible.
- Dr. Kazeem Okosun, your willingness to help at any time with the technicalities and your academic advice and encouragement is appreciated. I have known you for a few months but you have already impacted my life positively. Thank you and be blessed.
- Isaac Takaidza and Solly Lebelo, we have been together on this journey, and especially you Isaac, we have been together for years now. Thank you for the day to day collaboration that we always had. It helped.
- Dr. Kenneth Zimba, Head of VUT Mathematics Department, thank you for your support and willingness to allow me time out visiting my supervisor.
- My employer, Vaal University of Technology, thank you for funding my doctorate studies. I will forever be indebted.

DEDICATION

To Ashlynn, Tashinga, Nicola, Laura and Tinashe

My children, this is for you, let it inspire you.

To Rosebud

My beautiful wife, if this did not come to fruition, you too were going to be blamed. Thanks for everything.

To my mother, Martha

Suffice to say you are the strongest woman I have ever known. You are the rock upon which my life is rooted. To God be the glory.

ABSTRACT

The flow of reactive viscous fluids in porous media presents a theoretically challenging problem and has a broad range of scientific, technological and engineering applications. Real life areas where such flow systems are encountered include drying of food, geothermal energy extraction, nuclear waste disposal, the flow of heat and fluid inside human organs, insulation of buildings, groundwater movement, oil and gas production, astrophysical plasmas, magnetohydrodynamic (MHD) pumps and generators, metal extraction and granulation of metals, aerospace and ship propulsion and automobile exhaust systems. The reactions within such flow systems are inherently exothermic. It is in this view that we carry out studies of thermal effects and thermal stability criteria for unsteady flows of reactive variable viscosity non-Newtonian fluids through saturated porous media. The study focuses on non-Newtonian fluids mainly because the majority of industrial fluids exhibit non-Newtonian character. Particular focus will be on fluids of the differential type exemplified by third grade fluid.

Both analytical and numerical techniques were employed to solve the nonlinear partial differential equations that were derived from the conservation principles, namely the principles of conservation of mass, momentum and energy balance. Graphical representations were adopted in trying to explain the response of solutions to various flow parameter variations.

In chapter 1 we defined important terms and expressions, laid down a summary of important applications, carried out literature survey, stated the statement of the problem, the aims and objectives of the study as well as an outline of the envisaged research methodology. Chapter 2 focuses on the derivations of the fundamental equations that derive the flow system. These are the continuity equation, the momentum equation and the energy equation.

In chapter 3 we computationally investigated the unsteady flow of a reactive temperature dependent viscosity third grade fluid through a porous saturated medium with asymmetric convective boundary conditions. The response of velocity and temperature fields to each of the various flow parameters was analysed and interpreted. A transient increase in both the velocity and temperature profiles with an increase in the reaction strength, viscous heating and fluid viscosity parameter was observed. On the other hand, a transient decrease in the field properties was observed with increase in non-Newtonian character and the porous medium shape parameter. The reaction was noticed to blow-up if, depending on other flow parameters, the reaction strength is not carefully controlled.

In chapter 4 the effects of suction/injection on the flow system described in chapter 3 was analysed. The effects of the flow parameters on the temperature and velocity fields, the skin friction and the wall heat transfer rate were simulated and discussed. It was observed that the suction/injection Reynolds number has a retarding effect on the velocity and temperature fields and increases the wall shear stress. On the other hand the suction/injection Reynolds number was observed to diminish the rate of heat transfer at the channel walls.

The analysis of unsteady MHD reactive flow of a third grade fluid through a porous saturated medium with asymmetric boundary conditions was carried out in chapter 5. The major finding in this chapter is that the presence of the magnetic field decreases the velocity and temperature profiles. Blow up of solutions was also noticed to occur earlier than in the case of the problem in chapter 3.

Chapter 6 is a statement of concluding remarks as well as envisaged future work.

NOMENCLATURE

c_p specific heat at constant pressure

k thermal conductivity

a channel width

P pressure

$\bar{P}$ modified pressure

g acceleration due to gravity

Re Reynolds number

Pr Prandtl number

C_f dimensionless wall shear stress

Nu dimensionless wall heat transfer rate

T_0 initial fluid temperature

T_a ambient temperature

K permeability

R universal gas constant

l Planck's number

h Boltzmann's constant

C_0 initial concentration of the reactant species

E activation energy

Q heat of the reaction

A rate constant

Bi Biot number

S porous medium shape parameter

Ha Hartmann number

u velocity

t time

B_0 electromagnetic induction

Greek symbols

α variable viscosity parameter

θ dimensionless temperature

δ dimensionless material parameter

α_1, β_3 material coefficients

γ non-Newtonian parameter

ε activation energy parameter

μ fluid dynamic viscosity

σ electrical conductivity

Ω viscous heating parameter

λ Frank-Kamenetskii parameter

ρ fluid density

ν vibration frequency

τ shear stress

h_1, h_2 heat transfer coefficients at the lower and upper plates, resp.

$m \in \{-2, 0, 0.5\}$ numerical exponent for sensitized, Arrhenius and biomolecular kinetics

w dimensionless velocity

G pressure gradient parameter

θ_a ambient temperature parameter

Da Darcy number

TABLE OF CONTENTS

LIST OF FIGURES

LIST OF TABLES

CHAPTER ONE

INTRODUCTION

A fluid is a substance that deforms continuously, or flows, when subjected to shearing forces [35]. Alternatively, it can be defined as a substance that offers negligible resistance to a change of shape and is capable of flowing. Fluid mechanics (or dynamics) is concerned with the flow of fluids and is one of the most important of all the areas of physics. Its scope is varied and has wide applications. Physical phenomena are often dominated by fluids, and as such life would not exist without fluids and without the behaviour that fluids exhibit [49, 77]. Fluids play an important part in technology. It is thus inevitable that engineers must at least have a working knowledge of fluid behaviour in order for them to be able to efficiently analyse many of the systems they encounter and work with in everyday life.

1.1. Definition of terms

1.1.1. Channel flow

Channel flow (internal flow) refers to the flow of fluids in closed conduits like pipes or air ducts, and the flows are entirely in contact with the rigid boundaries of the conduits. Such flows are of great interest in science, engineering, technology and in everyday life. Most closed conduits in engineering applications are either circular or rectangular in cross section. Poiseuille flow and Couette flow are two examples of channel flow that are frequently encountered. Poiseuille flow is the flow resulting from pressure gradients in a long duct or pipe. Couette flow is the flow of fluid between infinite parallel flat plates driven by the motion of one or more plates [110].

A steady flow is one in which the flow field properties like velocity, pressure and cross section may differ from point to point but do not change with time. In contrast, if at any point in the fluid the conditions change with time, the flow is described as unsteady. A Laminar flow is one in which the fluid particles move in smooth layers, or laminas. A turbulent flow is one in which the fluid particles rapidly mix as they move along due to random three dimensional velocity fluctuations. A pictorial illustration of channel flow, as defined herein, is given in Figure 1.1.

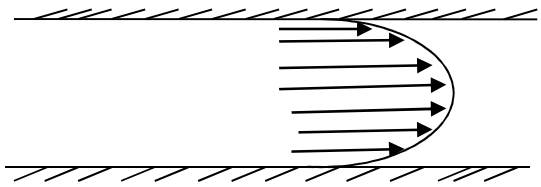

Figure 1.1. Poiseuille flow in a circular tube

1.1.2. Temperature dependent viscosity

Following [30], viscosity (dynamic viscosity) is the quantity that describes a fluid's resistance to shear or to flow. The cohesion and interaction between or among the molecules in a fluid brings about viscosity. When subjected to the same magnitude of the shear stress, different fluids deform differently. A major determinant of viscosity is temperature – viscosity varies with temperature. Engine oil and hydraulic fluids, for example, thicken appreciably on cold days and may significantly affect the performance of cars and other machinery during the cold periods. The viscosity of a liquid tends to decrease with increasing temperature, whereas for gases the opposite is true. A few models that describe the dependence of viscosity on temperature have been proposed. One of which is the Arrhenius-type equation, [70],

$$\mu(T) = \mu_0 e^{E/RT}$$

where μ_0 is dynamic viscosity at some reference temperature, E is the activation energy, R is the universal gas constant and T is temperature. The other common temperature dependent viscosity model is the exponential relationship, (see [69]),

$$\mu(T) = \mu_0 e^{-b(T-T_0)}$$

where b is a viscosity variation parameter and μ_0 is the fluid dynamic viscosity at temperature T_0.

A second kind of viscosity, the coefficient of kinematic viscosity [35], is the ratio of the dynamic (absolute) viscosity to the fluid density denoted by

$$\nu = \frac{\mu}{\rho}.$$

The SI unit of viscosity is the *pascal second (Pa s)* or *millipascal second (mPa s).* In Table 1.1, we list the viscosities, μ, of some selected materials at some specific temperatures.

Table 1.1. Viscosities of selected materials [30]

Simple liquids	T(℃)	$\mu(mPa\ s)$	**Complex materials**	T(℃)	$\mu(Pa\ s)$
alcohol, ethyl	20	1.1	Glass, room temp	25	10^{18}-10^{21}
alcohol, methyl	20	0.59	Glass, melting		10^{2}
blood	37	3 - 4	Honey	20	10
Ethylene glycol	25	16.1	Molasses	20	5
Ethylene glycol	100	1.98	Mustard	25	70
glycerin	20	1420	Peanut butter	20	150 – 250
glycerin	40	280	Syrup, chocolate	20	10 – 25
mercury	15	1.55	Tar	20	30000
milk	25	3	**Gases**	T(℃)	$\mu(\mu Pa\ s)$
Vegetable oil, canola	25	57	Air	15	17.9
Light machine oil	20	102	Hydrogen	0	8.42
Heavy machine oil	20	233	Helium (gas)	0	18.6
Motor oil, SAE 20	20	125	Nitrogen	0	16.7
water	0	1.79	Oxygen	0	18.1
water	100	0.28			

1.1.3. Non-Newtonian fluid

Fluid behaviour can be visualized in two ways namely Newtonian or non-Newtonian, depending on their general characteristic response to shear stress [35]. For a Newtonian fluid, shear stress is directly proportional to the rate of strain. If the deformation rate, rate of strain or shearing strain is defined by $\frac{du}{dy}$, where u is the fluid velocity in the x-direction, then the shear stress τ acting on a plane normal to the x-axis in a Newtonian fluid is such that $\tau \propto \frac{du}{dy}$, i.e.

$$\tau = \mu \frac{du}{dy}, \tag{1.1}$$

where μ is the absolute or dynamic viscosity. Equation (1.1) is Newton's law of viscosity for one dimensional flow. On the other hand, for a non-Newtonian fluid shear stress is not directly proportional to the rate of strain. Clay suspensions, polymer solutions, grease and toothpaste are examples of non-Newtonian fluids.

Over the years, many empirical equations have been proposed to model the observed relations between the shear stress τ and $\frac{du}{dy}$ for non-Newtonian fluids. The most common of such equations is the Power Law model

$$\tau = k\left(\frac{du}{dy}\right)^n = \left[k\left(\frac{du}{dy}\right)^{n-1}\right]\frac{du}{dy} \tag{1.2}$$

where k is called the consistency index and $\eta = \left(\frac{du}{dy}\right)^{n-1}$ is the flow behaviour index [35].

According to Sochi, [98], non-Newtonian fluids fall into three broad categories: time-independent, visco-elastic and time-dependent. Fluids exhibiting a combination of properties from more than one group are described as complex fluids. Time-independent fluids are those where the strain rate at a given point is solely dependent upon the instantaneous stress at that point. The fluid is described as thinning or pseudoplastic if the viscosity decreases, and thickening or dilatants if the viscosity increases with increasing shear rate.

Fluids that show partial elastic recovery upon the removal of a deforming stress are called viscoelastic fluids. They possess properties of both viscous fluids and elastic solids. Polymeric fluids are viscoelastic. Strong viscoelastic effects include shear-thinning, extension-thickening, normal stresses, and time-dependent rheology.

Time-dependent fluids are those for which the strain rate is a function of both the magnitude and the duration of stress and possibly of the time lapse between consecutive applications of stress. Two main categories of this type are thixotropic (work softening) and rheopectic (work hardening or anti-thixotropic) depending upon whether the stress decreases or increases with time at a given strain rate and constant temperature.

Yield-stress or viscoplastic fluids are characterised by their ability to sustain shear stresses. A certain amount of stress must be exceeded before the fluid starts to flow. Thus, an ideal yield-stress is a solid before yield and a fluid later. Accordingly, the viscosity of the substance changes from an infinite to a finite value. Yield-stress is a problematic phenomenon which is significantly difficult to model.

1.1.3.1. A note on fluids of the differential type

Following [28], fluids of the differential type are one of the earliest classes of materials bearing characteristics that cannot be adequately described by the classical linearly viscous fluid model (1.1). In such materials, only a very short (infinitesimal) part of the history of the deformation gradient has an influence on the stress. More specifically, in an incompressible fluid of differential type, apart from a constitutively indeterminate pressure, the stress is just a function of the velocity gradient and some number of its higher time derivatives. With the instantaneous cessation of all local motion, the stress becomes a pure pressure. One consequence of this is that, while they can experience the phenomenon of creep, these materials do not exhibit the phenomenon of stress relaxation. Fluids of differential type fall into various grades depending on the constitutive structure of the fluid's Cauchy stress. We omit the details here as the mechanics of fluids of differential type is a broad subject on its own. Suffice to say we have fluids of the differential type of grade 2, fluids of the differential type of grade 3, etc.

1.1.4. Magnetohydrodynamics

The study of flows in which the fluid is electrically conducting and moves in a magnetic field is known as magnetohydrodynamics (MHD) [11]. An example of an electrically conducting fluid is a liquid metal, for example, mercury or liquid sodium. According to Blanford and Thorne, [11], the major applications of MHD are in plasma physics. A plasma is a hot, ionized gas containing free electrons and ions. An example of an application of MHD is when strong magnetic fields are used to confine rings or columns of hot plasma that will be held in place long enough for thermonuclear fusion to occur resulting in power generation. Electricity is also generated when liquid metals are driven through a magnetic field. Other scientific and engineering applications are in spacecraft and ship propulsion, MHD pumps and generators, astrophysical plasmas, MHD flow control (reduction of turbulent drag), and in metallurgy (heating and flow control in metal processing).

1.1.4.1. Basic equations of MHD

The equations of MHD describe the motion of a conducting fluid in a magnetic field. Electric current is induced into a good conductor when it enters a magnetic field. The conductor creates its own magnetic field by Lenz's law. This induced magnetic field tends to cancel the original externally supported field thereby in effect excluding the magnetic field lines from the conductor. A Lorentz (or $\boldsymbol{j} \times \boldsymbol{B}$) force will act on the conducting fluid and modify its motion. The motion

modifies the field and the field, in turn, reacts back and modifies the motion. The theory is thus highly non-linear [11].

The set of MHD equations is as summarised below, see [11,104].

(Navier-Stokes equations with the Lorentz force)

$$\rho\left(\frac{\partial \boldsymbol{V}}{\partial t} + (\boldsymbol{V}\cdot\nabla)\boldsymbol{V}\right) = -\nabla p + \boldsymbol{j}\times\boldsymbol{B} + \mu_f\nabla^2\boldsymbol{V} + \rho\boldsymbol{g} \tag{1.3}$$

(Continuity equation)

$$\frac{\partial \rho}{\partial t} + \nabla\cdot\rho\boldsymbol{V} = 0 \tag{1.4}$$

(Faraday's Law)

$$\nabla\times\boldsymbol{E} = -\frac{\partial \boldsymbol{B}}{\partial t} \tag{1.5}$$

(Ampere's Law)

$$\nabla\times\boldsymbol{B} = \mu_m\boldsymbol{j} \tag{1.6}$$

(Ohm's law)

$$\boldsymbol{j} = \sigma(\boldsymbol{E} + \boldsymbol{V}\times\boldsymbol{B}) \tag{1.7}$$

μ_f is the fluid dynamic viscosity, μ_m is the magnetic permeability, σ fluid electrical conductivity, ρ is the fluid density, $\boldsymbol{V}$ is the fluid velocity, $\boldsymbol{E}$ is the electric field intensity and $\boldsymbol{B}$ is the magnetic field intensity. Equations (1.5) and (1.6) are together called Maxwell's equations and these are usually grouped together with equation (1.7) to give either a vector induction equation or a scalar equation for electric potential. Implicit in the five equations are the relations

$$\nabla\cdot\boldsymbol{B} = 0 \tag{1.8}$$

$$\nabla\cdot\boldsymbol{j} = 0 \tag{1.9}$$

Associated with all these equations is the energy equation with Joule heating [104]

$$\rho C_p\left(\frac{\partial T}{\partial t} + (\boldsymbol{V}\cdot\nabla)T\right) = k\nabla^2 T + \frac{j^2}{\sigma} + q''' \tag{1.10}$$

where T is temperature, k is the thermal conductivity and q''' is the heat produced by the reaction.

1.1.5. Porous medium

A porous medium is a material consisting of a solid matrix with an interconnected void (pores). The solid matrix is usually rigid, but it can undergo small deformation. The interconnectedness of the void allows the flow of one or more fluids through the material. In the simplest situation of a single-phase flow, the void is saturated by a single fluid whereas in the case of a two-phase flow a liquid and a gas share the void space [80]. Examples of porous media are sand, sandstone, lungs, packed catalyst beds, bread, automobile oil and air filters.

The mathematical description of the flow in porous media is extremely complex and involves many approximations [98]. The complexity arises from the irregular and tortuous nature of the pores. It is often sufficient and more practical to average the physical properties over many pores inside different sections of the particular reservoir rather than to consider the behaviour at a particular pore.

There are two important quantities describing the properties of a porous medium - the porosity ϕ and the permeability K. The porosity of a porous medium is defined as [80]:

$$\phi = \frac{pore\ volume}{matrix\ volume},$$

where the pore volume denotes the total volume of the pore space in the matrix and the matrix volume is the total volume of the particles or fibres and the pore space. Since the pore volume (volume of the pore space) is always less or equal to the matrix volume, it follows that $0 \leq \emptyset \leq 1$. For simplicity, the porosity is often chosen as a constant for the whole medium. The permeability K describes the ability of the fluid to flow through the porous medium and it is a quantity that depends on the geometry of the medium only. Figure 1.2 is a typical porous medium that is described in this section.

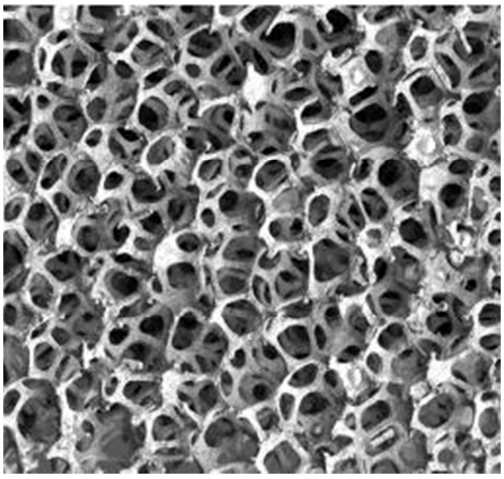

Figure 1.2: Porous medium: Aluminium foam

1.1.6. First law of thermodynamics

This law is a statement of conservation of energy. Energy can be changed from one form to another, but it cannot be created or destroyed. The Law states that the sum of work and heat added to a system will always equal to the increase of energy [12].

1.1.7. Planck's number

Planck's number, l, also called Planck's constant, is a physical constant reflecting the sizes of quanta in quantum mechanics. It is named after Max Planck, one of the founders of quantum theory, who discovered it in 1899. The Planck constant was first described as the proportionality constant between the energy (E) of a photon and frequency of its associated electromagnetic wave (ν). This relation between the energy and frequency is called the Planck relation or the Planck-Einstein equation $E = l\nu$. Since the frequency ν, wavelength λ, and speed of light c are related by $\lambda\nu = c$, the Planck relation can also be expressed as $E = \frac{lc}{\lambda}$ [114].

1.1.8. Boltzmann constant

The Boltzmann constant (h) is the physical constant relating energy at the individual particle level with temperature observed at the collective or bulk level. It is the universal gas constant divided by the Avogadro constant N_A: $h = \frac{R}{N_A}$. Boltzmann's constant is a bridge between

macroscopic and microscopic physics. It has the same units as entropy and is named after the Austrian physicist Ludwig Boltzmann [43].

1.1.9. Frank-kamenetskii parameter

The Frank-Kamenetskii parameter (λ) is a measure of how reactive the gases or reactants are, what the dimensions of the system involved, and the effect of ambient temperature on the system [37].

1.1.10. Prandtl number

The Prandtl number, Pr, is the ratio of momentum diffusivity (kinematic viscosity) to thermal diffusivity. It is named after the German physicist Ludwig Prandtl. Low Pr indicates strong conductive transfer whereas high Pr indicates strong convective transfer [17].

1.1.11. Biot number

The Biot number (Bi) is used in non-steady-state (or transient) heat transfer calculations. It is named after the French physicist Jean-Baptiste Biot (1774 – 1862), and gives a simple index of the ratio of the heat transfer resistances inside of and at the surface of a body. This ratio determines whether or not the temperatures inside a body will vary significantly in space, while the body heats or cools over time, from a thermal gradient applied to its surface. In general, problems involving small Biot numbers (much smaller than 1) are thermally simple, due to uniform temperature fields inside the body. Biot numbers much larger than 1 signal more complex problems due to non-uniformity of temperature fields within the object [29].

1.2. Applications

Flow of reactive fluids in porous media not only presents a theoretically challenging problem but also has a wide range of scientific, technological and engineering applications. This type of flow system can be found in, among others, packed bed chemical reactors, geothermal energy reservoirs, petroleum reservoirs, material processing industries, automobile exhaust systems, drying of food, waste disposal systems, insulation of buildings, groundwater movement, oil and gas production, surface catalysis of chemical reactions, regenerative heat exchange and adsorption, electricity generation, aerospace and ship propulsions, pollution dispersal, etc. The list is obviously inexhaustible as the presence of fluids in technological machinery is ubiquitous [77]. In Figure 1.3 we illustrate some of the devices or systems where the flow of fluids in porous media is applied.

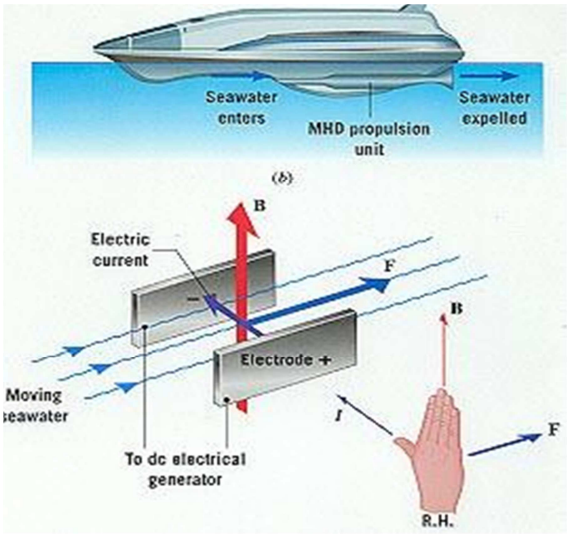

Propulsion force (Mitsubishi, 1991).

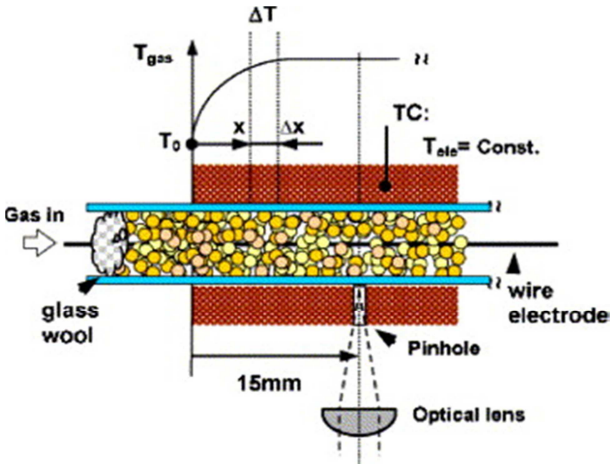

Packed-bed reactor

Petroleum Refinery, Saudi Arabia.

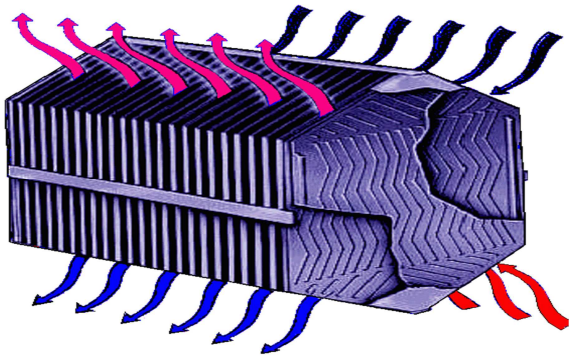

Heat exchanger

Figure 1.3. Applications of fluid flow

1.3. Literature review

Theoretical consideration of fluid flow in porous media has received great attention in recent years, and the interest is motivated by a wide range of scientific, technological and engineering applications, as mentioned earlier. Makinde, for example, has conducted wide research in this area. Some of his recent studies are found in [56 - 62, 71].

Makinde and Mhone [72] investigated the effect of magnetic field intensity and the permeability of the porous medium on the flow of an incompressible fluid. Makinde [56] studied the thermal effects of a reactive viscous flow through a channel filled with porous medium and isothermal walls. Makinde and Ogulu [74] investigated the effect of temperature-dependent viscosity on the

free convection flow of an optimally thick viscous incompressible electrically conducting fluid from a vertical porous flat plate in the presence of a transversely imposed magnetic field and radiation effect. Makinde [62] investigated thermal stability of a reactive viscous combustible fluid flowing steadily through a channel filled with saturated porous medium. Makinde and Maserumule [71] and Makinde and Moitsheki [73] studied thermal effects in variable viscosity Couette flow and on natural convection past a vertical plate imbedded in saturated porous medium respectively. In Makinde [60], stability of fluid flow in porous media was investigated using the Chebyshev collocation spectral approach. The major task in the papers cited in this paragraph was the investigation of thermal stability criteria. Procedure(s) that accurately obtain(s) the steady state thermal ignition criticality conditions were obtained successfully. It was discovered that an increase in the magnetic field intensity and a decrease in the porous medium permeability have a stabilising effect on the fluid flow. Convective cooling on the system was observed to enhance stability and to facilitate a delay in the occurrence of thermal blow-up.

Several other scholars have also done some work in the field of fluid flow through porous media. Parvazinia *et al* [84] investigated stability of laminar steady flow through a highly permeable porous media using multi-scale finite element modelling approach. Pathak and Ghiaasiaan [86] reported on simulations on understanding the solid-fluid heat transfer as well as thermal dispersion during laminar pulsating flow in generic porous media. It was revealed that the wall heat transfer rate and the thermal dispersion term were sensitive to porosity, Reynolds number, and pulsation frequency, and were significantly larger than their counterparts in steady flow. Sochi [98] presented a review of the single-phase flow of non-Newtonian fluids in porous media. The paper reviews the four main approaches for describing the flow through porous media in general, and such approaches mentioned are continuum models, bundle of tubes models, numerical methods and network modelling. Other recent works of Sochi are found in [96,97,99] where he studied pore-scale modelling of viscoelastic flow in porous media, flow of yield-stress fluids in porous media and computational techniques for modelling non-Newtonian flow in porous media respectively.

Bakier *et al* [9], Seddeek *et al* [92], Pal and Chatterjee [83] and Cortel [25] studied heat and mass transfer in MHD flow through porous media. A major finding from [9] and [92] is that the rate of heat transfer at the plate surfaces increases with increasing radiation parameter, mixed convection parameter, mass transfer coefficient, variable viscosity and magnetic field. In [25], it was observed that the effect of destructive chemical reaction on the reactant species is to

diminish the concentration of the boundary layer. Kumaran *et al* [48] as well as Hayat *et al* [42] studied stagnation point flow in porous media and obtained an analytical approximate solution of the classical two dimensional stagnation point flow. Nonlinear flows and/or effects in porous media were studied in Fourar *et al* [34], Cheng *et al* [19], Liu and Masliyah [53] and Pascal and Pascal [85]. Flow through fractured porous media was investigated by Lucas *et al* [54] and Grillo *et al* [39]. Chen *et al* [18] studied the flow and displacement in porous media of fluids with yield stress exemplified by a Bingham plastic. Non-Newtonian fluid flow through porous media was studied by, among other researchers, Al-Nimr *et al* [4], Liu and Masliyah [52], Akshin *et al* [2] and Dholkawala *et al* [27]. Khan *et al* [46] conducted an analytic investigation of unsteady flows of a magnetohydrodynamic (MHD) second grade fluid filling a porous media. Joseph *et al* [45] presented a mathematical model of reservoir flow of foamy oil which depends on velocity through Darcy's law, the pressure and the dispersed gas fraction. Chiem and Zhao [20] and Yang and Hwang [111] conducted numerical studies of steady/unsteady flow and heat transfer in porous media, and numerical simulation of turbulent flow and heat transfer characteristics in heat exchangers fitted with porous media respectively. The former revealed that altering some parametric values can have significant and interesting effects on both flow pattern as well as heat transfer characteristics, and the later found that introducing a porous medium into a fluid channel efficiently improves the heat transfer performance of fluid channels and heat transfer can be enhanced by using high thermal conductivity porous inserts. Teng and Zhao [103] studied an extension of Darcy's law to non-Stokes flow in porous media and Chai *et al* [15] studied non-Darcy flow in disordered porous media. Discontinuous Galerkin approximation of multiphase flows in porous media was studied in Natvig and Lie [78] and Ern *et al* [31]. Su [102] presented the N-dimensional fractional Fokker-Planck equation and its solutions for anomalous radial two-phase flow in porous media.

Nield [79] reported on the limitation of the Brinkman-Forchheimer equation in modelling flow in a saturated porous medium and at an interface. A lattice Boltzmann model for axisymmetric thermal flows through porous media was presented by Rong *et al* [89] and a lattice Boltzmann study of viscous coupling effects in immiscible two-phase flow in porous media was conducted by Yiotis *et al* [112]. Tyagi *et al* [107] presented a Lagrangian stochastic modelling framework for multi-phase flow in porous media. Other recent studies on porous media flow are found in [1, 14, 40, 47, 81, 106].

The interest by researchers on studies of fluid flow through porous media is evidently displayed by the enormous amount of recent studies in the area. It is reasonable to pin this interest on the

mathematical complexity of the studies as mentioned earlier and also on the abundance of crucial real-life applicable areas.

Most of the research that has been done to date in respect of fluid flow through porous media is mainly on Newtonian fluids (the fluid deformation is directly proportional to the applied shear stress). This is despite the fact that there are manifestations of fluid behaviour which cannot be adequately explained on the basis of the classical, linearly viscous model [105]. Geological materials, liquid foams, polymeric fluids, slurries, drilling mud, clay coatings, elastomers, emulsions, hydrocarbon oils, grease, and food products are among the many substances that are capable of flowing but which are non-Newtonian. 'Non-Newtonian' is a generic term that incorporates a variety of phenomena which are highly complex and require sophisticated mathematical modelling techniques for proper description [98]. The complications are worsened when considering flow through porous media [98].

1.4. Problem statement

Although, to a large extent, several studies involving heat and mass transfer in non-Newtonian fluids have been undertaken, most of these studies seem to lack a systematic and rational treatment of the thermodynamics of the problem with respect to the combined effects of porous media, unsteadiness, variable viscosity and asymmetric convective boundary conditions on the flow system. The flow of reactive viscous fluids in porous media gives rise to chemical reactions that are inherently exothermic. Studies of such thermal effects are important in handling reactive fluids as this ensures safety of property and life. Stability analysis as well as understanding thermal effects enables efficient operation of machinery. Numerous scientific and technical applications of such flows exist abundantly. For instance, Sasol industries located in the Vaal region of Gauteng and Secunda, Mpumalanga in South Africa produces a wide range of hydrocarbon oils and lubricants from plant material. The chemical reactions that take place in the manufacture and handling of these non-Newtonian fluids are inevitably exothermic and the processes are prone to explosions that can be fatal. The same can be said with power stations where the flows of electrically conducting fluids have many a time resulted in explosions.

So far no general methodology that can deal with all cases of non-Newtonian flow has been developed, and this situation is not expected to change in the foreseeable future, many challenges are still waiting to be overcome [98]. Thus, on a theoretical level this study will impact positively in pursuit of modelling strategies and techniques.

1.5. Aim and objective

This project aims to study the unsteady flow of reactive variable viscosity non-Newtonian fluid through a channel filled with saturated porous media.

The objective of this theoretical study is two-fold:

(i). to obtain and analyse a mathematical model for thermal effects of non-Newtonian fluid flow through a saturated porous media.

(ii). to determine the thermal stability criteria for non-Newtonian fluid flow through saturated porous media.

1.6. Research methodology

It is envisaged that both analytical techniques and numerical methods will be employed to tackle the nonlinear equations that will be derived from the law of conservation of mass, momentum and energy balance.

1.6.1. Finite difference method

The use of numerical methods to compute the solution for partial differential equations is necessitated by a geometry for which an analytical solution may not exist. Finite difference method is one of the many numerical methods for solving both ordinary and partial differential equations. Since this method will be employed to solve the nonlinear partial differential equations in this project, it is imperative that we give a description of the method. We follow [93].

1.6.1.1. Numerical differentiation of functions of a single variable

Let $y = y(x)$ and $\Delta x = h$. Using the Taylor series expansion around a point $x = x_0$, and ignoring higher order terms (since they vanish to 0), we obtain the following finite-difference approximations;

- the forward-difference approximation

$$y'_i = \frac{1}{h}[y_{i+1} - y_i] + O(h^2) \tag{1.11}$$

- the backward-difference approximation

$$y'_i = \frac{1}{h}[y_i - y_{i-1}] + O(h^2) \quad (1.12)$$

- the central difference approximation

$$y'_i = \frac{1}{2h}[y_{i+1} - y_{i-1}] + O(h^3) \quad (1.13)$$

- the second derivative

$$y''_i = \frac{1}{h^2}[y_{i+1} - 2y_i + y_{i-1}] + O(h^3) \quad (1.14)$$

1.6.1.2. Functions of two variables

Let $u = u(x,t)$, where (x,t) belongs to some two-dimensional area. Expansions in Taylor series around a point (i,j) results in the following approximations;

- the central-difference approximations for the two first order partial derivatives

$$(u_x)_{i,j} = \frac{1}{2\Delta x}\left[u_{i+1,j} - u_{i-1,j}\right] + O(\Delta x^3) \quad (1.15)$$

$$(u_t)_{i,j} = \frac{1}{2\Delta t}\left[u_{i,j+1} - u_{i,j-1}\right] + O(\Delta t^3) \quad (1.16)$$

- the approximations for the second-order partial derivatives

$$(u_{xx})_{i,j} = \frac{1}{\Delta x^2}\left[u_{i+1,j} - 2u_{i,j} + u_{i-1,j}\right] + O(\Delta x^3) \quad (1.17)$$

$$(u_{tt})_{i,j} = \frac{1}{\Delta t^2}\left[u_{i,j+1} - 2u_{i,j} + u_{i,j-1}\right] + O(\Delta t^3) \quad (1.18)$$

1.6.2. Shooting method

For most engineering and scientific applications numerical solutions are of particular interest due to the fact that exact solutions may not exist in closed form. Furthermore, numerical solution methods within the *dsolve* command in Maple, for instance, are applicable only to initial value problems. In view of this, Maple appears to be very limited in its ability to analyse the two-point (or more) boundary value problems that we wish to solve. The shooting method is a numerical technique that is utilised to solve two-point boundary value problems. It is an iterative algorithm that identifies appropriate initial conditions for a related initial value problem (IVP) that provides the solution to the original boundary value problem (BVP) [76].

Meade *et al* [76] developed the shooting technique for implementation in Maple. Suppose it is desired to compute the solution of the two-point BVP

$$\begin{aligned} \frac{dy}{dt} &= f(t, y(t)) \\ y_i(a) &= \alpha_i\ , \quad i = 1,2,\cdots, m_1 \\ y_{m_1+j}(b) &= \beta_j, \quad j = 1,2,\cdots, m_2 \end{aligned} \tag{1.19}$$

where the vector y contains the n unknown functions of the independent variable t. The unknown functions are ordered so that the first m_1 $(0 < m_1 < n)$ components of y have first kind boundary conditions at $t = a$, and the remaining $m_2 \coloneqq n - m_1$ components of the solution have first kind boundary conditions specified at a second point, $t = b$. The shooting method works by identifying a vector of parameters $\chi \in \mathbb{R}^{m_2}$ so that the solution, denoted by $y(t; \chi)$, to the IVP

$$\begin{aligned} \frac{dy}{dt} &= f(t, y(t; \chi)) \\ y_i(a; \chi) &= \alpha_i\ , \quad i = 1,2,\cdots, m_1 \\ y_{m_1+j}(a; \chi) &= \chi_j, \quad j = 1,2,\cdots, m_2 \end{aligned} \tag{1.20}$$

is equal to the solution of the BVP (1.19).

The translation of the simple shooting method into Maple programming language is enabled by a combination of Maple's facilities for symbolic manipulation and numerical solution of IVPs. This procedure, called *shoot*, has syntax closely similar to *dsolve*.

1.6.3. Runge-Kutta Integration method

The Runge-Kutta method for numerical solution of differential equations was developed by two German mathematicians Runge and Kutta [38]. Suppose we wish to find the numerical solution of the initial value problem

$$\frac{dy}{dx} = f(x, y), \ \ y(x_0) = y_0 \tag{1.21}$$

A simple second-order Runge-Kutta algorithm [38] for the solution of equation (1.21) is

$$y_{n+1} = y_n + \frac{1}{2}(k_1 + k_2)$$

$$k_1 = \ hf(x_n, y_n)$$

$$k_2 = hf(x_n + h, y_n + k_1)$$

where the increment to y is taken as a weighted average of the two estimates of the increment which are denoted k_1 and k_2.

The fourth-order Runge-Kutta method is a vast improvement of the second-order in terms of the closeness of its solution to the exact solution of the differential equation. Herewith the Runge-Kutta 4th order algorithm [38]:

$$y_{n+1} = y_n + \frac{1}{6}(k_1 + 2k_2 + 2k_3 + k_4),$$

$$k_1 = hf(x_n, y_n),$$

$$k_2 = hf\left(x_n + \tfrac{1}{2}h, y_n + \tfrac{1}{2}k_1\right),$$

$$k_3 = hf\left(x_n + \frac{1}{2}h, y_n + \frac{1}{2}k_2\right),$$

$$k_4 = hf(x_n + h, y_n + k_3),$$

Higher order Runge-Kutta algorithms; fifth-order, sixth-order, etc, have been developed.

The Runge-Kutta-Fehlberg method uses two Runge-Kutta methods of different orders. For example, it may use the fourth-order and the fifth-order to move from (x_n, y_n) to (x_{n+1}, y_{n+1}) and compare the results for y_{n+1}. The advantage of this process is that satisfactory results are achieved with fewer number of function evaluations. Algorithm for the Runge-Kutta-Fehlberg method is hereunder [38];

$k_1 = hf(x_n, y_n)$, $\quad k_2 = hf\left(x_n + \tfrac{1}{4}h, y_n + \tfrac{1}{4}k_1\right)$,

$k_3 = hf\left(x_n + \tfrac{3}{8}h, y_n + \tfrac{3}{32}k_1 + \tfrac{9}{32}k_2\right)$, $k_4 = hf\left(x_n + \tfrac{12}{13}h, y_n + \tfrac{1932}{2197}k_1 - \tfrac{7200}{2197}k_2 + \tfrac{7296}{2197}k_3\right)$,

$k_5 = hf\left(x_n + h, y_n + \tfrac{439}{216}k_1 - 8k_2 + \tfrac{3680}{513}k_3 - \tfrac{845}{4104}k_4\right)$,

$k_6 = hf\left(x_n + \tfrac{h}{2}, y_n - \tfrac{8}{27}k_1 + 2k_2 - \tfrac{3544}{2565}k_3 + \tfrac{1859}{4104}k_4 - \tfrac{11}{40}k_5\right)$;

$\hat{y}_{n+1} = y_n + \left(\tfrac{25}{216}k_1 + \tfrac{1408}{2565}k_3 + \tfrac{2197}{4104}k_4 - \tfrac{1}{5}k_5\right), with\ global\ error\ O(h^4)$;

$$y_{n+1} = y_n + \left(\frac{16}{135}k_1 + \frac{6656}{12825}k_3 + \frac{28561}{56430}k_4 - \frac{9}{50}k_5 + \frac{2}{55}k_6\right), with\ global\ error\ O(h^5),$$

Error, $E = \frac{1}{360}k_1 - \frac{128}{4275}k_3 - \frac{2197}{75240}k_4 + \frac{1}{50}k_5 + \frac{2}{55}k_6$.

The Runge-Kutta-Fehlberg Method is implemented in, among other programming languages, Maple (rkf45), Matlab (ode45, ode23) and Fortran (RKF45). In Maple it is used in conjunction with the shooting method to solve boundary value problems. In this project, we will rely on MAPLE to simulate solutions of the nonlinear partial differential equations governing our flow systems. It is for this reason that the shooting technique and the Runge-Kutta methods are summarised herein. Chapter 2 is devoted to the derivations of the fundamental equations governing the dynamics of fluid flow.

CHAPTER TWO

DERIVATION OF THE BASIC EQUATIONS

This chapter is devoted to the derivation of the continuity equation, the momentum equation and the energy equation. These are the three fundamental equations that govern the dynamics of fluid flow. The three equations are mathematical statements of the three physical principles, namely; conservation of mass, conservation of momentum (Newton's second law of motion) and conservation of energy (the first law of thermodynamics). We proceed following [91] and [109].

2.1. The substantial derivative

Following [109], consider an infinitesimally small fluid element moving with the unsteady flow depicted in Figure 2.1.

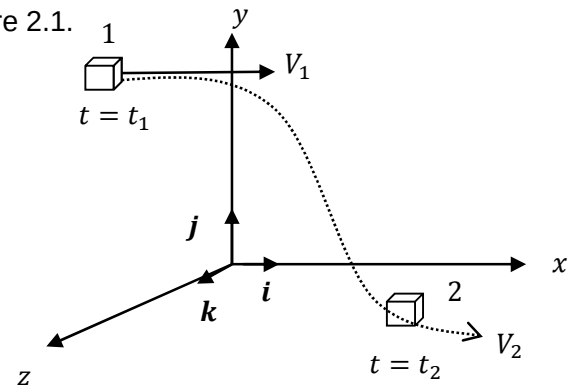

Figure 2.1. Fluid element moving in the flow field – illustration for the substantial derivative.

The velocity of the fluid element is

$$\boldsymbol{V} = u\boldsymbol{i} + v\boldsymbol{j} + w\boldsymbol{k},$$

where $u = u(x, y, z, t),\ v = v(x, y, z, t),\ w = w(x, y. z, t)$ are the x, y, z components of the velocity respectively. At time $t = t_1$ the density of the fluid element is $\rho_1(x_1, y_1, z_1, t_1)$ and at time $t = t_2$ it is $\rho_2(x_2, y_2, z_2, t_2)$. The Taylor series expansion of $\rho(x, y, z, t)$ about the initial point is

$$\rho_2 = \rho_1 + \left(\frac{\partial \rho}{\partial x}\right)_1 (x_2 - x_1) + \left(\frac{\partial \rho}{\partial y}\right)_1 (y_2 - y_1) + \left(\frac{\partial \rho}{\partial z}\right)_1 (z_2 - z_1) + \left(\frac{\partial \rho}{\partial t}\right)_1 (t_2 - t_1),$$

where we have ignored higher order terms. In the limit as $t_2 \longrightarrow t_1$, we have

$$\lim_{t_2 \to t_1}\left(\frac{\rho_2-\rho_1}{t_2-t_1}\right)=\left(\frac{\partial \rho}{\partial x}\right)_1 \lim_{t_2 \to t_1}\left(\frac{x_2-x_1}{t_2-t_1}\right)+\left(\frac{\partial \rho}{\partial y}\right)_1 \lim_{t_2 \to t_1}\left(\frac{y_2-y_1}{t_2-t_1}\right)+\left(\frac{\partial \rho}{\partial z}\right)_1 \lim_{t_2 \to t_1}\left(\frac{z_2-z_1}{t_2-t_1}\right)+\left(\frac{\partial \rho}{\partial t}\right)_1$$

Defining

$$\lim_{t_2 \to t_1}\left(\frac{\rho_2-\rho_1}{t_2-t_1}\right)=\frac{D\rho}{Dt},$$

gives

$$\frac{D\rho}{Dt}=u\frac{\partial \rho}{\partial x}+v\frac{\partial \rho}{\partial y}+w\frac{\partial \rho}{\partial z}+\frac{\partial \rho}{\partial t} \tag{2.1}$$

$\frac{D}{Dt}$ is called the substantial derivative. In this way, $\frac{D\rho}{Dt}$ is the rate of change of density of the fluid element as it moves through space. $\frac{\partial \rho}{\partial t}$ is the rate of change of density at a fixed point. In general, therefore, we have from equation (2.1) an expression for the substantial derivative in Cartesian coordinates

$$\frac{D}{Dt}=u\frac{\partial}{\partial x}+v\frac{\partial}{\partial y}+w\frac{\partial}{\partial z}+\frac{\partial}{\partial t}. \tag{2.2}$$

Since $\nabla = i\frac{\partial}{\partial x}+j\frac{\partial}{\partial y}+k\frac{\partial}{\partial z}$, we rewrite equation (2.2) as

$$\frac{D}{Dt}=\frac{\partial}{\partial t}+(\boldsymbol{V}\cdot\nabla) \tag{2.3}$$

$\boldsymbol{V}\cdot\nabla$ is called the convective derivative – the time rate of change due to the movement of the fluid element from one location to another in the flow field where the flow properties are spatially different. $\frac{\partial}{\partial t}$ is the local derivative. The substantial derivative applies to any flow field variable like temperature, static pressure, etc. For instance, the substantial derivative for temperature is

$$\frac{DT}{Dt}=\frac{\partial T}{\partial t}+(\boldsymbol{V}\cdot\nabla) \tag{2.4}$$

2.2. Continuity equation

The continuity equation is one of the equations governing the behaviour of the fluid. It is an expression of a fundamental conservation principle, namely, mass conservation. We adopt the derivation in Wendt [109].

Assuming a finite control volume fixed in space, the fundamental physical principle that mass is conserved means

$$\begin{Bmatrix} Net\ mass\ flow\ out \\ of\ control\ volume \\ through\ surface\ S \end{Bmatrix} = \begin{Bmatrix} time\ rate\ of\ decrease \\ of\ mass\ inside\ control \\ volume \end{Bmatrix}$$

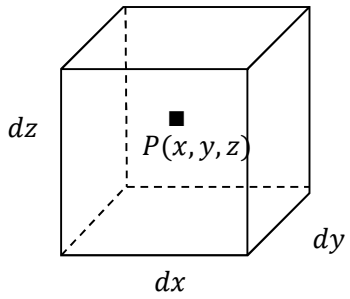

Figure 2.2. Volume element dV

In Figure 2.2, $P(x, y, z)$ is the centroid of the fluid element and the sides of the cube are fixed in space. Fluid can flow into and out of the volume element through the sides. Let the fluid density at $P(x, y, z)$ be $\rho(x, y, z)$ and suppose that this density is uniform throughout dV. The total mass contained within this volume element is thus

$$M = \int \rho dV = \int \rho dx dy dz. \tag{2.5}$$

The rate at which mass enters or leaves through the surface dS is $\frac{dM}{dt}$. A surface element $d\boldsymbol{S}$ is given by

$$d\boldsymbol{S} = \hat{\boldsymbol{n}} dS$$

where $\hat{\boldsymbol{n}}$ is a unit vector perpendicular to the surface. When $d\boldsymbol{S}$ is a side of a volume element dV, $\hat{\boldsymbol{n}}$ is assumed to point out of the volume element (i.e., from inside to outside). The flux mass

(mass/unit area/unit time) passing through a surface is $\rho\boldsymbol{V}$, where $\boldsymbol{V}$ is the fluid velocity. The mass per unit time flowing through $d\boldsymbol{S}$ is

$$\rho\boldsymbol{V}\cdot\ d\boldsymbol{S} = \rho\boldsymbol{V}\cdot\ \hat{\boldsymbol{n}}dS$$

and the total rate of flow of mass out of the volume dV is

$$\sum_{Faces} \rho\boldsymbol{V}\cdot\ d\boldsymbol{S}$$

Thus,

$$\oint_S \rho\boldsymbol{V}\cdot\ d\boldsymbol{S} = \oint_{\boldsymbol{S}} \rho\boldsymbol{V}\cdot\ \hat{\boldsymbol{n}}dS$$

where the integral is over the surface enclosing dV. In this way, we have

$$\frac{dM}{dt} = \frac{d}{dt}\int_V \rho dV = -\oint_S \rho\boldsymbol{V}\cdot\ \hat{\boldsymbol{n}}dS$$

The negative sign appears due to the fact that mass flow of the fluid is flowing out of the control volume.

We thus have,

$$\int_V \frac{\partial\rho}{\partial t}dV = -\oint_S \rho\boldsymbol{V}\cdot\ \hat{\boldsymbol{n}}dS$$

Now, by Gauss's theorem, namely "the normal surface integral of the function $\boldsymbol{F}$ over the boundary of a closed region is equal to the volume (space) integral of the divergence of $\boldsymbol{F}$ taken throughout the enclosed volume (space)", we have

$$\oint_S \rho\boldsymbol{V}\cdot\ \hat{\boldsymbol{n}}dS = \oint_V \nabla\cdot(\rho\boldsymbol{V})dV$$

Hence,

$$\int_V \left[\frac{\partial\rho}{\partial t} + \nabla\cdot(\rho\boldsymbol{V})\right]dV = 0.$$

This expression must hold for every arbitrarily shaped volume, and the only way it can be satisfied is if the integrand vanishes identically, or

$$\frac{\partial \rho}{\partial t} = -\nabla \cdot (\rho \boldsymbol{V}) \tag{2.6}$$

Equation (2.6), called the continuity equation, expresses conservation of mass in the finite control volume fixed in space model [91].

Now, an alternative derivation [91] is to consider the volume element dV co-moving with the fluid and assume that every point on the surface and within the volume is moving with the local velocity $\boldsymbol{V} = \frac{dx}{dt}\boldsymbol{i} + \frac{dy}{dt}\boldsymbol{j} + \frac{dz}{dt}\boldsymbol{k}$. Since each point on the boundary S moves with the fluid, no fluid can flow across the surface so that the total mass within the volume element is fixed in time. In this way we have

$$\frac{dM}{dt} = 0,$$

and the mass is automatically conserved. However, the density is time-dependent because the total volume of the moving fluid element can change as it distorts due to fluid motions. The statement of conservation of mass then becomes

$$\frac{dM}{dt} = 0 = \frac{d}{dt}\int_V \rho(t)dx(t)dy(t)dz(t) \tag{2.7}$$

The change in volume dV has to be accounted for. To do this, we rewrite equation (2.7) as

$$\frac{d}{dt}\int_V \rho(t)\delta x(t)\delta y(t)\delta z(t) = 0$$

$$\Rightarrow \int \left[\frac{d\rho}{dt}\delta x\delta y\delta z + \rho\frac{d}{dt}(\delta x\delta y\delta z)\right] = 0$$

$$\Rightarrow \int \left\{\frac{d\rho}{dt}\delta x\delta y\delta z + \rho\left[\frac{d\delta x}{dt}\delta y\delta z + \delta x\frac{d\delta y}{dt}\delta z + \delta x\delta y\frac{d\delta z}{dt}\right]\right\} = 0$$

$$\Rightarrow \int \left[\frac{d\rho}{dt}\delta x\delta y\delta z + \rho\delta x\delta y\delta z\left(\frac{\delta u}{\delta t} + \frac{\delta v}{\delta t} + \frac{\delta w}{\delta t}\right)\right] = 0$$

where we have used the fact that δ and d are both infinitesimals along with $\frac{dx}{dt} = u, \frac{dy}{dt} = v, \frac{dz}{dt} = w$ to write $\frac{d(\delta x)}{dt} = \delta\left(\frac{dx}{dt}\right) = \delta u$, $\frac{d(\delta y)}{dt} = \delta\left(\frac{dy}{dt}\right) = \delta v$, and $\frac{d(\delta z)}{dt} = \delta\left(\frac{dz}{dt}\right) = \delta w$.

Now, substituting $\nabla \cdot \boldsymbol{V} = \frac{\delta u}{\delta t} + \frac{\delta v}{\delta t} + \frac{\delta w}{\delta t}$ and $dV = \delta x \delta y \delta z$, results in

$$\int \left[\frac{d\rho}{dt} + \rho \nabla \cdot \boldsymbol{V}\right] dV = 0$$

and since this must hold for arbitrary volume elements, we require that

$$\frac{d\rho}{dt} + \rho \nabla \cdot \boldsymbol{V} = 0. \tag{2.8}$$

This is the expression for conservation of mass in this frame of reference. This equation must be consistent with equation (2.6) as they both express the law of conservation of mass. If we identify

$$\frac{d\rho}{dt} = \frac{\partial \rho}{\partial t} + \boldsymbol{V} \cdot \nabla \rho,$$

we can rewrite (2.6) as

$$\frac{\partial \rho}{\partial t} + \nabla \cdot (\rho \boldsymbol{V}) = \frac{\partial \rho}{\partial t} + \boldsymbol{V} \cdot \nabla \rho + \rho \nabla \cdot \boldsymbol{V} = 0 \tag{2.9}$$

which is consistent with (2.8).

The differential equation for conservation of mass (continuity equation) in component form is

$$\frac{\partial \rho}{\partial t} + \frac{\partial (\rho u)}{\partial x} + \frac{\partial (\rho v)}{\partial y} + \frac{\partial (\rho w)}{\partial z} = 0 \tag{2.10}$$

For incompressible flow ($\rho = constant$), the continuity equation reduces to

$$\frac{\partial u}{\partial x} + \frac{\partial v}{\partial y} + \frac{\partial w}{\partial z} = \nabla \cdot \boldsymbol{V} = 0 \tag{2.11}$$

The velocity field $\boldsymbol{V}(x, y, z, t)$ for incompressible flow must satisfy $\nabla \cdot \boldsymbol{V} = 0$. For steady flow, all field properties are, by definition, independent of time $\left(\frac{\partial \rho}{\partial t} = 0\right)$ and $\rho = \rho(x, y, z)$. Thus, for steady flow, the continuity equation becomes

$$\frac{\partial (\rho u)}{\partial x} + \frac{\partial (\rho v)}{\partial y} + \frac{\partial (\rho w)}{\partial z} = \nabla \cdot (\rho \boldsymbol{v}) = 0 \tag{2.12}$$

For a two-dimensional incompressible flow in the $xy-$plane, $\boldsymbol{V} = \boldsymbol{V}(x, y)$ and the continuity equation is

$$\frac{\partial u}{\partial x} + \frac{\partial v}{\partial y} = 0 \tag{2.13}$$

2.3. Momentum equation

The physical principle applied in deriving the momentum equation is Newton's second law of motion which states that

$$\boldsymbol{F} = m\boldsymbol{a},$$

where $\boldsymbol{F}$ is force, m is the mass and $\boldsymbol{a}$ is acceleration.

We assume the moving fluid element model as in Figure 2.3 and follow the derivation in [109].

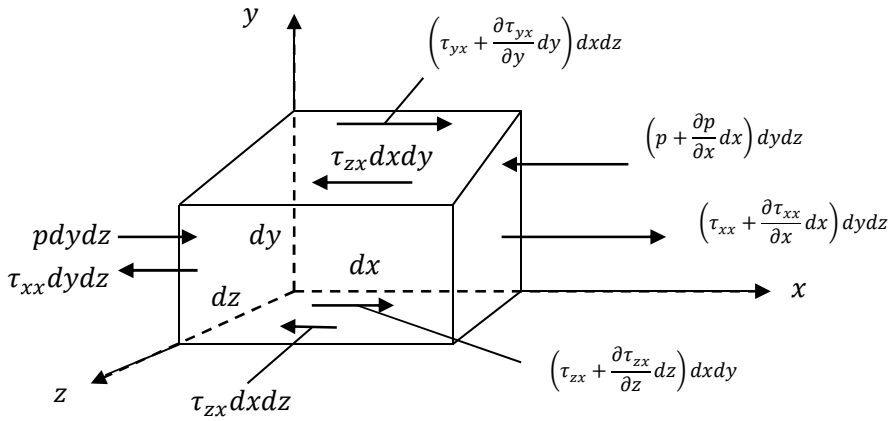

Figure 2.3. Infinitesimally small, moving fluid element. Only forces in the x-direction shown.

Newton's 2nd law states that "the net force on the fluid element equals its mass times the acceleration of the element". It is important to notice that this is a vector relation consisting of the x, y and z components. The x-component of Newton's 2nd law is thus

$$F_x = ma_x \tag{2.14}$$

F_x and a_x are the force and acceleration components respectively in the x-direction. The force comprises of the body forces and the surface forces. Body forces, e.g. gravitational force, act directly on the volumetric mass of the fluid element. Surface forces act directly on the surface of the fluid element. These are the pressure distribution acting on the surface imposed by the

outside fluid surrounding the fluid element, and the shear and normal stress distributions acting on the surface imposed by the outside fluid pushing on the surface by means of friction.

If we denote the body force per unit mass acting on the fluid element by $\boldsymbol{f}$, with f_x the x-component of this force, we get the body force on the fluid element acting in the x-direction as

$$\rho f_x dxdydz,$$

where, of course, $dxdydz$ is the volume of the fluid element. The surface forces in the x-direction exerted on the fluid element are shown in Figure 2.3.

$$\begin{Bmatrix} Net\ surface\ force \\ in\ the\ x-direction \end{Bmatrix} = \left[p - \left(p + \frac{\partial p}{\partial x}dx\right)\right] dydz + \left[\left(\tau_{xx} + \frac{\partial \tau_{xx}}{\partial x}dx\right) - \tau_{xx}\right] dydz + \left[\left(\tau_{yx} + \frac{\partial \tau_{yx}}{\partial y}dy\right) - \tau_{yx}\right] dxdz + \left[\left(\tau_{zx} + \frac{\partial \tau_{zx}}{\partial z}dz\right) - \tau_{zx}\right] dxdy \quad (2.15)$$

Summing results in

$$F_x = \left(-\frac{\partial p}{\partial x} + \frac{\partial \tau_{xx}}{\partial x} + \frac{\partial \tau_{yx}}{\partial y} + \frac{\partial \tau_{zx}}{\partial z}\right) dxdydz + \rho f_x dxdydz \quad (2.16)$$

Now,

$$m = \rho dxdydz$$

and, recalling the substantial derivative,

$$a_x = \frac{Du}{Dt}.$$

In this way equation (2.14) becomes

$$\rho \frac{Du}{Dt} = -\frac{\partial p}{\partial x} + \frac{\partial \tau_{xx}}{\partial x} + \frac{\partial \tau_{yx}}{\partial y} + \frac{\partial \tau_{zx}}{\partial z} + \rho f_x \quad (2.17)$$

Applying the same process to the y- and z- components, we get

$$\rho \frac{Dv}{Dt} = -\frac{\partial p}{\partial y} + \frac{\partial \tau_{xy}}{\partial x} + \frac{\partial \tau_{yy}}{\partial y} + \frac{\partial \tau_{zy}}{\partial z} + \rho f_y \quad (2.18)$$

$$\rho \frac{Dw}{Dt} = -\frac{\partial p}{\partial z} + \frac{\partial \tau_{xz}}{\partial x} + \frac{\partial \tau_{yz}}{\partial y} + \frac{\partial \tau_{zz}}{\partial z} + \rho f_z \quad (2.19)$$

Equations (2.17) – (2.19) are the $x-, y-$ and $z-$components respectively of the momentum equation. Since the fluid element is moving with the flow, the equations are in non-conservation form. These equations are called the Navier-Stokes equations.

Now, rewriting the left hand side of equation (2.17) using the definition of the substantial derivative, equation (2.3);

$$\rho\frac{Du}{Dt} = \rho\frac{\partial u}{\partial t} + \rho\boldsymbol{V}\cdot\nabla u$$

Observe that

$$\frac{\partial(\rho u)}{\partial t} = \rho\frac{\partial u}{\partial t} + u\frac{\partial \rho}{\partial t} \Longrightarrow \rho\frac{\partial u}{\partial t} = \frac{\partial(\rho u)}{\partial t} - u\frac{\partial \rho}{\partial t}$$

and

$$\nabla\cdot(\rho u\boldsymbol{V}) = u\nabla\cdot(\rho\boldsymbol{V}) + (\rho\boldsymbol{V})\cdot\nabla u$$

or

$$\rho\boldsymbol{V}\cdot\nabla u = \nabla\cdot(\rho u\boldsymbol{V}) - u\nabla\cdot(\rho\boldsymbol{V}).$$

Consequently,

$$\rho\frac{Du}{Dt} = \frac{\partial(\rho u)}{\partial t} - u\frac{\partial \rho}{\partial t} - \ u\nabla\cdot(\rho\boldsymbol{V}) + \nabla\cdot(\rho u\boldsymbol{V})$$

$$\rho\frac{Du}{Dt} = \frac{\partial(\rho u)}{\partial t} - u\left[\frac{\partial \rho}{\partial t} + \nabla\cdot(\rho\boldsymbol{V})\right] + \nabla\cdot(\rho u\boldsymbol{V})$$

and, from the continuity equation,

$$\rho\frac{Du}{Dt} = \frac{\partial(\rho u)}{\partial t} + \nabla\cdot(\rho u\boldsymbol{V}).$$

Equations (2.17), (2.18) and (2.19) therefore can be rewritten as

$$\frac{\partial(\rho u)}{\partial t} + \nabla\cdot(\rho u\boldsymbol{V}) = -\frac{\partial p}{\partial x} + \frac{\partial \tau_{xx}}{\partial x} + \frac{\partial \tau_{yx}}{\partial y} + \frac{\partial \tau_{zx}}{\partial z} + \ \rho f_x \qquad (2.20)$$

$$\frac{\partial(\rho v)}{\partial t} + \nabla\cdot(\rho v\boldsymbol{V}) = -\frac{\partial p}{\partial y} + \frac{\partial \tau_{xy}}{\partial x} + \frac{\partial \tau_{yy}}{\partial y} + \frac{\partial \tau_{zy}}{\partial z} + \ \rho f_y \qquad (2.21)$$

$$\frac{\partial(\rho w)}{\partial t} + \nabla \cdot (\rho w \boldsymbol{V}) = -\frac{\partial p}{\partial z} + \frac{\partial \tau_{xz}}{\partial x} + \frac{\partial \tau_{yz}}{\partial y} + \frac{\partial \tau_{zz}}{\partial z} + \rho f_z \qquad (2.22)$$

Equations (2.20) – (2.22) are Navier-Stokes equations in conservation form.

Assuming that the fluid in question is Newtonian, that is, the shear stresses in the fluid are proportional to the velocity gradients, we will rewrite the shear stresses as

$$\tau_{xx} = \eta \nabla \cdot \boldsymbol{V} + 2\mu \frac{\partial u}{\partial x}, \quad \tau_{yy} = \eta \nabla \cdot \boldsymbol{V} + 2\mu \frac{\partial v}{\partial x}, \qquad \tau_{zz} = \eta \nabla \cdot \boldsymbol{V} + 2\mu \frac{\partial w}{\partial x}$$

$$\tau_{xy} = \tau_{yx} = \mu\left(\frac{\partial v}{\partial x} + \frac{\partial u}{\partial y}\right), \quad \tau_{xz} = \tau_{zx} = \mu\left(\frac{\partial u}{\partial z} + \frac{\partial w}{\partial x}\right), \quad \tau_{yz} = \tau_{zy} = \mu\left(\frac{\partial w}{\partial y} + \frac{\partial v}{\partial z}\right),$$

where μ is the molecular viscosity coefficient and $\eta = -\frac{2}{3}\mu$ is the bulk viscosity coefficient. These are substituted into equations (2.20) – (2.22) to obtain

$$\frac{\partial(\rho u)}{\partial t} + \frac{\partial(\rho u^2)}{\partial x} + \frac{\partial(\rho uv)}{\partial y} + \frac{\partial(\rho uw)}{\partial z} = -\frac{\partial p}{\partial x} + \frac{\partial}{\partial x}\left(\eta \nabla \cdot \boldsymbol{V} + 2\mu \frac{\partial u}{\partial x}\right) + \frac{\partial}{\partial y}\left[\mu\left(\frac{\partial v}{\partial x} + \frac{\partial u}{\partial y}\right)\right] + \frac{\partial}{\partial z}\left[\mu\left(\frac{\partial u}{\partial z} + \frac{\partial w}{\partial x}\right)\right] + \rho f_x \qquad (2.23)$$

$$\frac{\partial(\rho v)}{\partial t} + \frac{\partial(\rho uv)}{\partial x} + \frac{\partial(\rho v^2)}{\partial y} + \frac{\partial(\rho vw)}{\partial z} = -\frac{\partial p}{\partial y} + \frac{\partial}{\partial x}\left[\mu\left(\frac{\partial v}{\partial x} + \frac{\partial u}{\partial y}\right)\right] + \frac{\partial}{\partial y}\left(\eta \nabla \cdot \boldsymbol{V} + 2\mu \frac{\partial v}{\partial x}\right) + \frac{\partial}{\partial z}\left[\mu\left(\frac{\partial w}{\partial y} + \frac{\partial v}{\partial z}\right)\right] + \rho f_y \qquad (2.24)$$

$$\frac{\partial(\rho w)}{\partial t} + \frac{\partial(\rho uw)}{\partial x} + \frac{\partial(\rho vw)}{\partial y} + \frac{\partial(\rho w^2)}{\partial z} = -\frac{\partial p}{\partial z} + \frac{\partial}{\partial x}\left[\mu\left(\frac{\partial u}{\partial z} + \frac{\partial w}{\partial x}\right)\right] + \frac{\partial}{\partial y}\left[\mu\left(\frac{\partial w}{\partial y} + \frac{\partial v}{\partial z}\right)\right] + \frac{\partial}{\partial z}\left(\eta \nabla \cdot \boldsymbol{V} + 2\mu \frac{\partial w}{\partial x}\right) + \rho f_z \qquad (2.25)$$

2.4. Energy equation

The physical principle that is used to derive the energy equation is that of conservation of energy (the first law of thermodynamics stated in section 1.1.6). Summarising the derivation given by Wendt [109], this principle applied to our fluid in Figure 2.3 becomes:

$$\begin{Bmatrix} Rate\ of\ change\ of \\ energy\ inside\ the \\ fluid\ element \end{Bmatrix} = \begin{Bmatrix} Net\ flux\ of \\ heat\ into \\ the\ element \end{Bmatrix} + \begin{Bmatrix} Rate\ of\ working\ done\ on \\ the\ element\ due\ to\ body \\ and\ surface\ forces \end{Bmatrix}$$

The rate of work done by the body force acting on the fluid element moving at a velocity $\boldsymbol{V}$ is given by $\rho \boldsymbol{F} \cdot \boldsymbol{V} dV = \rho \boldsymbol{F} \cdot \boldsymbol{V} dx dy dz$.

From Figure 2.4, the net rate of work done by pressure and shear stresses in the x-direction add up to $\left[-\frac{\partial(up)}{\partial x} + \frac{\partial(u\tau_{xx})}{\partial x} + \frac{\partial(u\tau_{yx})}{\partial y} + \frac{\partial(u\tau_{zx})}{\partial z}\right] dxdydz$. Similar expressions are obtained for the y- and z-directions. The total, net rate of work done on the moving fluid element is thus

$$\left[-\left(\frac{\partial(up)}{\partial x} + \frac{\partial(vp)}{\partial y} + \frac{\partial(wp)}{\partial z}\right) + \frac{\partial(u\tau_{xx})}{\partial x} + \frac{\partial(u\tau_{yx})}{\partial y} + \frac{\partial(u\tau_{zx})}{\partial z} + \frac{\partial(v\tau_{xy})}{\partial x} + \frac{\partial(v\tau_{yy})}{\partial y} + \frac{\partial(v\tau_{zy})}{\partial z} + \frac{\partial(w\tau_{xz})}{\partial x} + \frac{\partial(w\tau_{yz})}{\partial y} + \frac{\partial(w\tau_{zz})}{\partial z}\right] dxdydz + \rho \boldsymbol{F} \cdot \boldsymbol{V} dxdydz \quad (2.26)$$

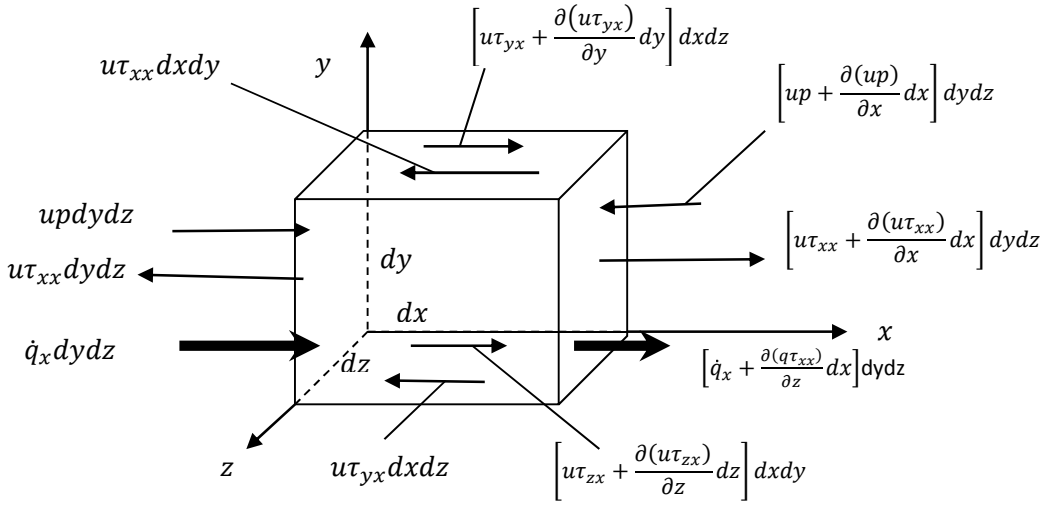

Figure 2.4. Energy fluxes associated with an infinitesimally small, moving fluid element. Only the fluxes in the x-direction are shown.

The volumetric heating of the element is $\rho \dot{q} dxdydz$, where $\dot{q}$ is the rate of volumetric heat addition per unit mass. The net heat transferred in the x-direction into the fluid element by thermal conduction is $\left[\dot{q_x} - \left(\dot{q_x} + \frac{\partial \dot{q_x}}{\partial x}dx\right)\right] dydz = -\frac{\partial \dot{q_x}}{\partial x} dxdydz$. This is added to similar expressions for the y- and z-directions to give the total heat of the fluid element by thermal induction as $-\left(\frac{\partial \dot{q_x}}{\partial x} + \frac{\partial \dot{q_y}}{\partial y} + \frac{\partial \dot{q_z}}{\partial z}\right) dxdydz$.

This, combined with volumetric heating of the fluid element, becomes

$$\{Net\ flux\ of\ heat\ into\ the\ element\} = \left[\rho\dot{q} - \left(\frac{\partial \dot{q}_x}{\partial x} + \frac{\partial \dot{q}_y}{\partial y} + \frac{\partial \dot{q}_z}{\partial z}\right)\right] dxdydz \tag{2.27}$$

Now, substituting $\dot{q}_x = -k\frac{\partial T}{\partial x}$; $\dot{q}_y = -k\frac{\partial T}{\partial y}$; $\dot{q}_z = -k\frac{\partial T}{\partial z}$, where k is the thermal conductivity, into equation (2.27) we obtain

$$\begin{Bmatrix} Net\ flux\ of \\ heat\ into \\ the\ element \end{Bmatrix} = \left[\rho\dot{q} + \frac{\partial}{\partial x}\left(k\frac{\partial T}{\partial x}\right) + \frac{\partial}{\partial y}\left(k\frac{\partial T}{\partial y}\right) + \frac{\partial}{\partial z}\left(k\frac{\partial T}{\partial z}\right)\right] dxdydz. \tag{2.28}$$

$$\{Rate\ of\ change\ of\ energy\ inside\ the\ fluid\ element\} = \rho\frac{D}{Dt}\left(E + \frac{V^2}{2}\right) dxdydz,$$

where E is the internal energy per unit mass and $\frac{V^2}{2}$ $(V^2 = u^2 + v^2 + w^2)$ is the kinetic energy per unit mass. We now have the energy equation as

$$\begin{aligned}\rho\frac{D}{Dt}\left(E + \frac{V^2}{2}\right) = {} & \rho\dot{q} + \frac{\partial}{\partial x}\left(k\frac{\partial T}{\partial x}\right) + \frac{\partial}{\partial y}\left(k\frac{\partial T}{\partial y}\right) + \frac{\partial}{\partial z}\left(k\frac{\partial T}{\partial z}\right) - \frac{\partial(up)}{\partial x} - \frac{\partial(vp)}{\partial y} - \frac{\partial(wp)}{\partial z} + \frac{\partial(u\tau_{xx})}{\partial x} \\ & + \frac{\partial(u\tau_{yx})}{\partial y} + \frac{\partial(u\tau_{zx})}{\partial z} + \frac{\partial(v\tau_{xy})}{\partial x} + \frac{\partial(v\tau_{yy})}{\partial y} + \frac{\partial(v\tau_{zy})}{\partial z} + \frac{\partial(w\tau_{xz})}{\partial x} + \frac{\partial(w\tau_{yz})}{\partial y} \\ & + \frac{\partial(w\tau_{zz})}{\partial z} + \rho\boldsymbol{F}\cdot\boldsymbol{V}\end{aligned} \tag{2.29}$$

The energy equation (2.29) can be written in various forms. In particular we can rewrite the equation in a form that involves just the internal energy E and replacing the viscous stress terms with their equivalent expressions in section 2.3.

$$\begin{aligned}\rho\frac{DE}{Dt} = {} & \rho\dot{q} + \frac{\partial}{\partial x}\left(k\frac{\partial T}{\partial x}\right) + \frac{\partial}{\partial y}\left(k\frac{\partial T}{\partial y}\right) + \frac{\partial}{\partial z}\left(k\frac{\partial T}{\partial z}\right) - p\left(\frac{\partial u}{\partial x} + \frac{\partial v}{\partial y} + \frac{\partial w}{\partial z}\right) + \eta\left(\frac{\partial u}{\partial x} + \frac{\partial v}{\partial y} + \frac{\partial w}{\partial z}\right)^2 \\ & + \mu\left[2\left(\frac{\partial u}{\partial x}\right)^2 + 2\left(\frac{\partial v}{\partial y}\right)^2 + 2\left(\frac{\partial w}{\partial z}\right)^2 + \left(\frac{\partial u}{\partial y} + \frac{\partial v}{\partial x}\right)^2 + \left(\frac{\partial u}{\partial z} + \frac{\partial w}{\partial x}\right)^2 \right. \\ & \left. + \left(\frac{\partial v}{\partial z} + \frac{\partial w}{\partial y}\right)^2\right]\end{aligned} \tag{2.30}$$

Equation (2.30) is the energy equation in terms of the flow field variables. The conservation form of the energy equation (2.30), written in terms of the internal energy is

$$\frac{\partial(\rho E)}{\partial t} + \nabla \cdot (\rho E \boldsymbol{v}) = \rho\dot{q} + \frac{\partial}{\partial x}\left(k\frac{\partial T}{\partial x}\right) + \frac{\partial}{\partial y}\left(k\frac{\partial T}{\partial y}\right) + \frac{\partial}{\partial z}\left(k\frac{\partial T}{\partial z}\right) - p\left(\frac{\partial u}{\partial x} + \frac{\partial v}{\partial y} + \frac{\partial w}{\partial z}\right) + \eta\left(\frac{\partial u}{\partial x} + \frac{\partial v}{\partial y} + \frac{\partial w}{\partial z}\right)^2 + \mu\left[2\left(\frac{\partial u}{\partial x}\right)^2 + 2\left(\frac{\partial v}{\partial y}\right)^2 + 2\left(\frac{\partial w}{\partial z}\right)^2 + \left(\frac{\partial u}{\partial y} + \frac{\partial v}{\partial x}\right)^2 + \left(\frac{\partial u}{\partial z} + \frac{\partial w}{\partial x}\right)^2 + \left(\frac{\partial v}{\partial z} + \frac{\partial w}{\partial y}\right)^2\right] \quad (2.31)$$

In this chapter we have derived the important equations that derive fluid dynamics. These equations will now be applied in the next chapters.

CHAPTER THREE

UNSTEADY FLOW OF A REACTIVE VARIABLE VISCOSITY NON-NEWTONIAN FLUID THROUGH A POROUS SATURATED MEDIUM WITH ASYMMETRIC CONVECTIVE BOUNDARY CONDITIONS

In this chapter we examine the thermal effects in an unsteady flow of a pressure driven, reactive, variable viscosity, third grade fluid through a porous saturated medium with asymmetrical convective boundary conditions. We assume that exothermic chemical reactions take place within the flow system and that the asymmetric convective heat exchange with the ambient at the surfaces follows Newton's law of cooling. The coupled nonlinear partial differential equations governing the problem are derived and solved numerically using a semi-implicit finite difference scheme. Graphical results will be presented and discussed qualitatively and quantitatively with respect to various parameters embedded in the problem.

3.1. Introduction

Flow of reactive fluids in porous media not only presents a theoretically challenging problem but also finds a wide range of technological and engineering applications [13]. This type of flow system can be, for example, found in packed bed chemical reactors, geothermal reservoirs, petroleum reservoirs, material processing industries, automobile exhaust systems, etc. Moreover, there are manifestations of fluid behaviour which cannot be adequately explained on the basis of the classical, linearly viscous model [105]. Geological materials, liquid foams, polymeric fluids, slurries, drilling mud, clay coatings, elastomers, many emulsions, hydrocarbon oils, grease, and food products are among the many substances which are capable of flowing but which exhibit flow characteristics that cannot be adequately described by the classical linearly viscous fluid model. In order to describe some of the departures from Newtonian behaviour evidenced by such materials, a number of idealized models have been suggested. Amongst these are fluids of the differential type of third grade [33, 88]. Meanwhile, the evaluation of thermal effects of a reactive non-Newtonian fluid in a porous medium is extremely important in order to ensure safety of life and property during handling and processing of such fluids [36, 100]. Al-Hadhrami *et al* [3] studied the thermal effects of steady flow of a Newtonian fluid in porous media across a range of permeability values. The pioneering papers by Aziz [8] and Makinde and Aziz [66] and the references therein introduced the idea of using the

convective boundary conditions in boundary layer flows. We adopt such boundary conditions in the current work. Makinde [55, 62] investigated the thermal effects of a reactive viscous flow through a channel filled with porous medium and with isothermal walls. Several studies involving heat and mass transfer in non-Newtonian third-grade fluids have been conducted [75, 94, 113], but most of these studies seem to lack a systematic and rational treatment of the thermodynamics of the problem with respect to the combined effects of porous media, unsteadiness, variable viscosity and asymmetric convective boundary conditions on the flow system.

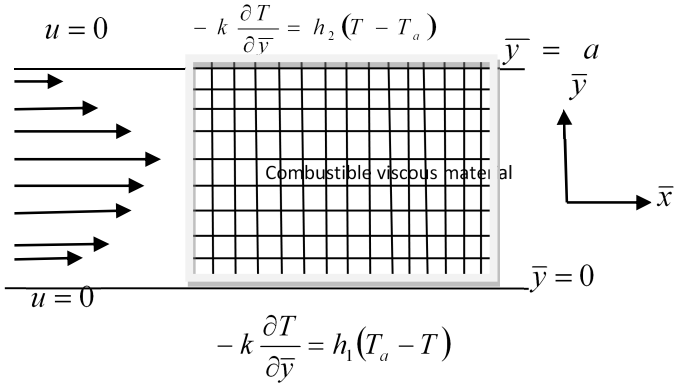

Figure 3.1: Geometry of the problem.

The objective of the present work is to study the unsteady flow of a reactive variable viscosity third-grade fluid between two parallel plates filled with a porous medium. Both the lower and upper walls of the channel are subjected to asymmetric convective heat exchange with the ambient. The mathematical formulation of the problem is established in section 3.2. In section 3.3 Graphical results are presented and discussed qualitatively and quantitatively with respect to various parameters in the system.

3.2. The mathematical model

Consider an unsteady flow of an incompressible, third-grade, variable viscosity, reactive fluid through a channel filled with a homogeneous and isotropic porous medium as illustrated in Figure 3.1. It is assumed that the plate surfaces are subjected to asymmetric convective heat exchange with the ambient due to unequal heat transfer coefficients and the fluid motion is induced by an applied axial pressure gradient. We choose the $\bar{x}$-axis parallel to the channel and the $\bar{y}$-axis normal to it.

Following [3, 13, 33, 36, 88, 100, 105], and the derivations in chapter 2, and neglecting the reacting viscous fluid consumption, the governing equations for the momentum and heat balance can be written as

$$\rho \frac{\partial u}{\partial \bar{t}} = -\frac{\partial \bar{P}}{\partial \bar{x}} + \frac{\partial}{\partial \bar{y}}\left[\bar{\mu}(T)\frac{\partial u}{\partial \bar{y}}\right] + \alpha_1 \frac{\partial^3 u}{\partial \bar{y}^2 \partial \bar{t}} + 6\beta_3 \frac{\partial^2 u}{\partial \bar{y}^2}\left(\frac{\partial u}{\partial \bar{y}}\right)^2 - \frac{\bar{\mu}(T)u}{\rho K} \tag{3.1}$$

$$\rho c_p \frac{\partial T}{\partial \bar{t}} = k\frac{\partial^2 T}{\partial \bar{y}^2} + \left(\frac{\partial u}{\partial \bar{y}}\right)^2\left(\bar{\mu}(T) + 2\beta_3\left(\frac{\partial u}{\partial \bar{y}}\right)^2\right) + \frac{\bar{\mu}(T)u^2}{K} + QC_0A\left(\frac{hT}{\nu l}\right)^m e^{-\frac{E}{RT}}. \tag{3.2}$$

The additional viscous dissipation term in equation (3.2) is due to [3] and is valid in the limit of very small and very large porous medium permeability. The appropriate initial and boundary conditions are

$$u(\bar{y}, 0) = 0, \quad T(\bar{y}, 0) = T_0, \tag{3.3}$$

$$u(0, \bar{t}) = 0, \quad -k\frac{\partial T}{\partial \bar{y}}(0, \bar{t}) = h_1[T_a - T(0, \bar{t})], \tag{3.4}$$

$$u(a, \bar{t}) = 0, \quad -k\frac{\partial T}{\partial \bar{y}}(a, \bar{t}) = h_2[T(a, \bar{t}) - T_a]. \tag{3.5}$$

T is the absolute temperature, ρ is the density, c_p is the specific heat at constant pressure, $\bar{t}$ is the time, h_1 is the heat transfer coefficient at the lower plate, h_2 is the heat transfer coefficient at the upper plate, T_0 is the fluid initial temperature, T_a is the ambient temperature, k is the thermal conductivity of the material, Q is the heat of reaction, A is the rate constant, E is the activation energy, R is the universal gas constant, C_0 is the initial concentration of the reactant species, a is the channel width, l is Planck's number, h is Boltzmann's constant, ν is the vibration frequency, K is the porous medium permeability, α_1 and β_3 are the material coefficients, $\bar{P}$ is the modified pressure, and m is the numerical exponent such that $m \in \{-2, 0, 0.5\}$, where the three values represent numerical exponents for sensitized, Arrhenius and bimolecular kinetics respectively (see [36, 55, 62]).

The temperature dependent viscosity ($\bar{\mu}$) can be expressed as

$$\bar{\mu}(T) = \mu_0 e^{-b(T-T_0)}, \tag{3.6}$$

as referred to in chapter 1, where b is a viscosity variation parameter and μ_0 is the initial fluid dynamic viscosity at temperature T_0. We introduce the following dimensionless variables into equations (3.1) to (3.6);

$$y = \frac{\bar{y}}{a},\ \alpha = \frac{bRT_0^2}{E},\ w = \frac{u\rho a}{\mu_0},\qquad \theta = \frac{E(T-T_0)}{RT_0^2},\qquad \theta_a = \frac{E(T_a-T_0)}{RT_0^2},$$

$$\gamma = \frac{\beta_3\mu_0}{\rho^2 a^4},\ \delta = \frac{\alpha_1}{\rho a^2},\qquad Bi_1 = \frac{h_1 a}{k},\qquad Bi_2 = \frac{h_2 a}{k},\ Da = \frac{K}{a^2},\qquad Pr = \frac{\mu_0 c_p}{k},$$

$$\varepsilon = \frac{RT_0}{E},\ x = \frac{\bar{x}}{a},\qquad P = \frac{\bar{P}\rho a^2}{\mu_0^2},\qquad G = -\frac{\partial \bar{P}}{\partial \bar{x}},\ S^2 = \frac{1}{Da},\qquad t = \frac{\bar{t}\mu_0}{\rho a^2},$$

$$\mu = \frac{\bar{\mu}}{\mu_0},\qquad \lambda = \left(\frac{hT_0}{vl}\right)^m \frac{QEAa^2C_0 e^{-\frac{E}{RT}}}{T_0^2 Rk},\qquad \Omega = \left(\frac{vl}{hT_0}\right)^m \frac{\mu_0^3 e^{\frac{E}{RT}}}{\rho^2 QAa^4 C_0} \tag{3.7}$$

and obtain the following dimensionless governing equations:

$$\frac{\partial w}{\partial t} = G - S^2 we^{-\alpha\theta} + e^{-\alpha\theta}\frac{\partial^2 w}{\partial y^2} - \alpha e^{-\alpha\theta}\frac{\partial\theta}{\partial y}\frac{\partial w}{\partial y} + \delta\frac{\partial^3 w}{\partial y^2 \partial t} + 6\gamma\frac{\partial^2 w}{\partial y^2}\left(\frac{\partial w}{\partial y}\right)^2, \tag{3.8}$$

$$Pr\frac{\partial\theta}{\partial t} = \frac{\partial^2\theta}{\partial y^2} + \lambda\left\{(1+\varepsilon\theta)^m exp\left(\frac{\theta}{1+\varepsilon\theta}\right) + \Omega\left[S^2 w^2 e^{-\alpha\theta} + \left(\frac{\partial w}{\partial y}\right)^2\left(e^{-\alpha\theta} + 2\gamma\left(\frac{\partial w}{\partial y}\right)^2\right)\right]\right\}, \tag{3.9}$$

$$w(y,0) = 0,\ \ \theta(y,0) = 0, \tag{3.10}$$

$$w(0,t) = 0,\quad \frac{\partial\theta}{\partial y}(0,t) = -Bi_1[\theta_a - \theta(0,t)], \tag{3.11}$$

$$w(1,t) = 0,\quad \frac{\partial\theta}{\partial y}(1,t) = -Bi_2[\theta(1,t) - \theta_a], \tag{3.12}$$

where λ represent the Frank-Kamenetskii parameter, Pr is the Prandtl number, Bi is the Biot number, ε is the activation energy parameter, δ is the material parameter, γ is the non-Newtonian parameter, G is the pressure gradient parameter, Da is the Darcy number, α is the variable viscosity parameter, Ω is the viscous heating parameter, θ_a is the ambient temperature parameter, and S is the porous medium shape parameter.

The other dimensionless quantities of interest are the skin friction (C_f) and the wall heat transfer rate (Nu) given as

$$C_f = -\frac{dw}{dy}(1,t),\quad Nu = -\frac{d\theta}{dy}(1,t). \tag{3.13}$$

In the following section, equations (3.8) to (3.13) are solved numerically using a semi-implicit finite difference scheme.

3.3. Numerical solution

Our numerical algorithm is based on the semi-implicit finite difference scheme [21 - 23, 67, 68]. Implicit terms are taken at the intermediate time level $(N+\xi)$ where $0 \le \xi \le 1$. The discretization of the governing equations is based on a linear Cartesian mesh and uniform grid on which finite differences are taken. We approximate both the second and first spatial derivatives with second-order central differences. The equations corresponding to the first and last grid points are modified to incorporate the boundary conditions. The semi-implicit scheme for the velocity component is

$$\frac{\partial}{\partial t}\left(w-\delta\frac{\partial^2 w}{\partial y^2}\right)=G-S^2e^{-\alpha\theta^{(N)}}w^{(N+\xi)}+e^{-\alpha\theta^{(N)}}\frac{\partial^2}{\partial y^2}w^{(N+\xi)}$$

$$-\left[\alpha e^{-\alpha\theta}\frac{\partial\theta}{\partial y}\frac{\partial w}{\partial y}\right]^{(N)}+6\gamma\left(\frac{\partial}{\partial y}w^{(N)}\right)^2\frac{\partial^2}{\partial y^2}w^{(N+\xi)} \qquad (3.14)$$

In equation (3.14), it is understood that $\partial\,\#/\partial t \coloneqq \left(\#^{(N+1)}-\#^{(N)}\right)/\Delta t$. The equation for $w^{(N+1)}$ then becomes

$$-r_1w_{j-1}^{(N+1)}+r_2w_{j-1}^{(N+1)}-r_1w_{j+1}^{(N+1)}=\text{ explicit terms}, \qquad (3.15)$$

where $r_1=\frac{1}{\Delta y^2}\left[\delta+\xi\Delta t(\mu+6\gamma\dot{\gamma}^2)^{(N)}\right]$, $r_2=\left(1+\xi\Delta tS^2\mu^{(N)}+2r_1\right)$, with

$\mu=\exp(-\alpha\theta)$ and $\dot{\gamma}=w_y$. The solution procedure for $w^{(N+1)}$ thus reduces to inversion of tri-diagonal matrices, which is an advantage over a full implicit scheme. The semi-implicit integration scheme for the temperature equation is similar to that for the velocity component. Unmixed second partial derivatives of the temperature are treated implicitly:

$$Pr\frac{\theta^{(N+1)}-\theta^{(N)}}{\Delta t}=\frac{\partial^2}{\partial y^2}\theta^{(N+\xi)}+\lambda\left\{\left[(1+\varepsilon\theta)^m exp\left(\frac{\theta}{1+\varepsilon\theta}\right)\right]^{(N)}+\Omega\left[S^2w^2e^{-\alpha\theta}+\dot{\gamma}^2\left(e^{-\alpha\theta}+2\gamma\dot{\gamma}^2\right)\right]^{(N)}\right\}. \qquad (3.16)$$

The equation for $\theta^{(N+1)}$ thus becomes

$$-r\theta_{j-1}^{(N+1)}+(\mathrm{Pr}+2r)\theta_j^{(N+1)}-r\theta_{j+1}^{(N+1)}=\ \text{explicit terms,} \tag{3.17}$$

where $r=\xi\Delta t/\Delta y^2$. The solution procedure again reduces to inversion of tri-diagonal matrices. The schemes (3.15) and (3.17) were checked for consistency. For $\xi=1$, these are first order accurate in time but second-order accurate in space. The schemes in [21] have $\xi=\frac{1}{2}$ which improves the accuracy in time to second order. Following the work in [22, 23] we use $\xi=1$ so that the choice of larger time steps is possible and still obtain convergence to the steady solutions.

3.4. Results and discussion

Unless otherwise stated, we employ the parameter values:
$G=1,\mathrm{Pr}=10,\theta_a=0.1,\delta=0.1,\lambda=0.1,Bi_1=1,Bi_2=1,m=0.5,\varepsilon=0.1,\alpha=0.1,\Omega=0.1,\gamma=0.1,S=1,$
$\Delta y=0.02,\Delta t=0.01$ and $t=40.$ These will be the default values in this work and hence in any graph where any of these parameters is not explicitly mentioned, it will be understood that such parameters take on the default values.

3.4.1. Transient and steady state flow profiles

We display the transient solutions in Figure 3.2. The figures show a transient increase in both fluid velocity, Figure 3.2(a), and temperature, Figure 3.2(b), until a steady state is reached.

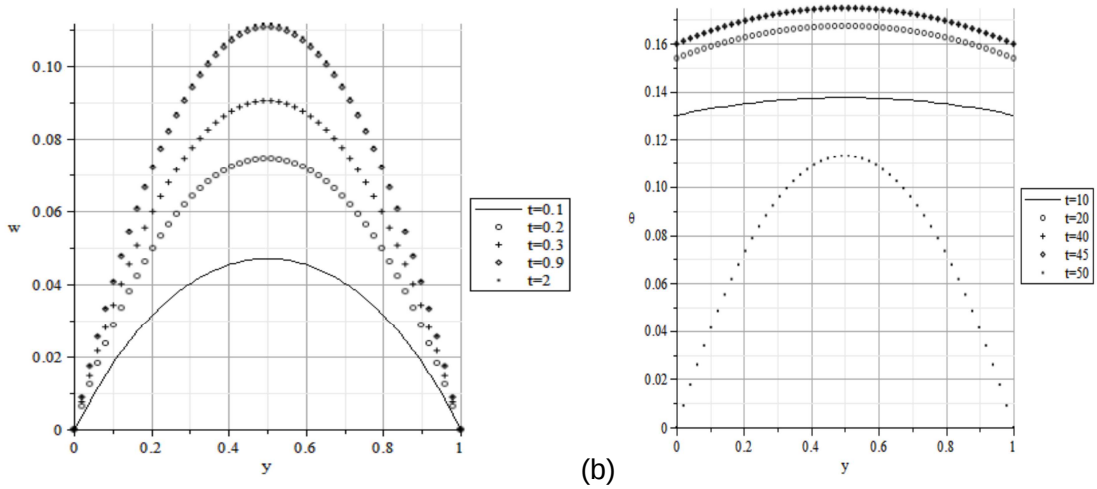

(a) (b)

Figure 3.2: Transient and steady state profiles.

3.4.1.1. Blow-up of solutions

We need to point out early on that depending on certain parameter values in the problem, the steady temperature and velocity profiles such as those in Figure 3.2 may not be attainable. In particular, the reaction parameter λ will need to be carefully controlled as "large" values can easily lead to blow-up of solutions as illustrated in Figure 3.3.

As shown in Figure 3.3, larger values of λ would lead to finite time temperature blow-up since the terms associated with λ are strong heat sources.

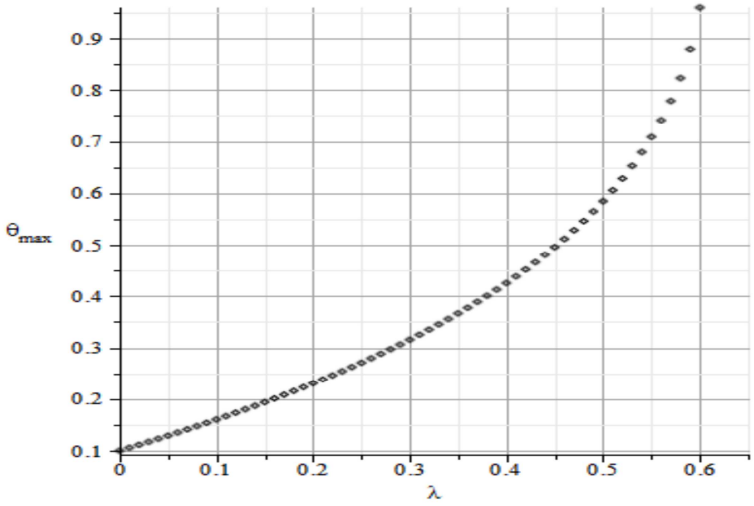

Figure 3.3: Blow-up of the fluid temperature for large λ.

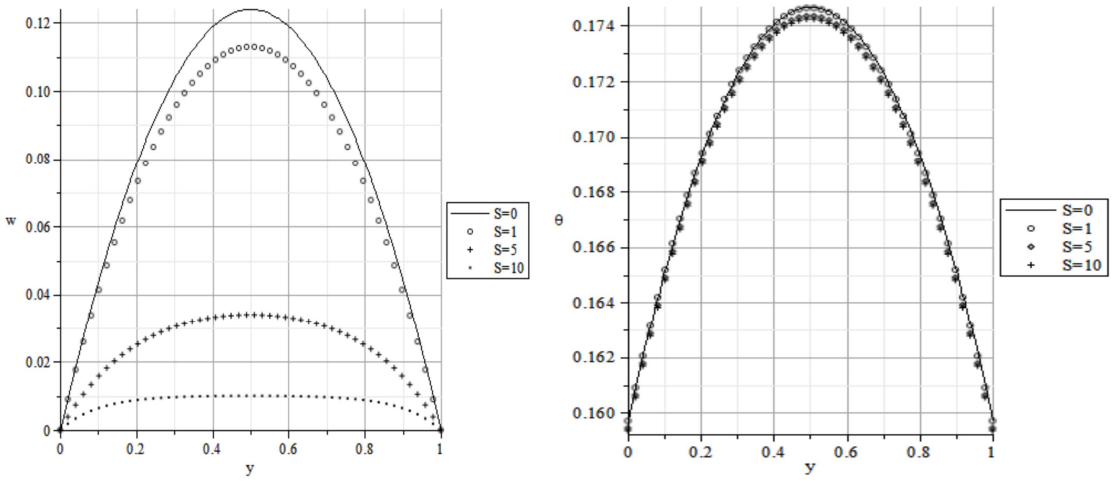

(a) (b)

Figure 3.4: Effects of the porous medium parameter, S

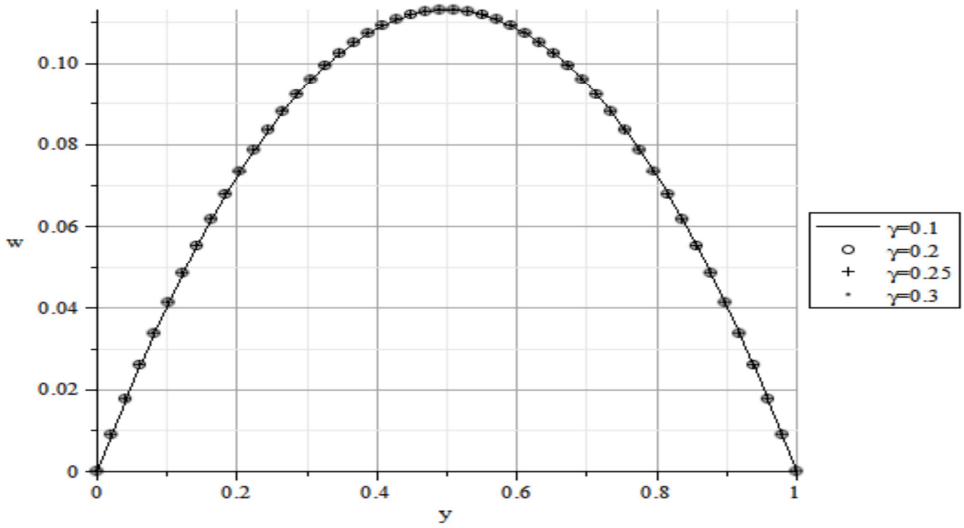

Figure 3.5: Effects of the non-Newtonian parameter (γ) on velocity.

3.4.2. The parameter dependence of solutions

The response of the velocity and temperature to varying values of the porous medium parameter (S) is illustrated in Figure 3.4. An increase in the porous medium parameter S leads to corresponding increases in damping properties in the flow due to reduced porosity. This results in increased resistance to flow and thus explains the reduction in fluid velocity with increasing porous medium parameter as shown in Figure 3.4 (a). The reduced velocity in turn decreases the viscous heating source terms in the temperature equation and hence correspondingly decreases the fluid temperature as shown in Figure 3.4 (b).

The response of the velocity to varying values of the non-Newtonian parameter (γ) is illustrated in Figure 3.5. An increase in the parameter γ leads to corresponding increases in those non-Newtonian properties of the fluid, say (visco)elasticity, that would result in increased resistance to flow and thus explain the slight reduction in fluid velocity with increasing non-Newtonian character as measured by the parameter γ; see Figure 3.5. The reduced velocity in turn decreases the viscous heating source terms in the temperature equation and hence correspondingly decreases the fluid temperature. Since however the parameter γ only enters the temperature equation implicitly through the velocity field, the effects of γ on the fluid temperature are not as noticeable as those on the fluid velocity.

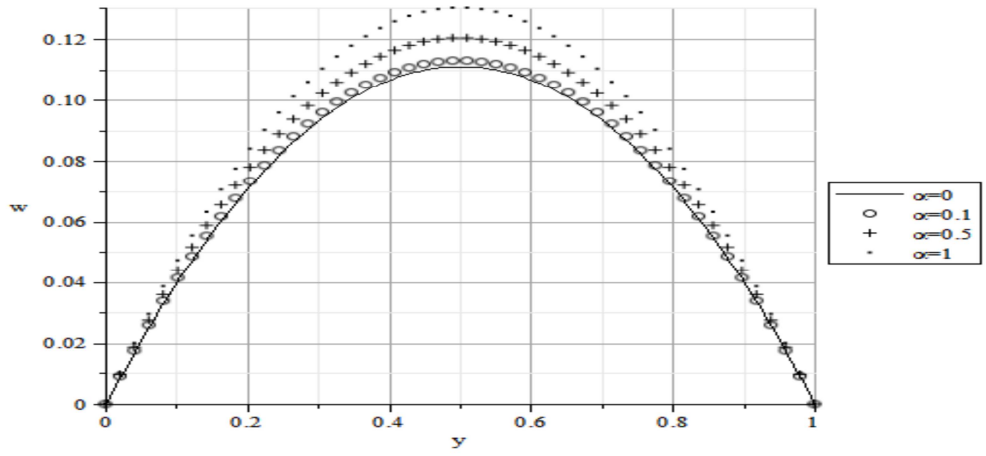

Figure 3.6: Effects of the variable viscosity parameter (α) on the velocity.

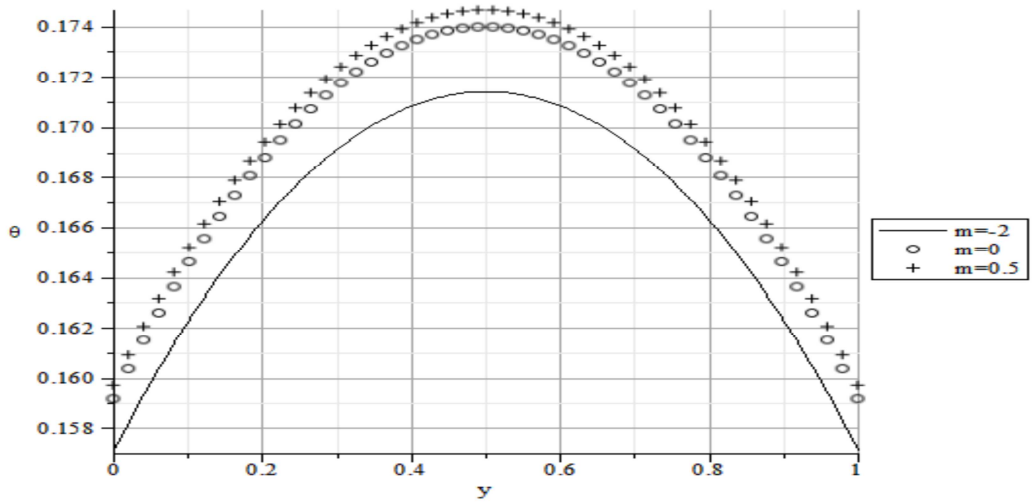

Figure 3.7: Effects of the parameter m on the temperature.

The influence of the variable viscosity parameter on the velocity profile is shown in Figure 3.6. Increasing the parameter α reduces the fluid viscosity and hence correspondingly diminishes the fluid's resistance to flow. This necessarily leads to increased fluid velocity as illustrated in Figure 3.6. The increased velocity in turn increases the viscous heating source terms in the temperature equation and hence correspondingly increases the fluid temperature. However, as with the non-Newtonian parameter, the viscous effects are more pronounced in the velocity equation than in the temperature equation and this explains why the effects of α on the fluid temperature are not as noticeable as in the fluid velocity.

The effects of the chemical kinetics exponent m on the temperature profile are shown in Figure 3.7. Figure 3.7 shows that the internal heat generated in the fluid during a bimolecular type of exothermic chemical reaction ($m = 0.5$) is higher than that generated under reaction of either the Arrhenius ($m = 0$) or the sensitized ($m = -2$) type. This is so since an increase in the parameter m leads to corresponding increases in the strengths of the chemical reaction source terms in the temperature equation. This leads to increased fluid temperatures as shown in Figure 3.7. The increased temperature in turn leads to a reduction in fluid viscosity and hence indirectly to increased fluid velocity. Since however the parameter m only enters the velocity equation implicitly through the temperature/viscosity coupling, the effects of m on the fluid velocity look at best marginal and are not as pronounced as on the fluid temperature. The effects of the activation energy parameter ε on the temperature profile are shown in Figure 3.8. The parameter ε plays a more-or-less similar role (both mathematically and physically) to the parameter m described earlier in Figure 3.7 and hence its effects are similarly explained.

The graphs of Figure 3.8 correspond to the case of bimolecular reactions ($m = 0.5$). It should however be noted that in the cases sensitized and Arrhenius reactions (in which $m \le 0$) both temperature and velocity are expected to decrease with increasing ε; see Figure 3.9(a) and (b). This is due to the fact that the function

$$(1+\varepsilon\theta)^m \exp\left(\frac{\theta}{1+\varepsilon\theta}\right), m \le 0$$

decreases as ε increases. Since this function represents source terms in the temperature equation, the fluid temperature, as expected, decreases with increasing ε, so the maximum temperature is recorded for $\varepsilon = 0$ as shown in Figure 3.9(a) and (b).

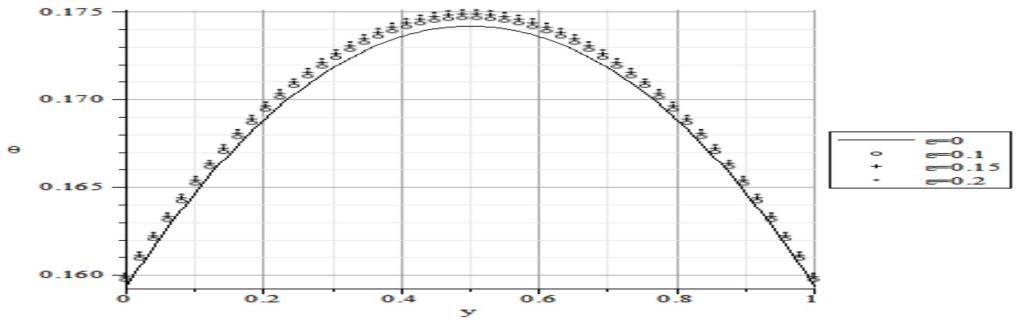

Figure 3.8: Effects of the activation energy parameter (ε) on the temperature.

(a) (b)

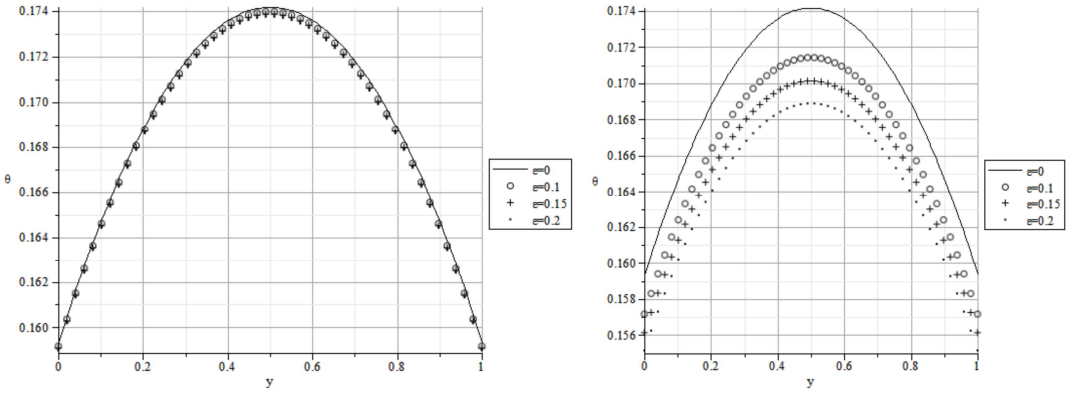

Figure 3.9: Effects of the activation energy parameter (ε) on temperature, for $m = 0$ and $m = -2$.

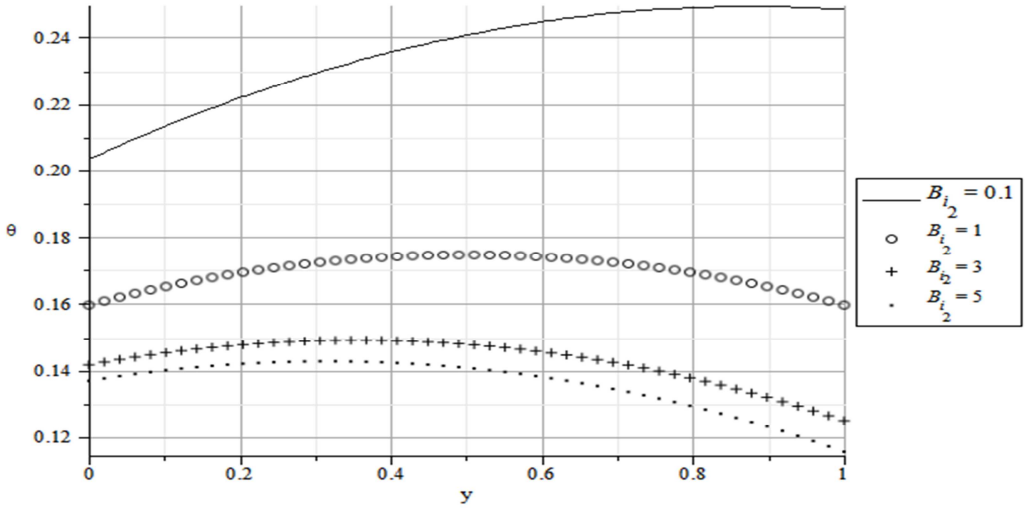

Figure 3.10: Effects of the Biot number (Bi_2) on the temperature.

The effects of the Biot number Bi_2 on the temperature profile are illustrated in Figure 3.10. As seen from the boundary condition (3.12), higher Biot numbers mean correspondingly higher degrees of convective cooling at the channel walls and hence lead to lower temperatures at the channel walls and also in the bulk fluid. The overall temperature profiles thus decrease with increasing Biot number as the bulk fluid continually adjusts to the lower wall temperatures. The reduced temperatures correspondingly decrease the fluid viscosity and hence also marginally decrease the fluid velocity through the viscosity coupling. As noted earlier, such a coupling

depending on other parameters as well (say α) does not necessarily result in drastic changes in velocity profiles even though the temperature profiles show well pronounced changes.

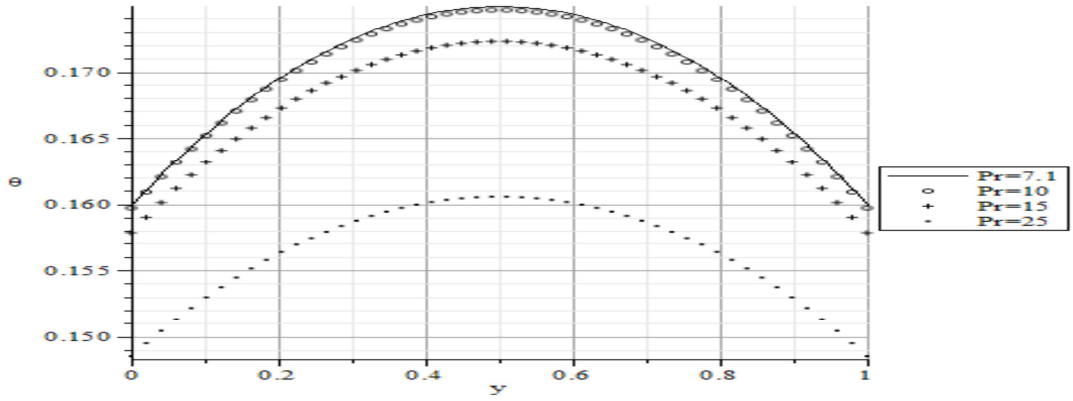

Figure 3.11: Effects of the Prandtl number (Pr) on the temperature.

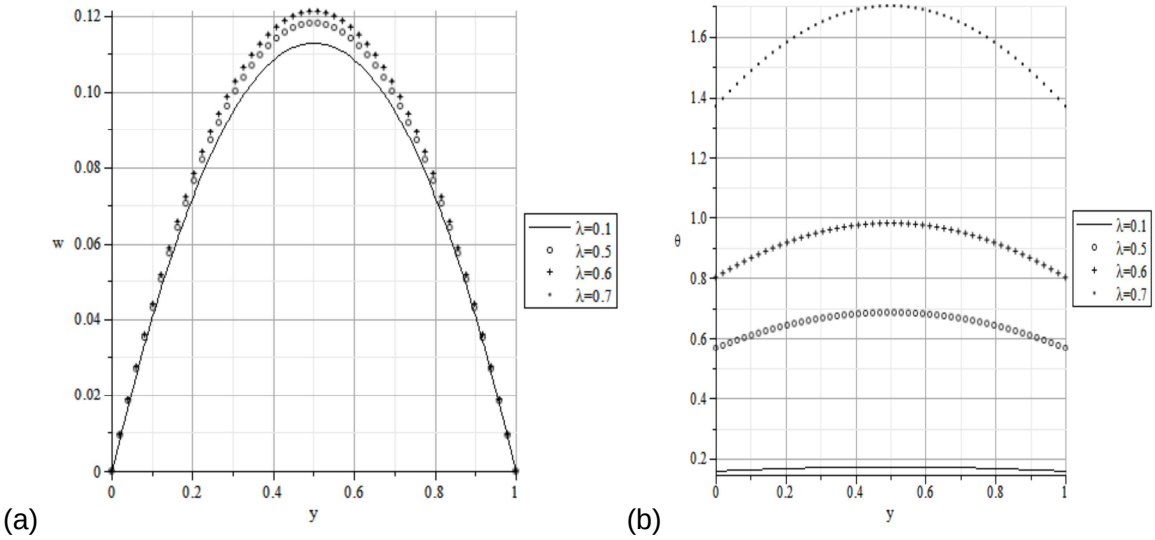

(a) (b)

Figure 3.12: Effects of the reaction parameter, λ .

The effects of the Prandtl number Pr on the temperature profile are illustrated in Figure 3.11. Larger values of the Prandtl number correspondingly decrease the strength of the source terms in the temperature equation and hence in turn reduce the overall fluid temperature, as clearly illustrated in Figure 3.11. As pointed out earlier, the reduced temperature results in decreased fluid viscosity and hence (implicitly) reduces the fluid velocity. The effects of the Prandtl number on the velocity are however, as expected and previously explained, quite marginal.

The effects of the reaction parameter λ on the velocity and temperature profiles are illustrated in Figure 3.12. The reaction parameter λ plays a roughly opposite role to the Prandtl number just described. Increased values of λ lead to significant increases in the reaction and viscous heating source terms and hence significantly increase the fluid temperature as shown in Figure 3.12 (b) and also in the blow-up Figure 3.3. The significant temperature rise in response to the increased λ means that the viscosity coupling to the velocity is no longer weak and hence significant reductions in the viscosity lead to appreciable increases in the fluid velocity, as shown in Figure 3.12(a).

The effects of the viscous heating parameter Ω on the temperature profile are illustrated in Figure 3.13. The effects of Ω mirror those of λ, albeit on a smaller scale since Ω is not connected to the exponentially increasing reaction source terms but only to the viscous heating terms. The wall shear stress dependence on the reaction parameter λ is illustrated in Figure 3.14 (a) for varying values of the viscosity variation parameter α. Similarly, the wall heat transfer rate dependence on λ is illustrated in Figure 3.14 (b) for varying values of α. Figure 3.15 (a) shows the wall shear stress dependence on λ for varying values of the non-Newtonian parameter γ and similarly, Figure 3.15 (b) shows the wall shear stress dependence on λ for varying values of the porous medium parameter S. In general, parameters that decrease the fluid velocity correspondingly decrease the wall shear stress. On the other hand parameters that increase the fluid velocity also increase the wall shear stress.

Both the wall heat transfer dependence on λ for varying values of the non-Newtonian parameter γ and the wall heat transfer dependence on λ for varying values of the porous medium parameter S are similar to the behaviour illustrated in Figure 3.14 (b). As with the wall shear stress, parameters that decrease the fluid temperature correspondingly decrease the wall heat transfer. Those that increase the fluid temperature also increase the wall heat transfer rate. In fact, since both the parameters α and γ only marginally increase the temperature, their effects on the wall heat transfer are also similarly marginal. All the results for the wall shear stress and the wall heat transfer were obtained at time $t = 5$.

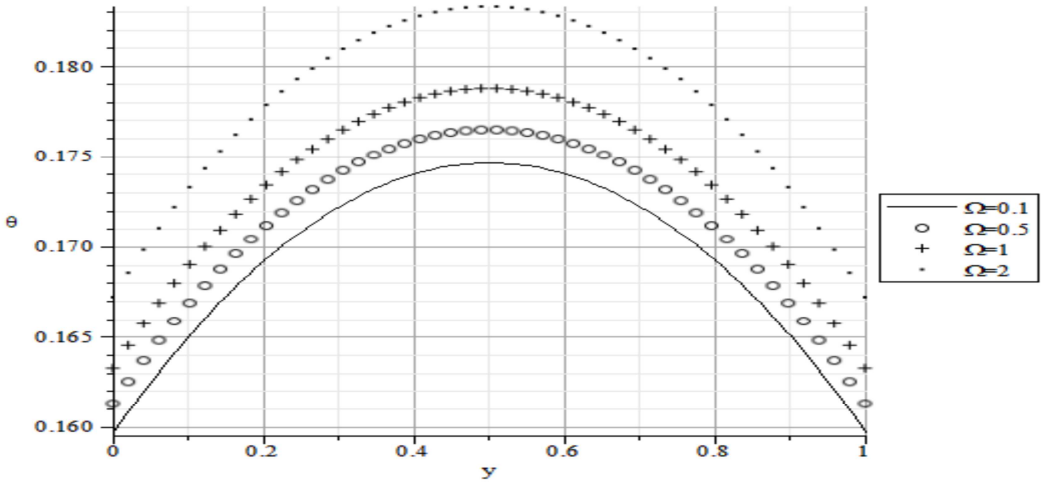

Figure 3.13: Effects of the viscous heating parameter (Ω) on the temperature.

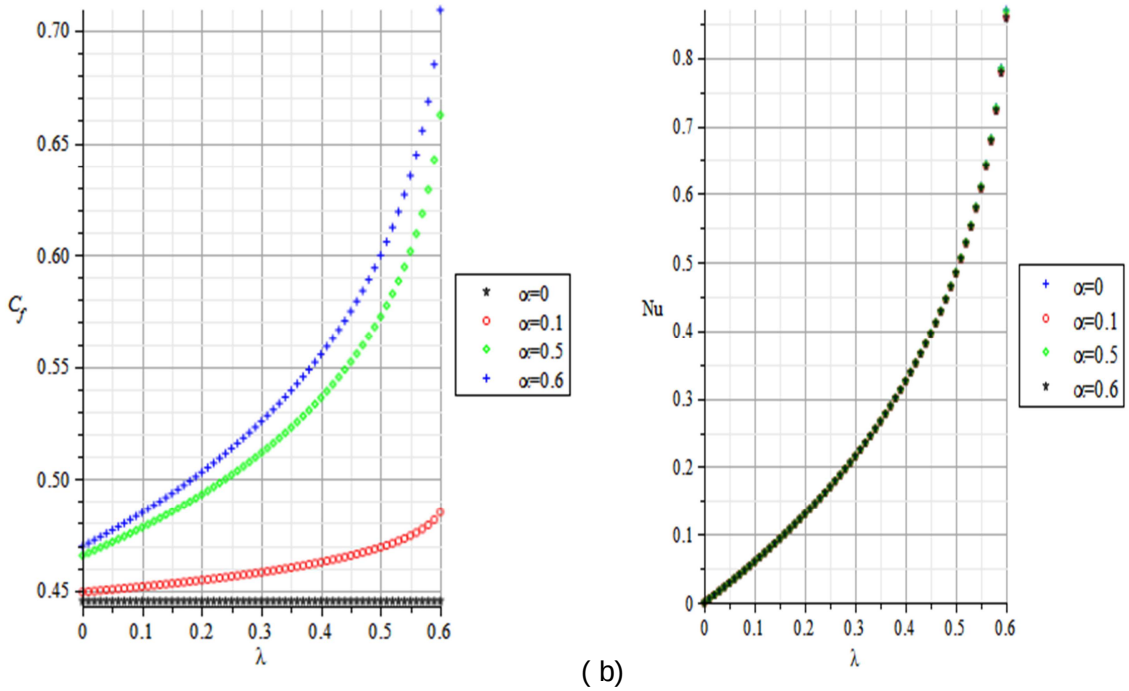

(a) (b)

Figure 3.14: Variation, with λ and α, of (a) the wall shear stress and (b) the wall heat transfer rate.

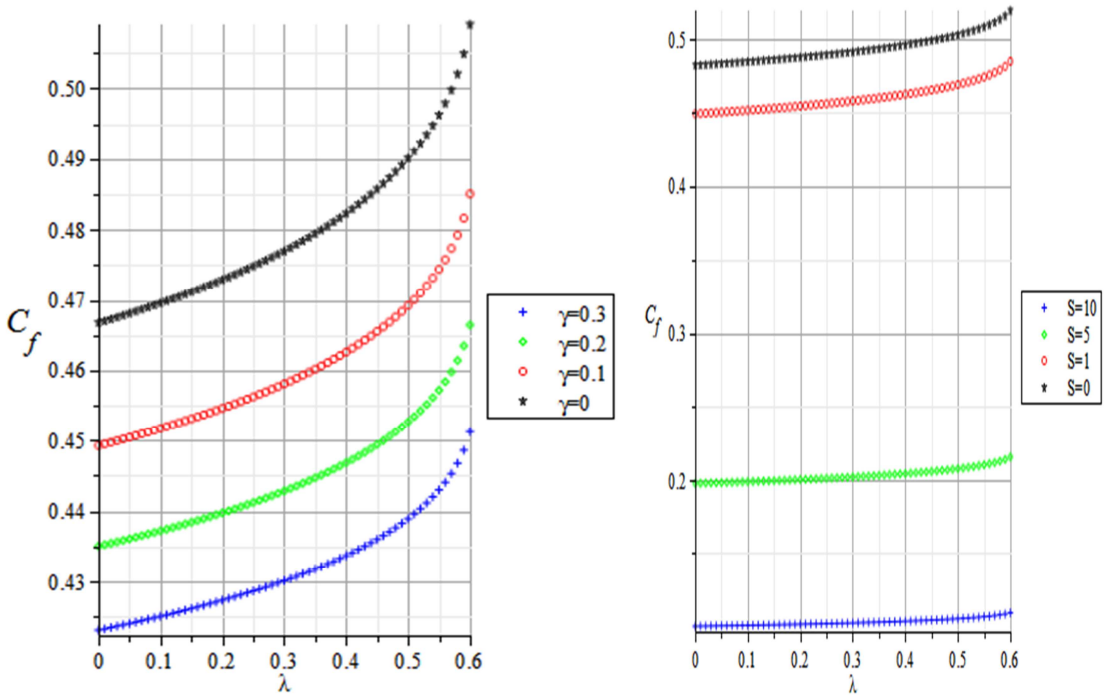

(a) (b)

Figure 3.15: Variation of the wall shear stress with (a) λ and γ and (b) with λ and S .

3.5. Conclusion

We computationally investigated the transient flow of a reactive variable viscosity non-Newtonian fluid through a porous saturated medium with asymmetric convective cooling. We observed that there is a transient increase in both fluid velocity and temperature with an increase in the reaction strength, viscous heating and fluid viscosity parameter (which decreases the viscosity). A transient decrease in both fluid velocity and temperature is observed with increase in the non-Newtonian character and porous medium parameter (which decreases the porosity in the flow). The possible finite time blow-up of solutions means that the reaction strength needs to be carefully controlled. We also noticed that due to the nature of the coupling of the source terms, the fluid velocity and temperature either both increase or both decrease, together. Parameters that increase the fluid velocity and temperature would also increase the skin friction and the wall heat transfer rate respectively, and similarly those parameters that decrease the said field properties would correspondingly decrease the skin friction and the wall heat transfer rate respectively.

CHAPTER FOUR

EFFECTS OF SUCTION/INJECTION ON UNSTEADY REACTIVE VARIABLE VISCOSITY NON-NEWTONIAN FLUID FLOW IN A CHANNEL FILLED WITH POROUS MEDIUM AND CONVECTIVE BOUNDARY CONDITIONS

A study on thermal effects of the suction/injection Reynolds number, in conjunction with other flow parameters, on an unsteady reactive temperature dependent viscosity third grade fluid in a porous channel filled with saturated porous medium is presented. This is an extension of the problem in chapter 3. As in chapter 3, it is assumed that the channel walls are subjected to asymmetric convective heat exchange with the surrounding medium and that exothermic chemical reactions take place within the flow system. The heat exchange with the ambient at the surfaces is assumed to obey Newton's law of cooling. The equations governing the flow system are expressed in non-dimensional form and a semi-implicit finite difference scheme is utilised to obtain the velocity and temperature profiles. The effects of the flow parameters on the temperature and velocity fields, the skin friction and the wall heat transfer rate are simulated and discussed. The suction/injection Reynolds number is observed to retard the velocity field. It is also observed that the suction/injection Reynolds number, the porous medium parameter, the Prandtl number and the Biot number have a retarding effect on the temperature field. The variable viscosity parameter and the suction injection Reynolds number increases the skin fiction while the porous medium parameter and the Prandtl number diminish it. It is also revealed that the suction injection Reynolds number, the porous medium parameter and the Prandtl number have a diminishing effect on the rate of heat transfer at the channel walls.

4.1. Introduction

The flow of viscous fluids in channels with porous walls filled with or without porous media have been investigated and studied by several scholars, e.g.,[6, 24, 32, 64, 65, 70, 108] for various physical situations. In such flow systems, consideration of thermal effects and thermal stability criteria ought to be a major part of the analysis. Diverse applications are found in geothermal energy extraction, drying of food, nuclear waste disposal, heat and fluid exchange inside human organs, insulation of buildings, groundwater movement, oil and gas production, surface catalysis of chemical reactions, regenerative heat exchange and adsorption, etc. In some of these physical systems, the fluids involved belong to the wide class of non-Newtonian fluids owing to their failure in obeying the classical linear viscosity model. The heuristics and mathematical

computations underlying the rheology of such fluids, in particular fluids of the differential type, are cumbersome and complex as to evoke the interest of many scholars. In an incompressible fluid of differential type, apart from a constitutively indeterminate pressure, the stress is just a function of the velocity gradient and a number of its higher time derivatives [33].

Beg and Makinde [10] presented a theoretical analysis of a two-dimensional steady, laminar flow of an incompressible, viscous elastic fluid with species diffusion in a parallel plate channel with porous walls containing a homogeneous, isotropic porous medium with high permeability. The Runge-Kutta integration scheme with a modified version of the Newton-Raphson shooting method imbedded in the MAPLE software was used to numerically solve the transformed similarity of the ordinary differential equations governing the system. Makinde and Chinyoka [24, 70] analysed unsteady flow of a variable viscosity reactive fluid and heat transfer in a circular pipe with porous walls and in a slit with wall suction or injection respectively. Makinde and Ogulu [74] investigated the effects of thermal radiation on the heat and mass transfer flow of a variable viscosity fluid past a vertical porous plate permeated by a transverse magnetic field. Wang *et al* [108] conducted a theoretical investigation of the flow distribution and pressure drop in a channel with porous walls. Attia [6] studied the effect of suction and injection on the unsteady flow between parallel plates with variable viscosity and thermal conductivity. The effect of suction and injection on magnetohydrodynamic three dimensional couette flow and heat transfer through a porous medium was studied by Das [26].

In this study we seek to conduct an in-depth succinct analysis whereby we outline longitudinal velocity and temperature profiles of an unsteady reactive temperature dependent viscosity third grade fluid flow between two permeable parallel plates filled with a saturated porous medium. The dependence of the velocity and temperature fields, the skin friction and the Nusselt number on the many flow parameters, in particular the suction/injection Reynolds number, is extensively analysed. The ultimate aim is to characterise thermal effects and thermal stability criteria of the flow regime as dictated by the underlying parameters. Such detailed thermodynamics investigation has far reaching implications on safety in the industries dealing with flow systems of this nature.

The organisation of the rest of the chapter is as follows: The physical problem is presented and formulated mathematically in section 4.2. The solution process, a semi-implicit finite difference scheme based on [21, 23], is implemented in section 4.3. Section 4.4 comprises of the simulations of the velocity and temperature profiles together with the discussion of the results.

4.2. Mathematical formulation

We examine an unsteady flow of an incompressible variable viscosity, reactive non-Newtonian fluid through a channel filled with a homogeneous and isotropic porous medium. It is assumed that the channel walls are uniformly porous such that fluid injection and suction take place at the lower and upper walls respectively as illustrated in Figure 4.1. The plate surfaces are also subjected to asymmetric convective heat exchange with the ambient due to unequal heat transfer coefficients and the fluid motion is induced by an applied axial pressure gradient. We choose the $\bar{x}$ -axis parallel to the channel and the $\bar{y}$ -axis normal to it.

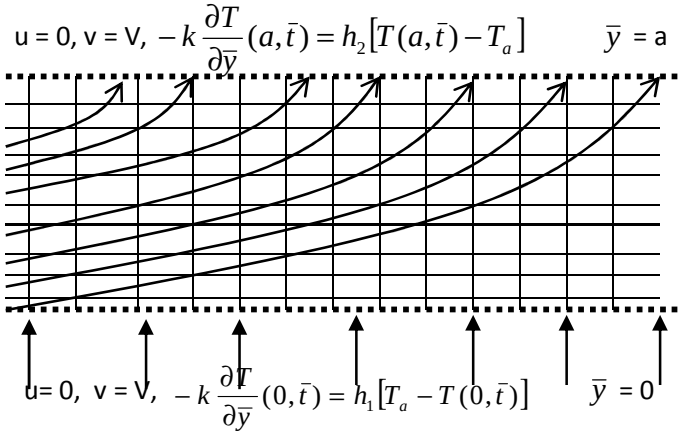

Figure 4.1. **Schematic diagram of the problem**.

Following [3, 13, 33, 36, 88, 100, 105] and neglecting the reacting viscous fluid consumption, the governing equations for the momentum and heat balance can be written as;

$$\rho\left(\frac{\partial u}{\partial \bar{t}} + V\frac{\partial u}{\partial \bar{y}}\right) = \frac{\partial \bar{P}}{\partial \bar{x}} + \frac{\partial}{\partial \bar{y}}\left[\bar{\mu}(T)\frac{\partial u}{\partial \bar{y}}\right] + \alpha_1\frac{\partial^3 u}{\partial \bar{y}^2\partial \bar{t}} + 6\beta_3\frac{\partial^2 u}{\partial \bar{y}^2}\left(\frac{\partial u}{\partial \bar{y}}\right)^2 - \frac{\bar{\mu}(T)u}{\rho K}, \tag{4.1}$$

$$\rho c_p\left(\frac{\partial T}{\partial \bar{t}} + V\frac{\partial T}{\partial \bar{y}}\right) = k\frac{\partial^2 T}{\partial \bar{y}^2} + \left(\frac{\partial u}{\partial \bar{y}}\right)^2\left(\bar{\mu}(T) + 2\beta_3\left(\frac{\partial u}{\partial \bar{y}}\right)^2\right) + \frac{\bar{\mu}(T)u^2}{K} + QC_0A\left(\frac{hT}{\nu l}\right)^m e^{-\frac{E}{RT}}. \tag{4.2}$$

The additional viscous dissipation term in equation (4.2) is valid in the limit of very small and very large porous medium permeability. The appropriate initial and boundary conditions are

$$u(\bar{y},0) = 0, \qquad T(\bar{y},0) = T_0\ , \tag{4.3}$$

$$u(0,\bar{t}) = 0, \qquad -k\frac{\partial T}{\partial \bar{y}}(0,\bar{t}) = h_1\left[T_a - T(0,\bar{t})\right], \tag{4.4}$$

$$u(a,\bar{t}) = 0, \qquad -k\frac{\partial T}{\partial \bar{y}}(a,\bar{t}) = h_2\left[T(a,\bar{t}) - T_a\right]. \tag{4.5}$$

V is the suction/injection velocity. The other symbols and parameters are as defined in chapter 3. The temperature dependent viscosity $(\bar{\mu})$ is given by (3.6).

We introduce the dimensionless variables (3.7), together with

$$Re = \frac{V\alpha\rho}{\mu_0}$$

into equations (4.1) – (4.5) and obtain the following dimensionless governing equations:

$$\frac{\partial w}{\partial t} + \mathrm{Re}\frac{\partial w}{\partial y} = G - S^2 w e^{-\alpha\theta} + e^{-\alpha\theta}\frac{\partial^2 w}{\partial y^2} - \alpha e^{-\alpha\theta}\frac{\partial\theta}{\partial y}\frac{\partial w}{\partial y} + \delta\frac{\partial^3 w}{\partial y^2\partial t} + 6\gamma\frac{\partial^2 w}{\partial y^2}\left(\frac{\partial w}{\partial y}\right)^2, \tag{4.6}$$

$$\mathrm{Pr}\frac{\partial\theta}{\partial t} + \mathrm{Pr}\,\mathrm{Re}\frac{\partial\theta}{\partial y} = \frac{\partial^2\theta}{\partial y^2} + \lambda\left\{(1+\varepsilon\theta)^m \exp\left(\frac{\theta}{1+\varepsilon\theta}\right) + \Omega\left[S^2 w^2 e^{-\alpha\theta} + \left(\frac{\partial w}{\partial y}\right)^2\left(e^{-\alpha\theta} + 2\gamma\left(\frac{\partial w}{\partial y}\right)^2\right)\right]\right\} \tag{4.7}$$

$$w(y,0) = 0, \quad \theta(y,0) = 0, \tag{4.8}$$

$$w(0,t) = 0, \quad \frac{\partial\theta}{\partial y}(0,t) = -Bi_1\left[\theta_a - \theta(0,t)\right], \tag{4.9}$$

$$w(1,t) = 0, \quad \frac{\partial\theta}{\partial y}(1,t) = -Bi_2\left[\theta(1,t) - \theta_a\right], \tag{4.10}$$

where *Re* is the Suction /Injection Reynolds number and the other parameters are as defined in chapter 3.

The other dimensionless quantities of interest are the skin friction (C_f) and the wall heat transfer rate (Nu) given by (3.13).

In the following section, equations (4.6) – (4.10) together with equations (3.6) and (3.13) are solved numerically using a semi-implicit finite difference scheme.

4.3. Numerical procedure

We adopt the semi-implicit finite difference scheme given in [21, 23]. Implicit terms are taken at the intermediate time level $(N+\xi)$ where $0 \le \xi \le 1$. The discretization of the governing equations is based on a linear Cartesian mesh and uniform grid on which finite differences are taken. Both the second and first spatial derivatives are approximated by second-order central differences. The equations corresponding to the first and last grid points are modified to incorporate the boundary conditions. We thus have the semi-implicit scheme for the velocity component as

$$\frac{\partial}{\partial t}\left(w - \delta \frac{\partial^2 w}{\partial y^2} \right) = G - S^2 e^{-\alpha\theta(N)} w^{(N+\xi)} - \mathrm{Re}\frac{\partial}{\partial y} w^{(N)} + e^{-\alpha\theta(N)} \frac{\partial^2}{\partial y^2} w^{(N+\xi)} - \left[\alpha e^{-\alpha\theta} \frac{\partial \theta}{\partial y} \frac{\partial w}{\partial y} \right]^{(N)} + 6\gamma \left(\frac{\partial}{\partial y} w^{(N)} \right)^2 \frac{\partial^2}{\partial y^2} w^{(N+\xi)} \tag{4.11}$$

In equation (4.11), it is understood that $\frac{\partial \#}{\partial t} := \left(\#^{(N+1)} - \#^{(N)} \right) / \Delta t$. The equation for $w^{(N+\xi)}$ then becomes

$$-r_1 w_{j-1}^{(N+1)} + r_2 w_j^{(N+1)} - r_1 w_{j+1}^{(N+1)} = \text{explicit terms} \tag{4.12}$$

where

$$r_1 = \frac{1}{\Delta y^2}\left[\delta + \xi \Delta t \left(\mu + 6\gamma \left(\dot{\gamma} \right)^2 \right)^{(N)} \right], \qquad r_2 = \left(1 + \xi \Delta t S^2 \mu^{(N)} + 2 r_1 \right), \quad \text{with}$$

$\mu = \exp(-\alpha\theta)$ and $\dot{\gamma} = w_y$. The solution procedure for $w^{(N+1)}$ thus reduces to inversion of tri-diagonal matrices, which is an advantage over a full implicit scheme. The semi-implicit integration scheme for the temperature equation is similar to that for the velocity component. Unmixed second partial derivatives of the temperature are treated implicitly:

$$\Pr\frac{\theta^{(N+1)}-\theta^{(N)}}{\Delta t}=\frac{\partial^2}{\partial y^2}\theta^{(N+\xi)}-\Pr\mathrm{Re}\frac{\partial}{\partial y}\theta^{(N)}+$$
$$\lambda\left\{\left[\left(1+\varepsilon\theta\right)^m\exp\left(\frac{\theta}{1+\varepsilon\theta}\right)\right]^{(N)}+\Omega\left[S^2w^2e^{-\alpha\theta}+\left(\dot{\gamma}\right)^2\left(e^{-\alpha\theta}+2\gamma\left(\dot{\gamma}\right)^2\right)\right]^{(N)}\right\} \tag{4.13}$$

The equation for $\theta^{(N+1)}$ thus becomes

$$-r\theta_{j-1}^{(N+1)}+\left(\Pr+2r\right)\theta_j^{(N+1)}-r\theta_{j+1}^{(N+1)}=\text{explicit terms} \tag{4.14}$$

where $r=\xi\Delta t/\Delta y^2$. The solution procedure again reduces to inversion of tri-diagonal matrices. The schemes (4.12) and (4.14) were checked for consistency. For $\xi=1$, these are first order accurate in time but second-order accurate in space. The schemes in [21] have $\xi=\frac{1}{2}$ which improves the accuracy in time to second order. Following the work in [23] we use $\xi = 1$ so that the choice of larger time steps is possible and still obtain convergence to the steady solutions.

4.4. Results and discussion

4.4.1. Transient and steady state profiles

We will display all steady solutions at $t=40$ although solutions were observed to have converged to steady state far earlier than this time. In the absence of suction/injection, i.e. if the channel walls are impermeable, we obtain parabolic velocity and temperature profiles as depicted by Figure 4.2. The 3 dimensional graphs in Figure 4.3 clearly reveal that maximum velocity is recorded at the centre of the channel whereas maximum temperature is recorded at the channel walls.

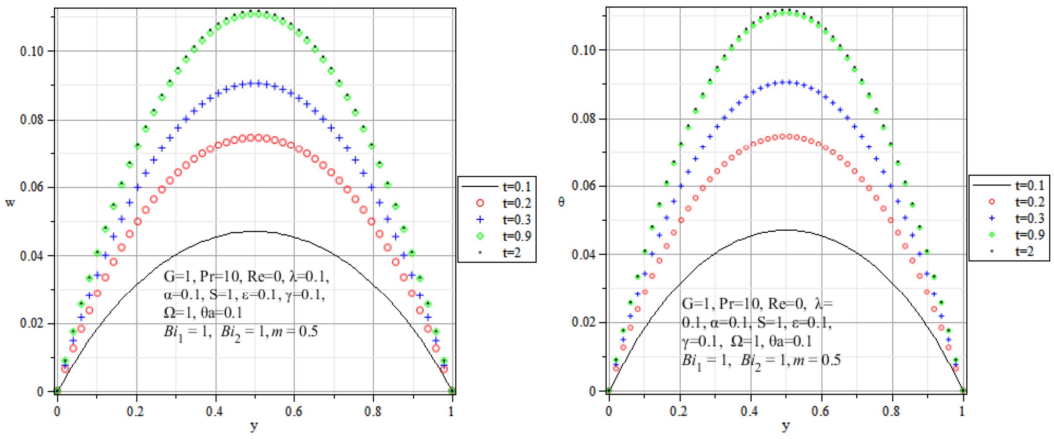

Figure 4.2. Evolution of velocity and temperature with no suction/injection.

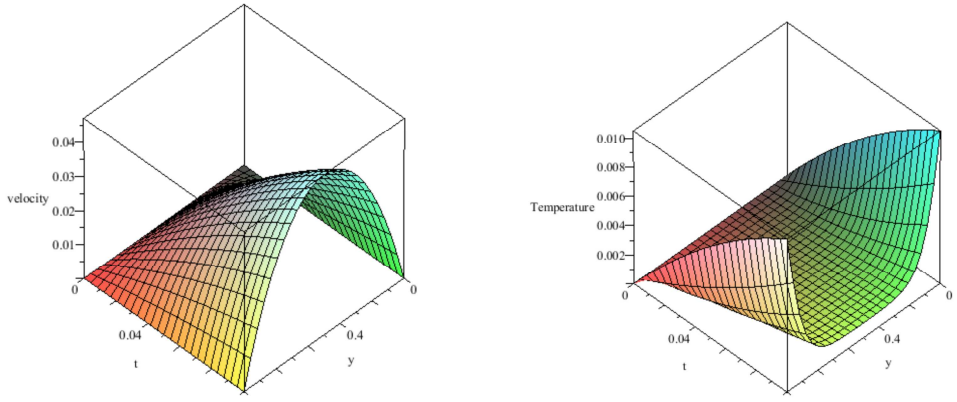

Figure 4.3. 3 dimensional representation of velocity and temperature profiles, $\mathrm{Re} = 0$**.**

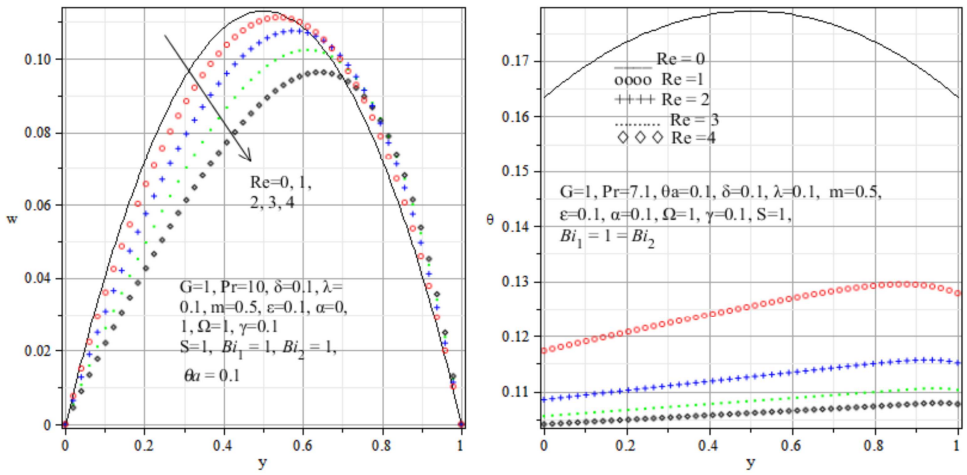

Figure 4.4. Effects of suction/injection Reynolds number on velocity and temperature.

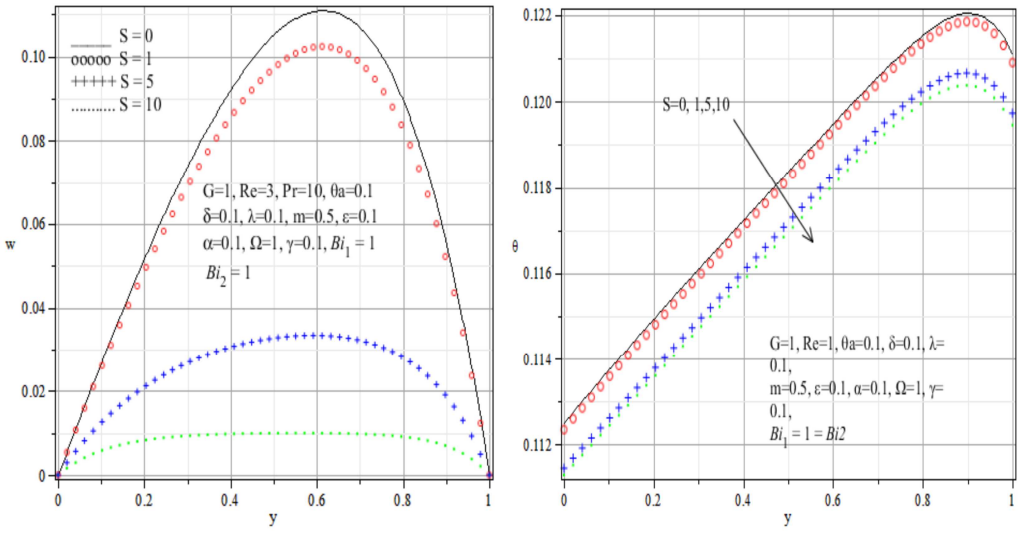

Figure 4.5. Response of velocity and temperature to medium shape parameter, S.

4.4.2. Parameter dependence of solutions

In all the cases we consider, fluid is injected uniformly through the lower wall and corresponding suction out of the upper wall. The effect of this is that velocity and temperature profiles are shifted considerably towards the upper wall.

If the injection/suction Reynolds number is increased gradually, velocity and temperature profiles are both seen to decrease as a result, see Figure 4.4. The increased velocity near the upper plate causes increased rate of heat transfer out of the upper plate and this explains the drop in temperature. The response of velocity and temperature profiles to increasing porous medium shape parameter S, seen in Figure 4.5, follows a similar trend as that in Figure 4.4. An increase in S reduces permeability of the pore spaces in the matrix. As a result velocity decreases. The reduced velocity slows down the temperature through the reduction of viscous heating source terms in the temperature equation.

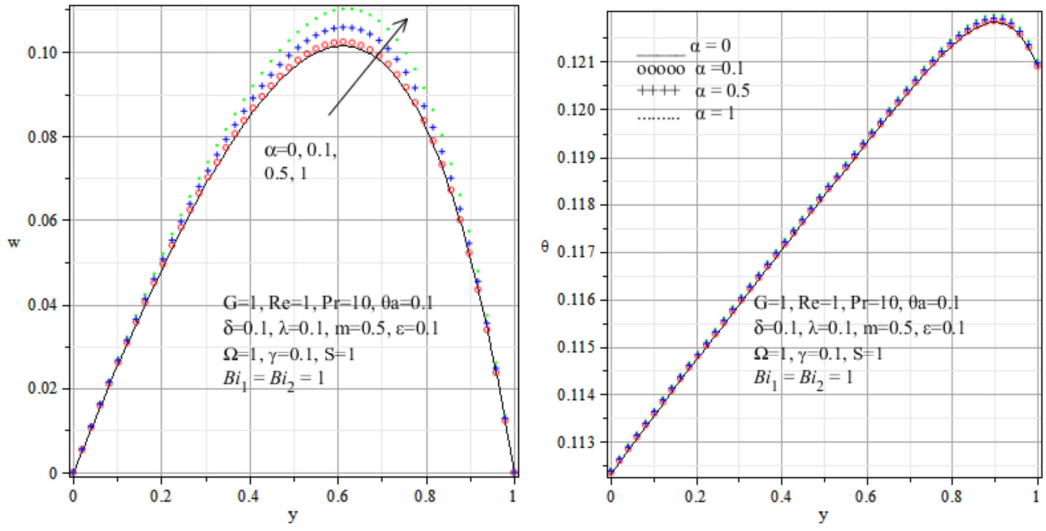

Figure 4.6. Effects of the variable viscosity parameter, α.

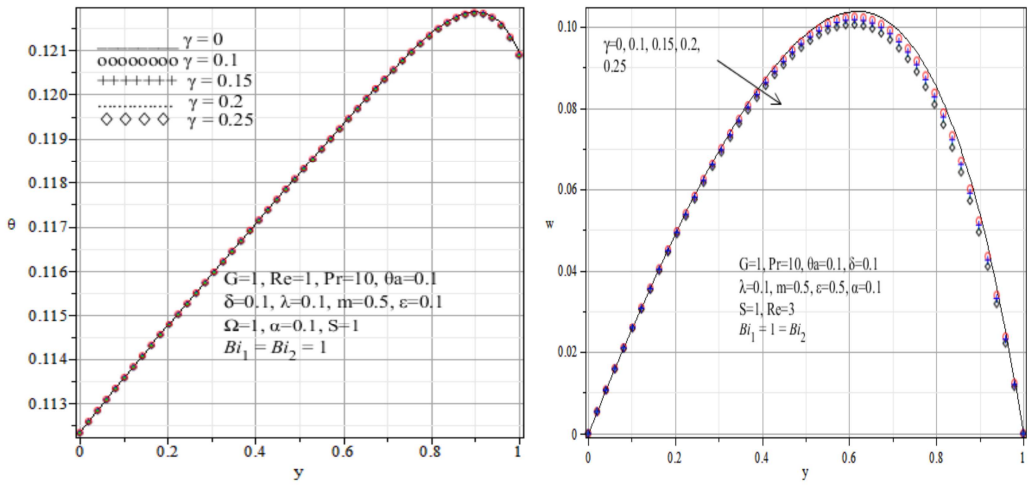

Figure 4.7. Effects of the non-Newtonian parameter, γ.

Figures 4.6 and 4.7 explain the effects of increasing the variable viscosity parameter, α and the non-Newtonian parameter, γ. With all other parameters constant, increasing α reduces fluid viscosity which in turn increases flow rate. On the other hand increasing γ increases the non-Newtonian properties of the fluid whose effects are to damp the flow. In both cases the effects on fluid temperature are marginal.

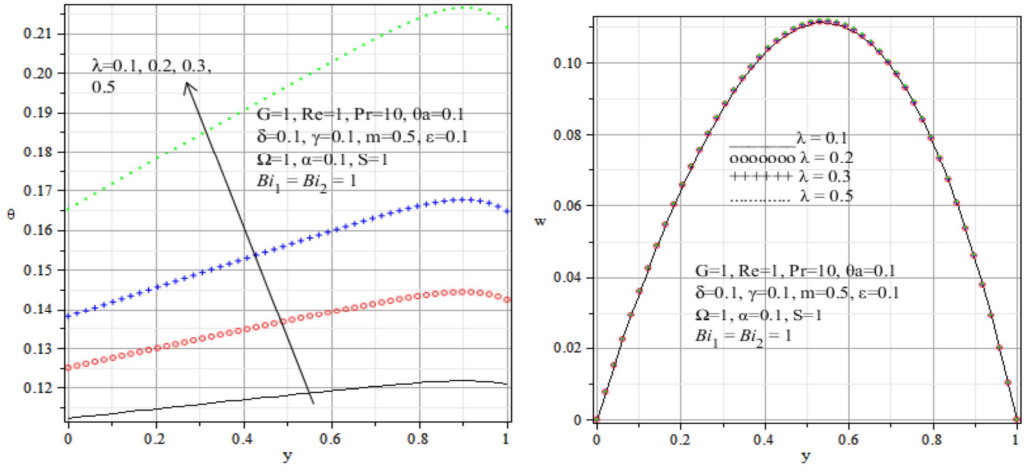

Figure 4.8. Effects of the reaction parameter, λ.

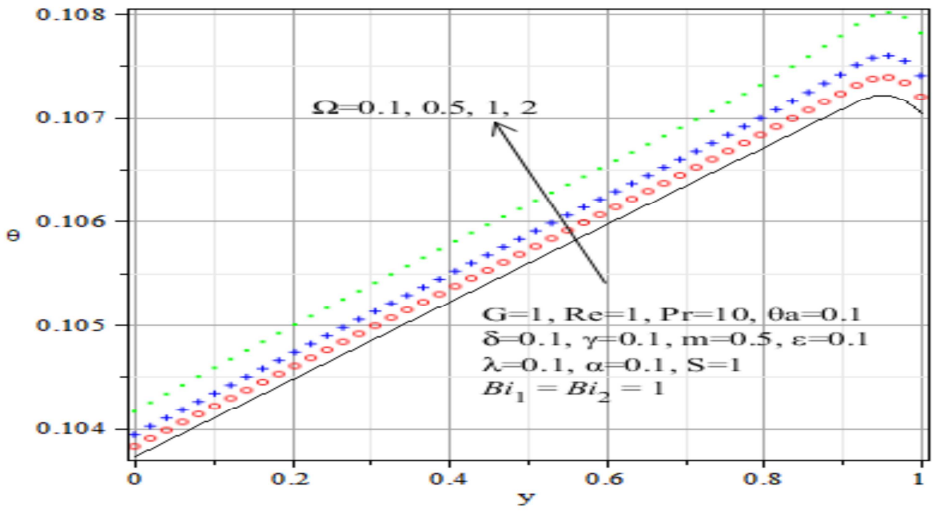

Figure 4.9. Effects of the viscous heating parameter, Ω, on temperature.

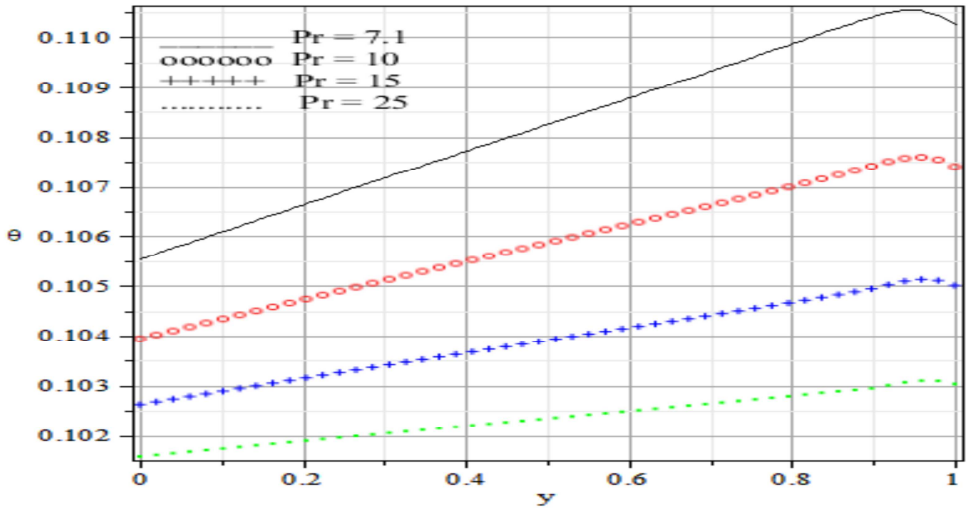

Figure 4.10. Efffects of the Prandtl number on temperature, $\mathrm{Re} = 3$.

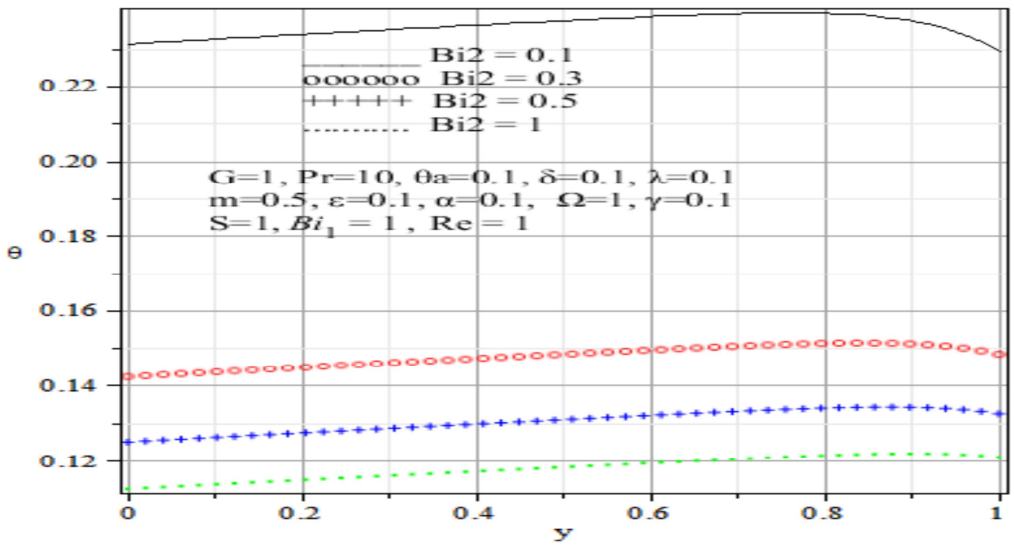

Figure 4.11. Effects of the Biot number, Bi_2, on temperature.

Figure 4.8 shows flow quantities increasing with the reaction parameter, λ. This is not surprising at all because increasing the reaction parameter results in increased reaction rate. The same trend is seen in figure 4.9. In Figures 4.10 and 4.11, fluid temperature is seen to decrease with increasing Prandtl number and Biot number respectively. Generally the Prandtl number decreases the fluid thermal conductivity whereas higher Biot numbers mean higher degrees of convective cooling at the channel walls and this naturally leads to lower fluid temperatures at the channel walls and so is in the bulk of the fluid.

The physical quantities of engineering significance are the wall shear stress (skin friction) and the wall heat transfer rate. We display variation of these quantities with the reaction parameter λ and the suction/injection Reynolds number, the porous medium shape parameter, the variable viscosity parameter and the Prandtl number in Figures 4.12 and 4.13. The figures are plotted until the solution blow-up values of λ are reached. The skin friction is seen to increase with increasing suction/injection Reynolds number Re as well as variable viscosity parameter α. On the contrary, the influence of the porous medium shape parameter and the Prandtl number on the skin friction is to decrease it.

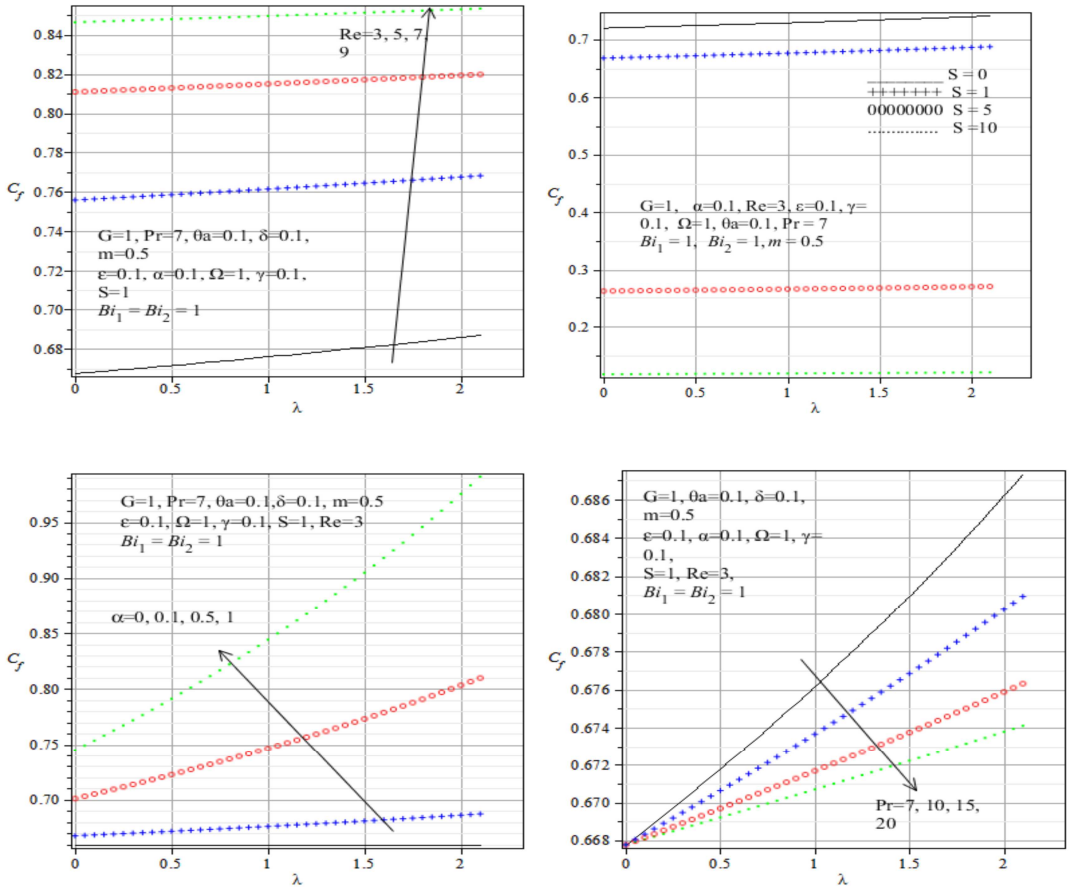

Figure 4.12. Variation with λ and $\mathrm{Re}, S, \alpha, \mathrm{Pr}$ of the wall shear stress

In Figure 4.13, it is observed that as the values of the suction/injection Reynolds number, the porous medium shape parameter and the Prandtl number are increased, the rate at which heat is transferred at the upper wall decreases. On the other hand, increasing the variable viscosity parameter marginally increases the rate of heat transfer at the wall.

Table 4.1 lists computations of the thermal criticality values of λ for various parameter variations. This is an exercise of crucial importance as, depending on other flow parameters, values of the reaction parameter above a certain threshold inevitably lead to blow up of solutions. It is thus important to know a priori the blow up values of the reaction parameter in relation to the behaviour of other parameters. It is particularly noted from the table that the thermal criticality values of λ increase with increasing suction/injection Reynolds number and the Prandtl number. This trend is also revealed by Figure 4.14.

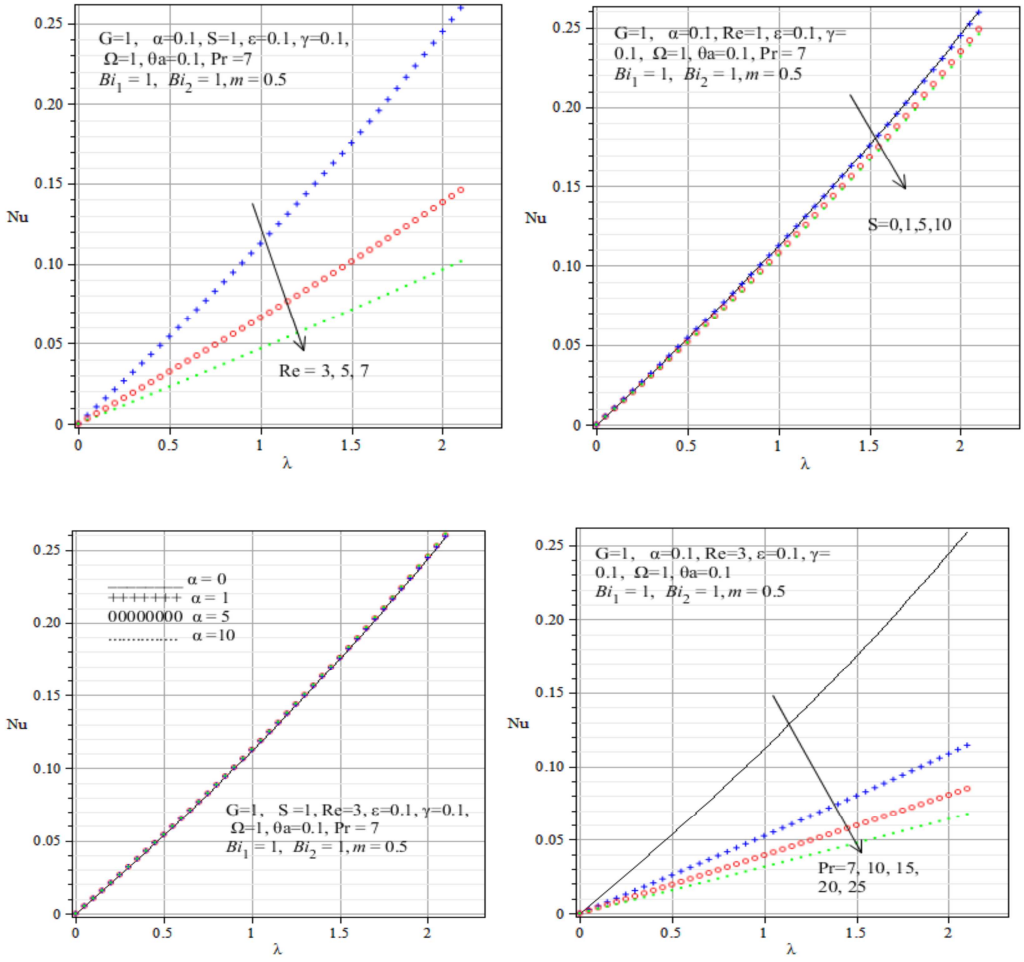

Figure 4.13. Variation with λ and $\mathrm{Re}, S, \alpha, \mathrm{Pr}$ of the wall heat transfer rate.

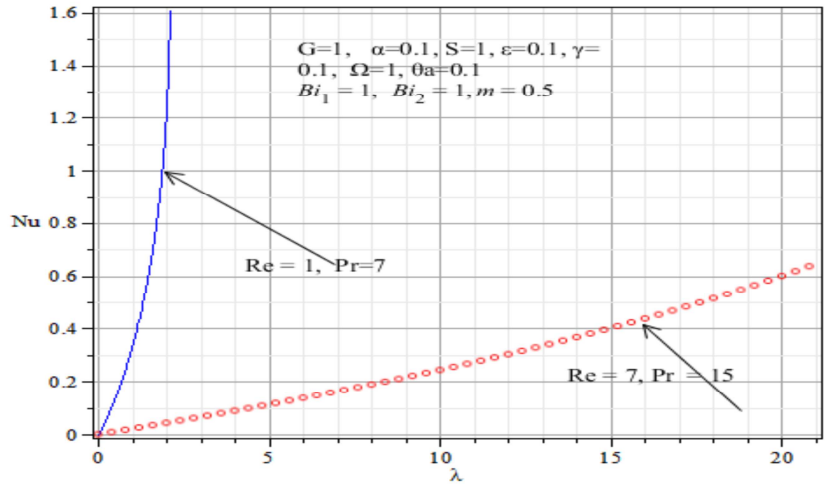

Figure 4.14. Blow up of solutions

Table 4.1. Thermal criticality values of λ for different parameter values

Re	S	α	δ	Pr	γ	Bi_2	m	ε	Ω	Nu	λ_c
0	1	0.1	0.1	7.2	0.1	1	0.5	0.1	1	1.009898	0.594012
1	1	0.1	0.1	7.2	0.1	1	0.5	0.1	1	1.896763	2.128543
5	1	0.1	0.1	7.2	0.1	1	0.5	0.1	1	2.541587	12.127745
10	1	0.1	0.1	7.2	0.1	1	0.5	0.1	1	1.046734	18.810380
1	3	0.1	0.1	7.2	0.1	1	0.5	0.1	1	1.585287	2.128543
1	5	0.1	0.1	7.2	0.1	1	0.5	0.1	1	1.813598	2.178044
1	10	0.1	0.1	7.2	0.1	1	0.5	0.1	1	1.694715	2.178044
1	1	0.5	0.1	7.2	0.1	1	0.5	0.1	1	1.745310	2.079042
1	1	0.8	0.1	7.2	0.1	1	0.5	0.1	1	1.612351	2.029541
1	1	1	0.1	7.2	0.1	1	0.5	0.1	1	1.754748	2.029541
1	1	0.1	0.5	7.2	0.1	1	0.5	0.1	1	1.871694	2.128543
1	1	0.1	1	7.2	0.1	1	0.5	0.1	1	1.846684	2.128543
1	1	0.1	0.1	1	0.1	1	0.5	0.1	1	0.743134	0.594012
1	1	0.1	0.1	3	0.1	1	0.5	0.1	1	0.963442	0.891018
1	1	0.1	0.1	7.2	0.5	1	0.5	0.1	1	2.048847	2.128543
1	1	0.1	0.1	7.2	-0.5	1	0.5	0.1	1	1.771495	2.128543
1	1	0.1	0.1	7.2	0.1	5	0.5	0.1	1	5.537611	2.128543
1	1	0.1	0.1	7.2	0.1	10	0.5	0.1	1	7.452527	2.128543
1	1	0.1	0.1	7.2	0.1	1	0	0.1	1	1.700805	2.227545
1	1	0.1	0.1	7.2	0.1	1	-2	0.1	1	2.710665	3.069062
1	1	0.1	0.1	7.2	0.1	1	0.5	0.3	1	3.369335	2.623553
1	1	0.1	0.1	7.2	0.1	1	0.5	0.5	1	11.129398	4.257086
1	1	0.1	0.1	7.2	0.1	1	0.5	0.1	1.5	1.740303	2.079042
1	1	0.1	0.1	7.2	0.1	1	0.5	0.1	2	1.641712	2.029541

4.5. Conclusion

Thermal effects of the suction/injection Reynolds number, in conjunction with other flow parameters, on an unsteady reactive temperature dependent viscosity third grade fluid in a porous channel filled with saturated porous medium and with asymmetric convective boundary conditions have been analysed. It is concluded that the velocity field is retarded by the increase in suction/injection Reynolds number. The porous medium parameter, the Prandtl number, the Biot number and the suction/injection Reynolds number have a retarding effect on the temperature field. The suction/injection Reynolds number and the variable viscosity parameter increase the wall shear stress, while the porous medium shape parameter and the Prandtl number have the opposite effect. The rate of heat transfer at the wall is diminished by increasing the suction/injection Reynolds number, the porous medium shape parameter and the Prandtl number. Values of the reaction parameter for which blow up of solutions occur are higher at larger suction/injection Reynolds numbers and Prandtl numbers.

CHAPTER FIVE

ANALYSIS OF UNSTEADY MHD REACTIVE FLOW OF A NON-NEWTONIAN FLUID THROUGH A POROUS SATURATED MEDIUM WITH ASYMMETRIC CONVECTIVE BOUNDARY CONDITIONS

In this chapter we extend the problem in chapter 3 by analyzing thermal effects in an unsteady hydromagnetic flow of a pressure driven, reactive, variable viscosity, electrically conducting third-grade fluid through a porous saturated medium with asymmetrical convective boundary conditions. It is assumed that the chemical kinetics in the flow system are exothermic and that the asymmetric convective heat exchange with the surrounding medium at the surfaces follows Newton's law of cooling. A semi-implicit finite difference scheme will again be used to numerically solve the underlying coupled nonlinear partial differential equations governing the flow and heat transfer.

5.1. Introduction

The current apparent surge in research interest in studies of phenomena connected with convective hydromagnetic fluid flow can be explained by its wide applications in science, engineering and technology. The flow of electrically conducting viscous fluid between two parallel plates in the presence of a transversely applied magnetic field has applications in many devices such as magnetohydrodynamic (MHD) power generators, MHD pumps, accelerators, aerodynamics heating, electrostatic precipitation, polymer technology, petroleum industry, cooling of nuclear reactors, geothermal energy extraction, metal purification, etc [7, 16, 61, 67, 69]. Following the pioneering work of Hartmann [41], the rheological community has undertaken to investigate hydromagnetic fluid flow and heat transfer in different geometries under varied physical effects. Makinde and Mhone [72] investigated hydromagnetic instability of viscous incompressible fluid in a channel filled with saturated porous medium. Chamkha [16] studied mixed convection of hydromagnetic fully developed laminar flow in a vertical channel with symmetric and asymmetric wall heating conditions in the presence or absence of heat generation or absorption effects. Convection flow of an electrically conducting fluid past a vertical porous plate in the presence of a transversely imposed magnetic field was studied in [61, 74]. Liu [50, 51] studied hydromagnetic flow over a stretching sheet subject to a transverse magnetic field.

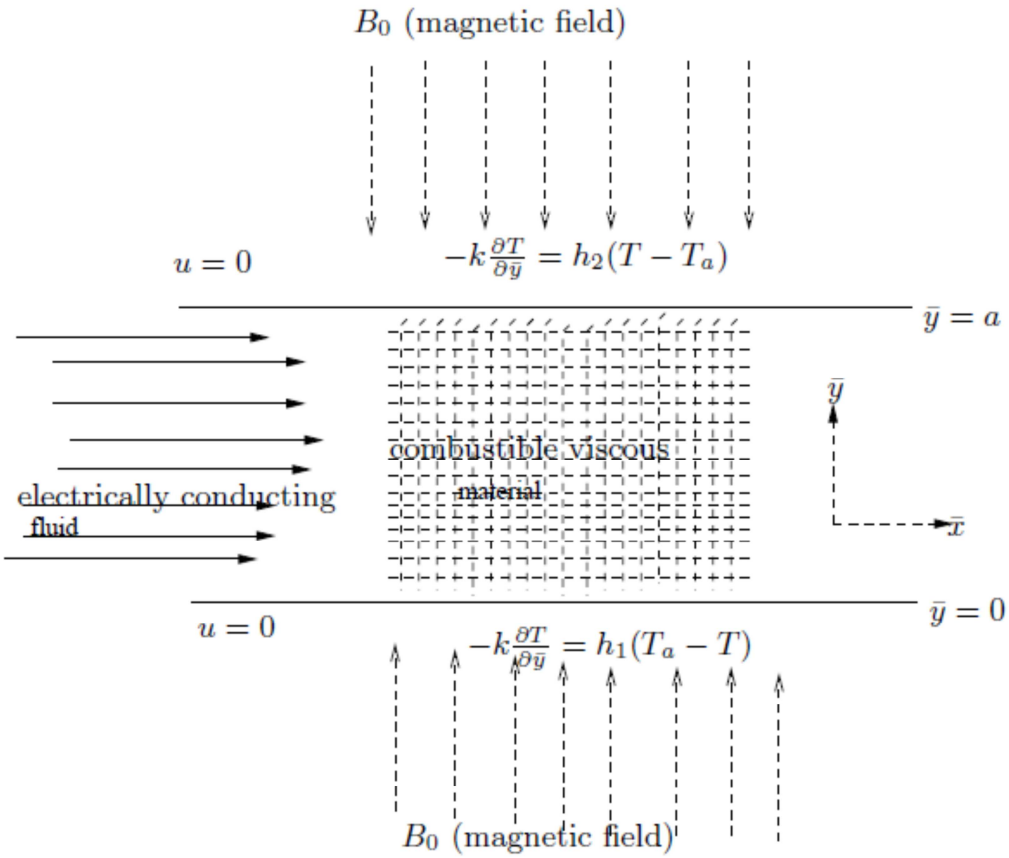

Figure 5.1: Problem schematics and coordinate system

As mentioned earlier, one particular dimension that has been of particular interest in recent years is the study of flow of fluids that exhibit non-Newtonian character. Prasad *et al* [87] explored the effects of thermal buoyancy on a non-Newtonian power law fluid flow past a vertical continuous stretching sheet, while Olajuwon [82] examined convection heat and mass transfer in a hydromagnetic flow of a second grade fluid past a semi-infinite stretching sheet in the presence of thermal radiation and thermal diffusion. Makinde and Chinyoka [69] studied unsteady hydromagnetic Generalized Couette flow and heat transfer characteristics of a reactive variable viscosity incompressible electrically conducting third grade fluid in a channel with asymmetric convective cooling at the walls in the presence of a uniform transverse magnetic field. Literature survey reveals that studies as in [69] have still not been widely exhausted, in particular the concept of reactive variable viscosity electrically conducting non-Newtonian fluid as well as asymmetric convection as opposed to symmetric convection.

In section 5.2, mathematical model formulation is presented and the solution process is implemented in section 5.3. Numerical and graphical results as well as their discussion are presented in section 5.4.

5.2. Mathematical model formulation

An unsteady flow of an incompressible electrically conducting, third-grade, variable viscosity reactive fluid through a channel filled with a homogeneous and isotropic porous medium is considered. It is assumed that the flow is subjected to the influence of an externally applied homogeneous magnetic field as depicted in Figure 5.1. The fluid has small electrical conductivity so that the electromagnetic force produced has small magnitude. The plate surfaces are subjected to asymmetric convective heat exchange with the ambient due to unequal heat transfer coefficients and the fluid motion is induced by an applied axial pressure gradient. We choose the $\bar{x}$-axis parallel to the channel and the $\bar{y}$-axis normal to it.

Under the above assumptions, and neglecting the reacting viscous fluid consumption, the governing equations for momentum and heat balance are formulated as in chapter 3, [3, 36, 58, 59, 63, 75, 90], and can be written as

$$\rho\frac{\partial u}{\partial \bar{t}} = -\frac{\partial \bar{P}}{\partial \bar{x}} + \frac{\partial}{\partial \bar{y}}\left[\bar{\mu}(T)\frac{\partial u}{\partial \bar{y}}\right] + \alpha_1\frac{\partial^3 u}{\partial \bar{y}^2\partial \bar{t}} + 6\beta_3\frac{\partial^2 u}{\partial \bar{y}^2}\left(\frac{\partial u}{\partial \bar{y}}\right)^2 - \frac{\bar{\mu}(T)u}{\rho K} - \sigma B_0^2 u \tag{5.1}$$

$$\rho c_p\frac{\partial T}{\partial \bar{t}} = k\frac{\partial^2 T}{\partial \bar{y}^2} + \sigma B_0^2 u^2 + \left(\frac{\partial u}{\partial \bar{y}}\right)^2\left(\bar{\mu}(T) + 2\beta_3\left(\frac{\partial u}{\partial \bar{y}}\right)^2\right) + \frac{\bar{\mu}(T)u^2}{K} + QC_0A\left(\frac{hT}{\nu l}\right)^m e^{-\frac{E}{RT}}. \tag{5.2}$$

The appropriate initial and boundary conditions are

$$u(\bar{y},0) = 0, \quad T(\bar{y},0) = T_0, \tag{5.3}$$

$$u(0,\bar{t}) = 0, \quad -k\frac{\partial T}{\partial \bar{y}}(0,\bar{t}) = h_1[T_a - T(0,\bar{t})], \tag{5.4}$$

$$u(a,\bar{t}) = 0, \quad -k\frac{\partial T}{\partial \bar{y}}(a,\bar{t}) = h_2[T(a,\bar{t}) - T_a]. \tag{5.5}$$

σ is the fluid electrical conductivity and B_0 is the electromagnetic induction. The other symbols and parameters are as defined in chapter 3. The temperature dependent viscosity ($\bar{\mu}$) is given by equation (3.6).

We introduce the dimensionless variables in (3.7) together with

$$Ha^2 = \frac{\sigma B_0^2 a^2}{\mu_0}$$

into equations (5.1) to (5.5);

and obtain the following dimensionless governing equations:

$$\frac{\partial w}{\partial t} = G - Ha^2 w - S^2 w e^{-\alpha\theta} + e^{-\alpha\theta}\frac{\partial^2 w}{\partial y^2} - \alpha e^{-\alpha\theta}\frac{\partial\theta}{\partial y}\frac{\partial w}{\partial y} + \delta\frac{\partial^3 w}{\partial y^2 \partial t} + 6\gamma\frac{\partial^2 w}{\partial y^2}\left(\frac{\partial w}{\partial y}\right)^2, \tag{5.6}$$

$$Pr\frac{\partial\theta}{\partial t} = \frac{\partial^2\theta}{\partial y^2} + \lambda\left\{(1+\varepsilon\theta)^m exp\left(\frac{\theta}{1+\varepsilon\theta}\right) + \Omega\left[Ha^2 w^2 + S^2 w^2 e^{-\alpha\theta} + \left(\frac{\partial w}{\partial y}\right)^2\left(e^{-\alpha\theta} + 2\gamma\left(\frac{\partial w}{\partial y}\right)^2\right)\right]\right\}, \tag{5.7}$$

$$w(y,0) = 0, \quad \theta(y,0) = 0, \tag{5.8}$$

$$w(0,t) = 0, \quad \frac{\partial\theta}{\partial y}(0,t) = -Bi_1[\theta_a - \theta(0,t)], \tag{5.9}$$

$$w(1,t) = 0, \quad \frac{\partial\theta}{\partial y}(1,t) = -Bi_2[\theta(1,t) - \theta_a], \tag{5.10}$$

where Ha is the Hartmann number and all the other parameters are as defined in chapter 3.

The other dimensionless quantities of interest are the skin friction (C_f) and the wall heat transfer rate (Nu) given by equations (3.13).

In the following section, equations (5.6) to (5.10) together with equations (3.13) are solved numerically using a semi-implicit finite difference scheme.

5.3. Numerical solution

The semi-implicit finite difference scheme given in [21] is adopted. Following [22, 23], implicit terms are taken at the intermediate time level $(N+\xi)$ where $0 \leq \xi \leq 1$. The discretization of the governing equations is based on a linear Cartesian mesh and uniform grid on which finite differences are taken. Both the second and first spatial derivatives are approximated by second-order central differences. The equations corresponding to the first and last grid points are modified to incorporate the boundary conditions. The semi-implicit scheme for the velocity component is

$$\frac{\partial}{\partial t}\left(w-\delta\frac{\partial^2 w}{\partial y^2}\right)=G-S^2e^{-\alpha\theta^{(N)}}w^{(N+\xi)}-Ha^2w^{(N+\xi)}+e^{-\alpha\theta^{(N)}}\frac{\partial^2}{\partial y^2}w^{(N+\xi)}$$

$$-\left[\alpha e^{-\alpha\theta}\frac{\partial\theta}{\partial y}\frac{\partial w}{\partial y}\right]^{(N)}+6\gamma\left(\frac{\partial}{\partial y}w^{(N)}\right)^2\frac{\partial^2}{\partial y^2}w^{(N+\xi)} \qquad (5.11)$$

In (5.11), it is understood that $\partial\,\#/\partial t \coloneqq \left(\#^{(N+1)}-\#^{(N)}\right)/\Delta t$. The equation for $w^{(N+1)}$ then becomes

$$-r_1w_{j-1}^{(N+1)}+r_2w_{j-1}^{(N+1)}-r_1w_{j+1}^{(N+1)}=\Delta tG+(w+\delta w_{yy})^{(N)}-\alpha\Delta t\left(e^{-\alpha\theta}\theta_y\dot{\gamma}\right)^{(N)}-\Delta tS^2e^{-\alpha\theta^{(N)}}(1-\xi)w^{(N)}-\Delta tHa^2(1-\xi)w^{(N)}+\Delta t(1-\xi)\left(e^{-\alpha\theta}+6\gamma\dot{\gamma}^2\right)^{(N)}w_{yy}^{(N)}\ , \qquad (5.12)$$

where $r_1=\frac{1}{\Delta y^2}\left[\delta+\xi\Delta t(\mu+6\gamma\dot{\gamma}^2)^{(N)}\right]$, $r_2=\left(1+\xi\Delta tS^2\mu^{(N)}+\xi\Delta tHa^2+2r_1\right)$, with $\mu=\exp(-\alpha\theta)$ and $\dot{\gamma}=w_y$. The solution procedure for $w^{(N+1)}$ thus reduces to inversion of tri-diagonal matrices, which is an advantage over a full implicit scheme. The semi-implicit integration scheme for the temperature equation is similar to that for the velocity component. Unmixed second partial derivatives of the temperature are treated implicitly:

$$Pr\frac{\theta^{(N+1)}-\theta^{(N)}}{\Delta t}=\frac{\partial^2}{\partial y^2}\theta^{(N+\xi)}+\lambda\left\{\left[(1+\varepsilon\theta)^m exp\left(\frac{\theta}{1+\varepsilon\theta}\right)\right]^{(N)}+\Omega\left[Ha^2w^2+S^2w^2e^{-\alpha\theta}+\dot{\gamma}^2\left(e^{-\alpha\theta}+2\gamma\dot{\gamma}^2\right)\right]^{(N)}\right\}. \qquad (5.13)$$

The equation for $\theta^{(N+1)}$ thus becomes

$$-r\theta_{j-1}^{(N+1)}+(Pr+2r)\theta_j^{(N+1)}-r\theta_{j+1}^{(N+1)}=\theta^{(N)}+\Delta t(1-\xi)\theta_{yy}^{(N)}+\lambda\Delta t\left[(1+\varepsilon\theta)^m exp\left(\frac{\theta}{1+\varepsilon\theta}\right)\right]^{(N)}+\Omega\Delta t\left[Ha^2w^2+S^2w^2e^{-\alpha\theta}+\dot{\gamma}^2\left(e^{-\alpha\theta}+2\gamma\dot{\gamma}^2\right)\right]^{(N)}, \qquad (5.14)$$

where $r=\xi\,\Delta t/\Delta y^2$. The solution procedure again reduces to inversion of tri-diagonal matrices. The schemes (5.12) and (5.14) were checked for consistency. For $\xi=1$, these are first order accurate in time but second-order accurate in space. The schemes in [21] have $\xi=\frac{1}{2}$ which improves the accuracy in time to second order. Following the work in [22, 23] we use $\xi=1$ so

that the choice of larger time steps is possible and still obtain convergence to the steady solutions.

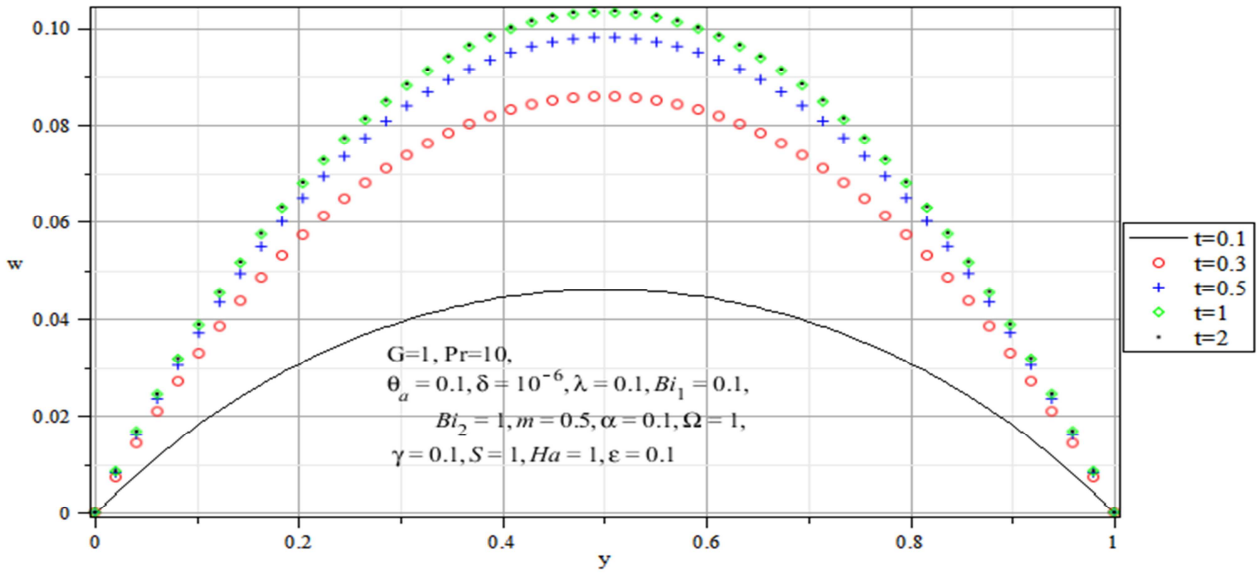

Figure 5.2: Transient and steady state velocity profiles.

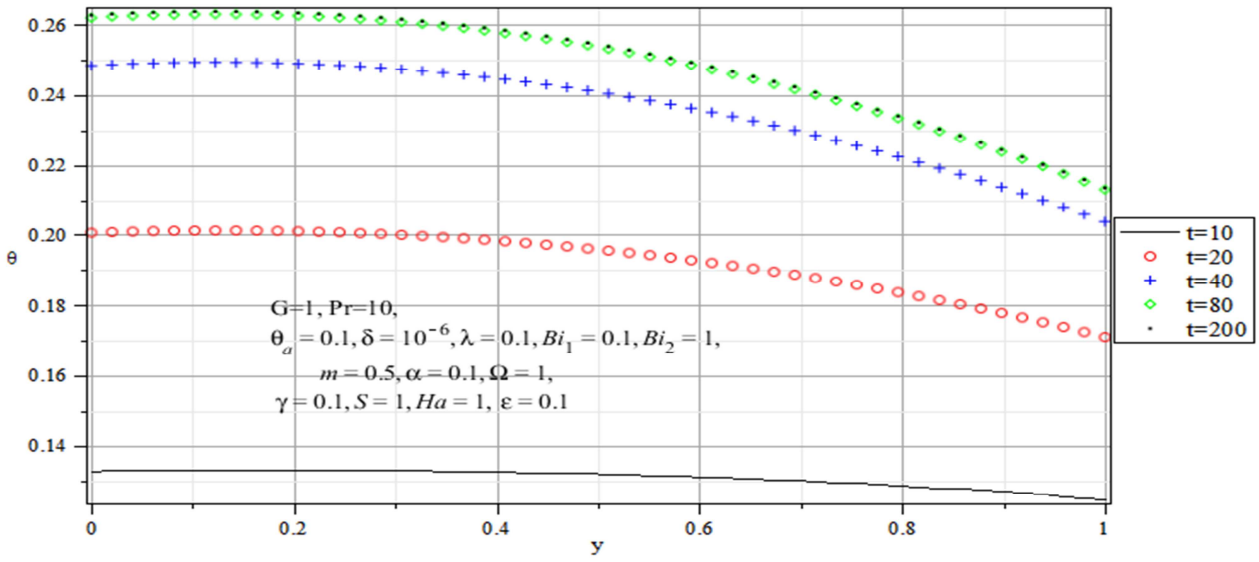

Figure 5.3: Transient and steady state temperature profiles.

5.4. Results and discussion

Figure 5.2 and Figure 5.3 are plots of the steady state velocity and temperature profiles. Both graphs show transient increase until steady state is reached.

As depicted by Figure 5.4, if the reaction parameter λ is not carefully controlled, it may not be possible to attain steady state velocity and temperature profiles as in Figure 5.2 and Figure 5.3. The terms associated with λ are strong heat sources. It is clear from Figure 5.4 that values of $\lambda \geq 0.3$ lead to finite temperature blow up.

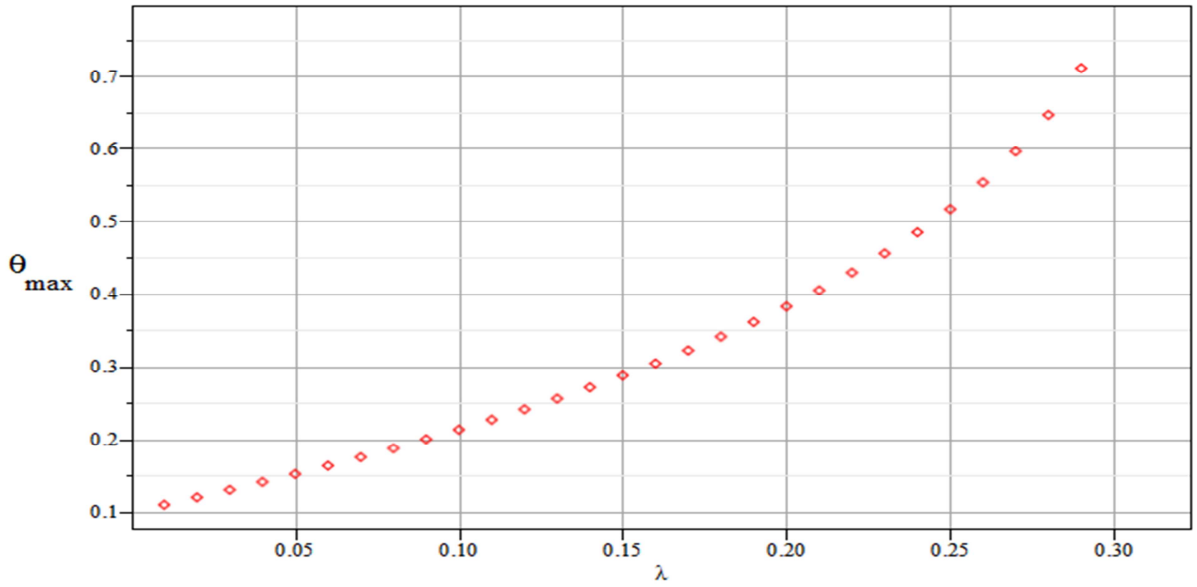

Figure 5.4: Blow up of fluid temperature for large λ.

5.4.1. Parameter variation analysis

Figure 5.5 to Figure 5.9 show the behaviour of fluid velocity in response to varying values of the Hartmann number (Ha), the porous medium shape parameter (S), the non-Newtonian parameter (γ), the variable viscosity parameter (α) and the reaction parameter (λ) respectively. Velocity is seen to decrease with an increase in the Hartmann number, the porous medium shape parameter as well as the non-Newtonian parameter. An increase in the Hartmann number means an increase in the damping properties of the magnetic field, and these damping forces result in increased resistance to flow and fluid velocity decreases as seen in Figure 5.5. An increase in the porous medium shape parameter S increases the complexity

(tortuosity) of the porous medium and the same effect as with the Hartmann number is observed (Figure 5.6). Increasing the non-Newtonian parameter γ means increasing the non-Newtonian properties of the fluid and these cause increased resistance to flow as well. As a result fluid velocity is also observed to decrease (Figure 5.7) with γ, albeit on a far much smaller scale when compared to the former two parameters.

The other two diagrams, Figure 5.8 and Figure 5.9 show velocity profile increasing with the variable viscosity parameter α and the reaction parameter λ respectively. The variable viscosity parameter reduces fluid viscosity which in turn leads to reduced resistance to flow resulting in increased velocity of the fluid. An increase in the parameter λ leads to significant increase in the reaction rate and this increase the viscous heating source terms. Fluid temperature increases drastically as a result (see Figure 5.18) and this significant temperature rise renders the viscosity coupling to the velocity stronger and this reduces the viscosity significantly leading to significant increase in the fluid velocity as seen in Figure 5.9.

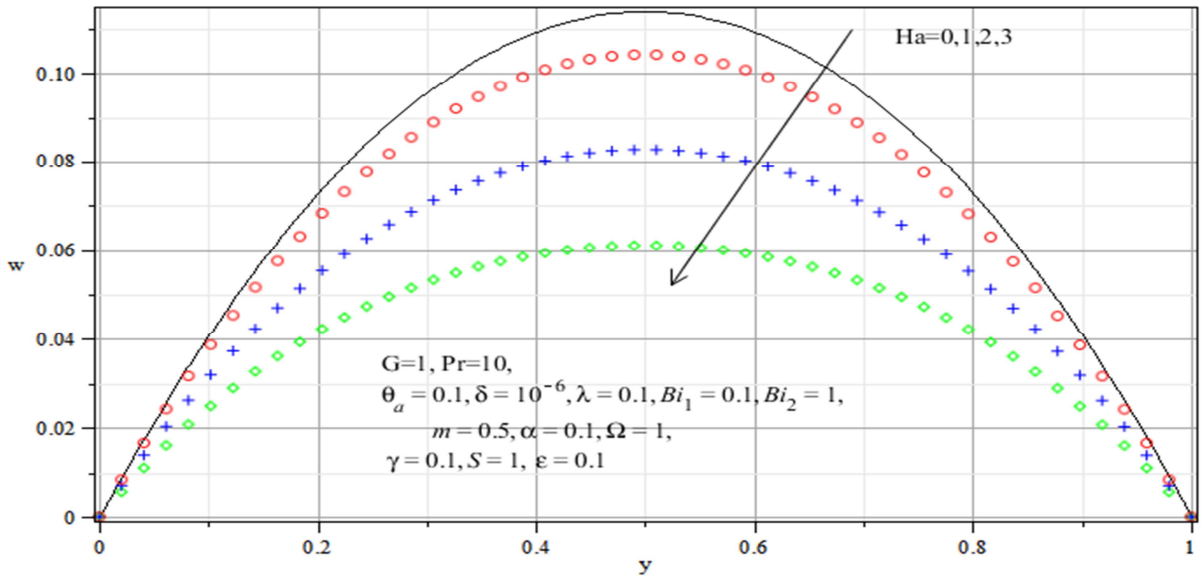

Figure 5.5: Effects of Hartmann number (Ha) on velocity.

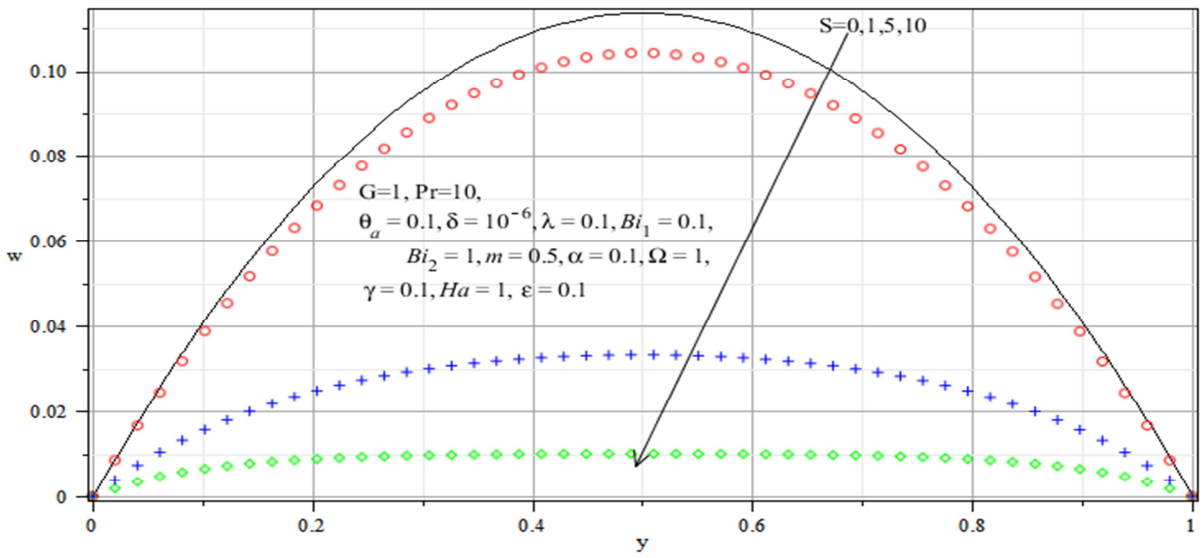

Figure 5.6: Effects of porous medium shape parameter (S) on velocity.

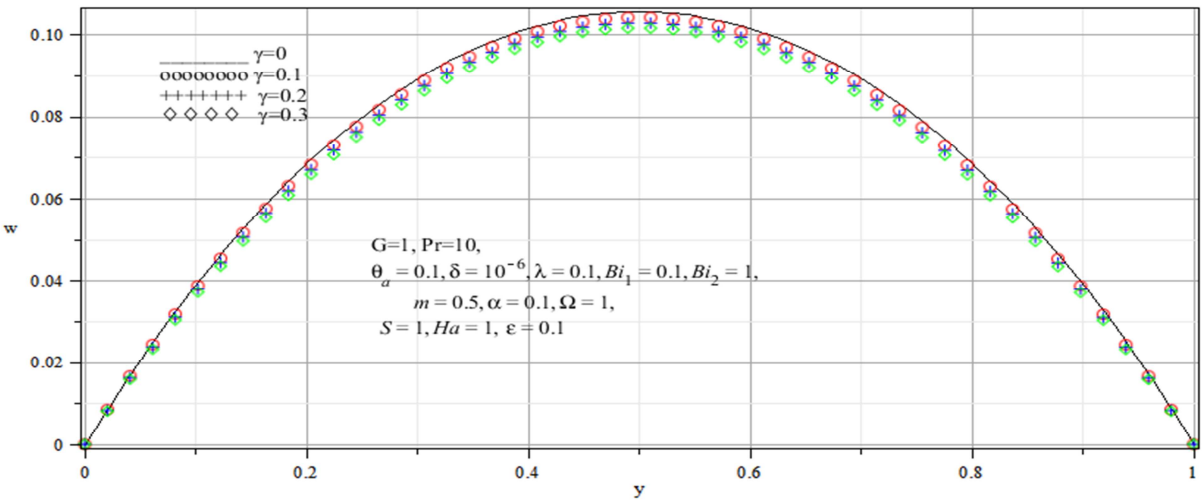

Figure 5.7: Effects of the non-Newtonian parameter (γ) on velocity.

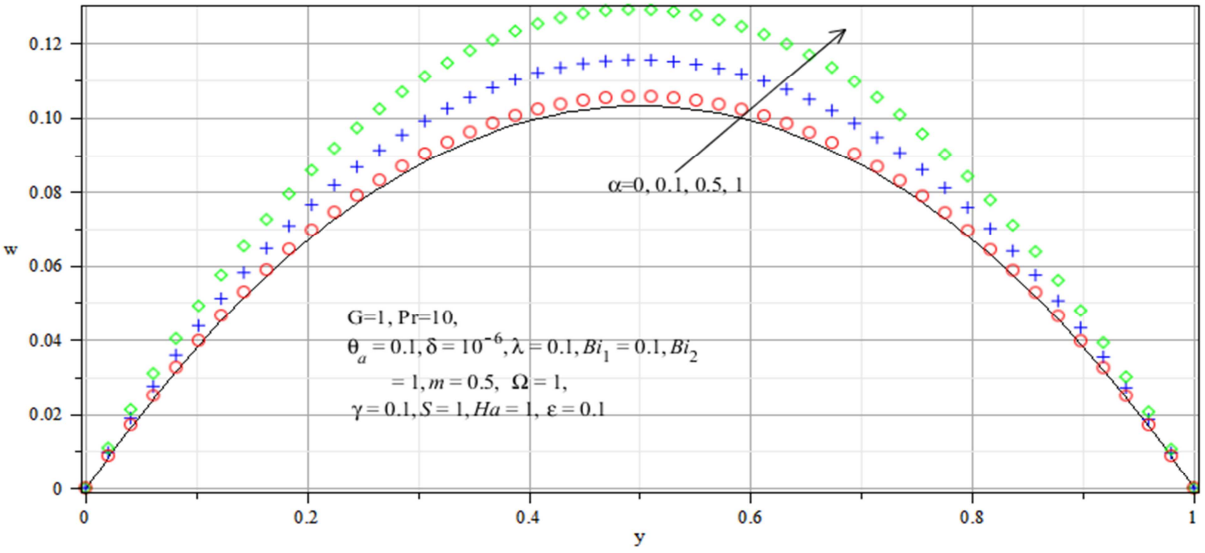

Figure 5.8: Effects of the variable viscosity parameter (α) on velocity.

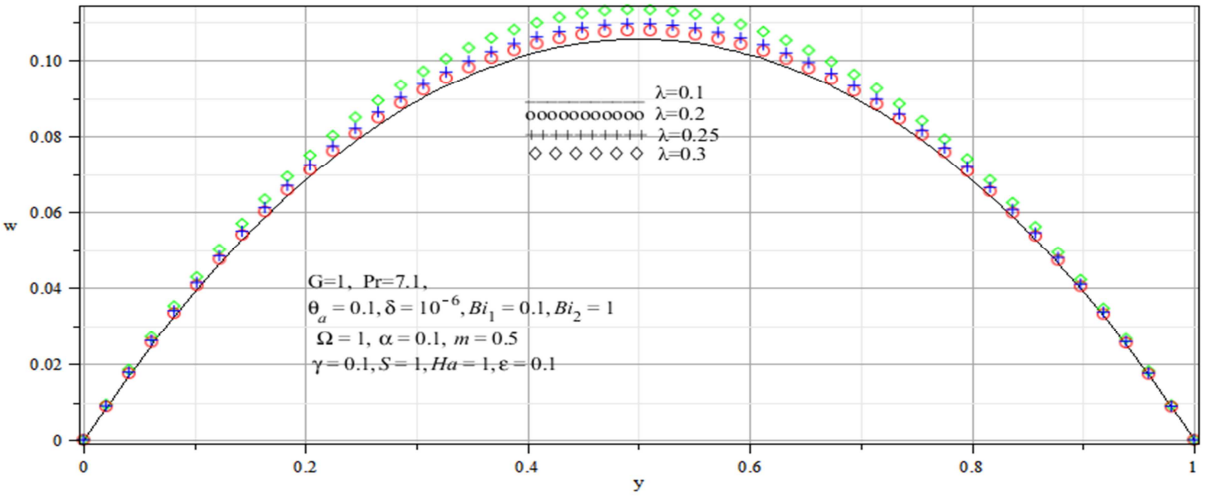

Figure 5.9: Effects of the reaction parameter (λ) on velocity.

Figures 5.10, 5.11, 5.12, 5.16 and 5.17 display fluid temperature profiles decreasing in response to increasing values of the Hartmann number (Ha), the porous medium shape parameter (S), the non-Newtonian parameter (γ), the Biot number (Bi) and Prandtl number ($\Pr$), respectively. The behaviour of the profiles in Figures 5.10, 5.11 and 5.12 is as a result of the coupling effect – as the velocity decreases, explained earlier, as a result of increasing Hartmann number, porous medium shape parameter and the non-Newtonian parameter it decreases the viscous heating

source terms in the temperature equation thereby causing a decrease in the fluid temperature. As for Figure 5.16, higher Biot numbers increase convective cooling at the channel walls and this extends to the bulk of the fluid as well resulting in overall temperature drop. The Prandtl number tends to decrease the contribution of the heating source terms in the temperature equation and hence in turn reduces the fluid temperature (see Figure 5.17). Boundary condition (5.10) explains the observed effect of the Biot number on the channel walls. In both cases the reduced temperature increases fluid viscosity which in turn reduces the velocity owing to viscosity coupling. However the effects on velocity are marginal and almost unnoticeable. It must be noted that the coupling is also affected by other parameters as well. Figures 5.13, 5.14, 5.15, 5.18 and 5.19 show temperature profiles increasing directly with increasing variable viscosity parameter α, parameter m, the activation energy parameter ε ($m = 0.5$) the reaction parameter λ and the viscous heating parameter Ω respectively. The reaction parameter λ has already been observed to drastically increase the rate of the reaction and this inevitably increases the fluid temperature. The same holds for the activation energy parameter ε and the viscous heating parameter Ω. The effect of the variable viscosity parameter α is as a result of the already explained coupling effect. In respect of Figure 5.14, an increase in the parameter m leads to corresponding increases in the strengths of the chemical reaction source terms in the temperature equation. As a result, the internal heat generated in the fluid during a bimolecular type of exothermic chemical reaction ($m = 0.5$) is higher than that generated under reaction of either the Arrhenius ($m = 0$) or the sensitised ($m = -2$) reaction types. In this way the temperature profile is seen to increase with the parameter m.

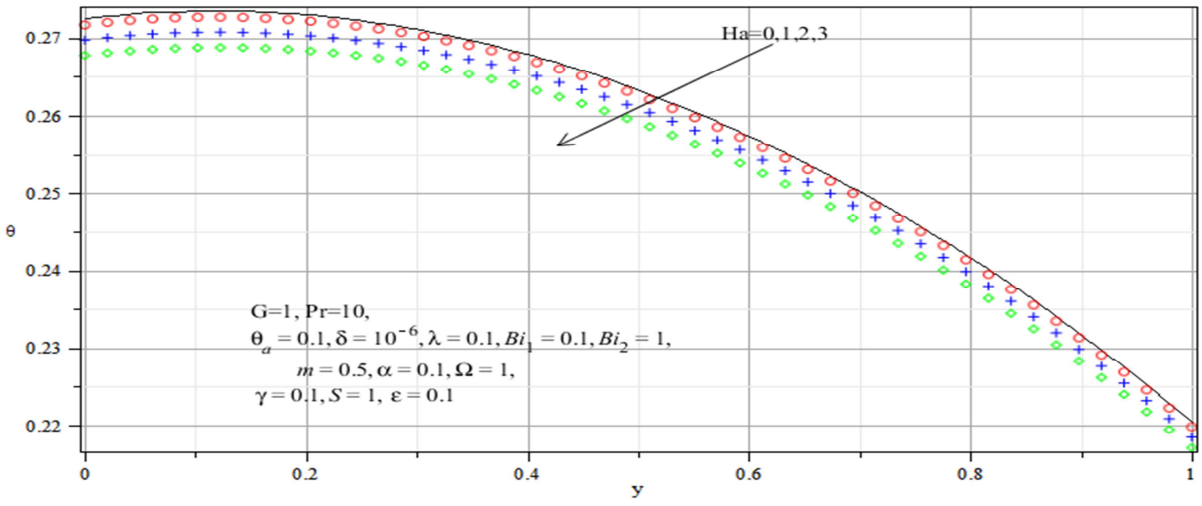

Figure 5.10: Effects of the Hartmann number (Ha) on temperature.

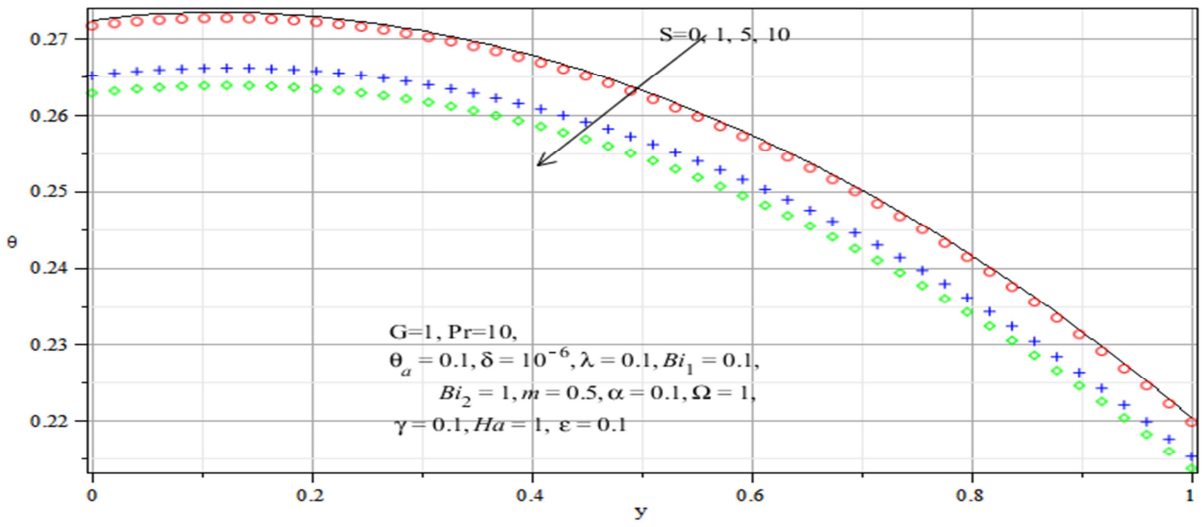

Figure 5.11: Effects of the porous medium shape parameter (S) on temperature.

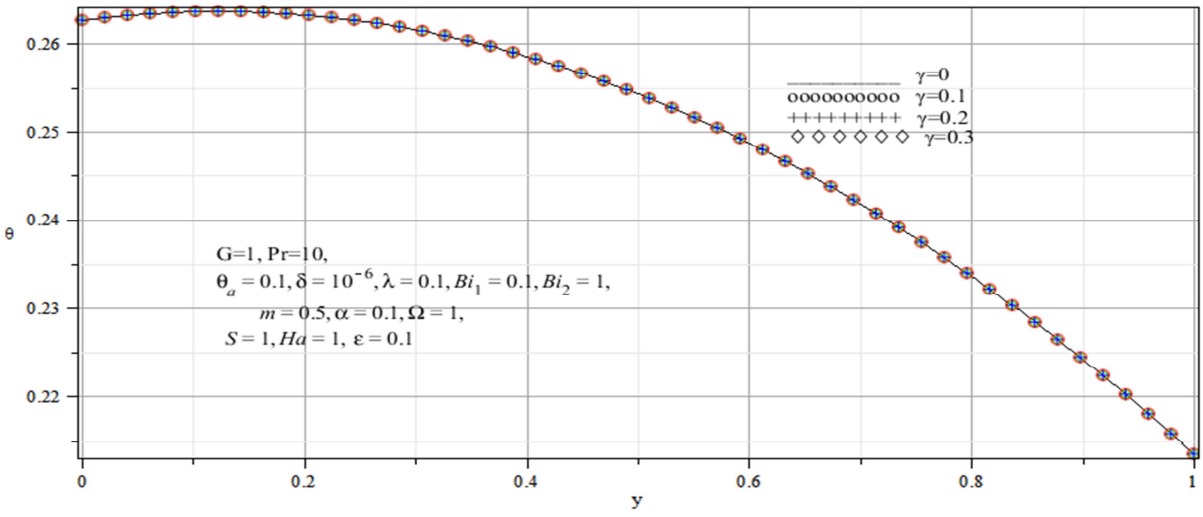

Figure 5.12: Effects of the non-Newtonian parameter (γ) on temperature.

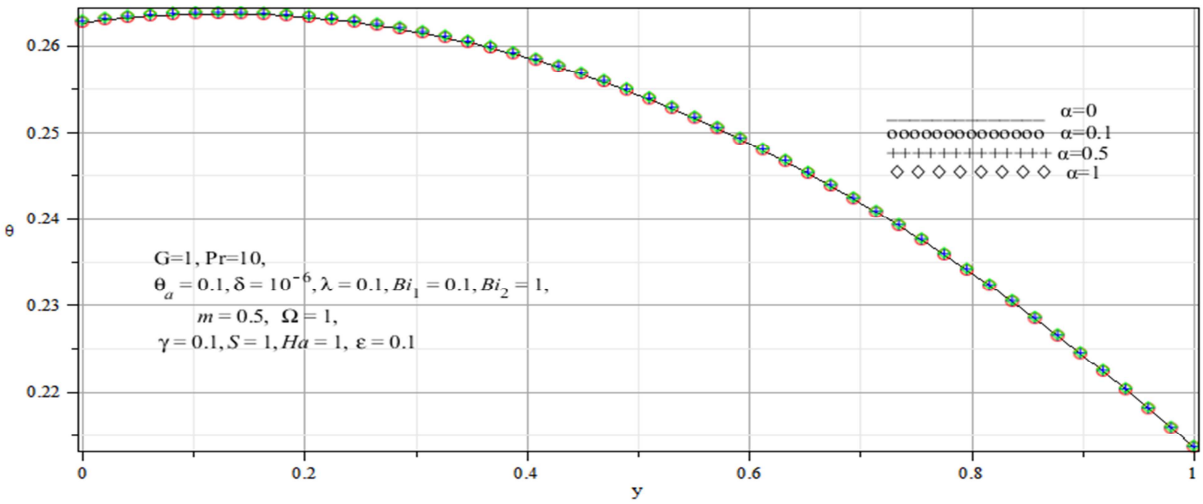

Figure 5.13: Effects of the variable viscosity parameter (α) on temperature.

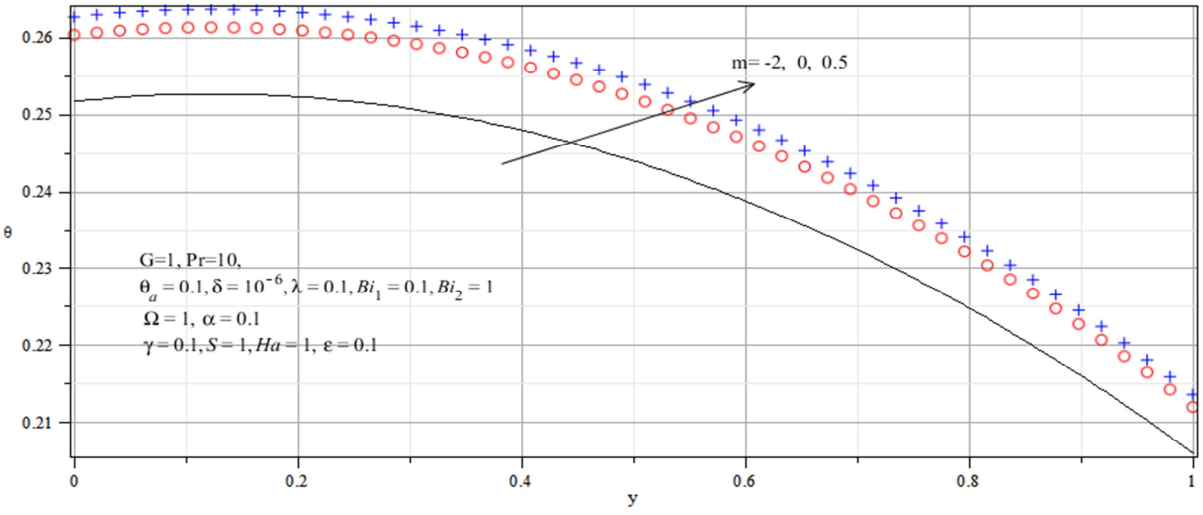

Figure 5.14: Effects of the parameter m on temperature.

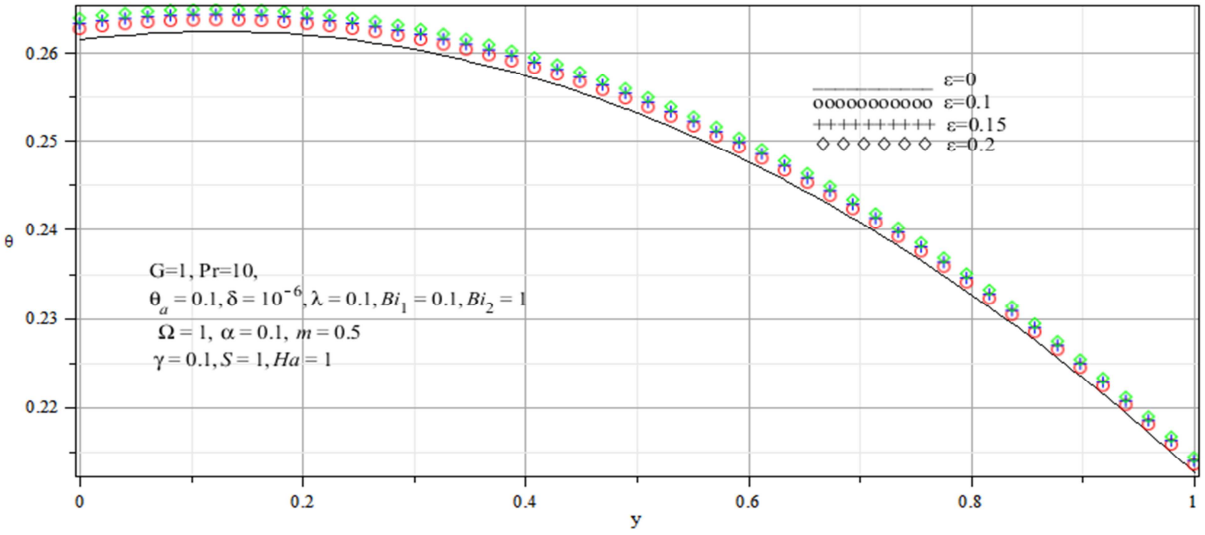

Figure 5.15: Effects of the activation energy parameter (ε) on temperature, $m = 0.5$

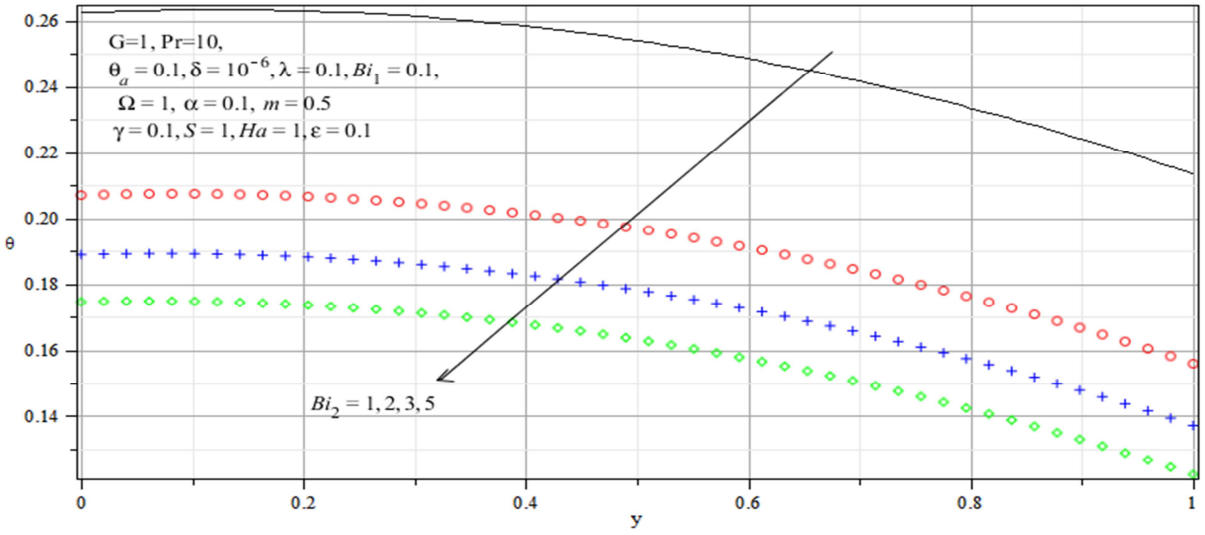

Figure 5.16: Effects of the Biot number (Bi_2) on temperature.

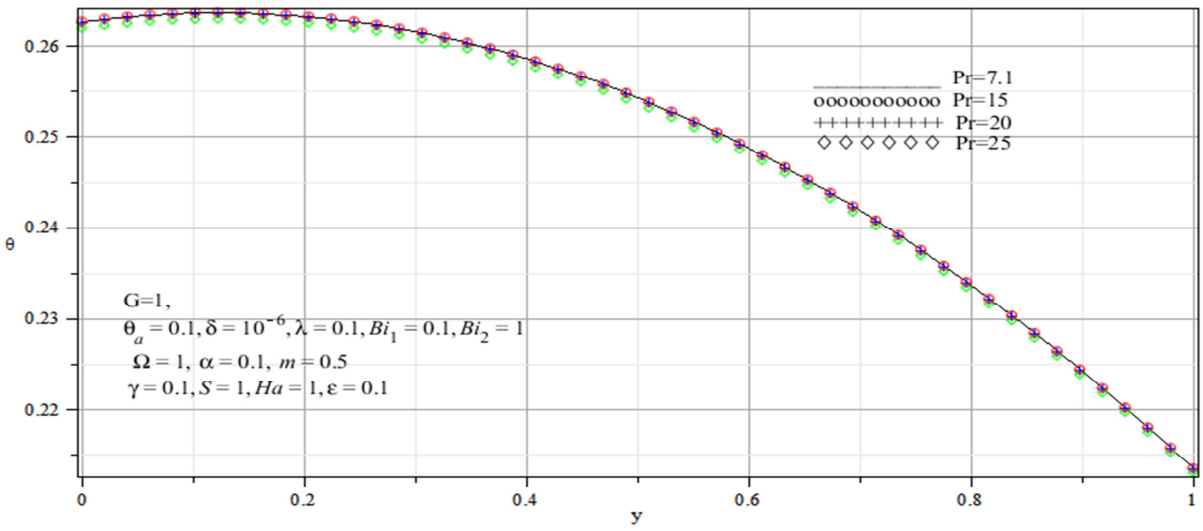

Figure 5.17: Effects of the Prandtl number (Pr) on temperature.

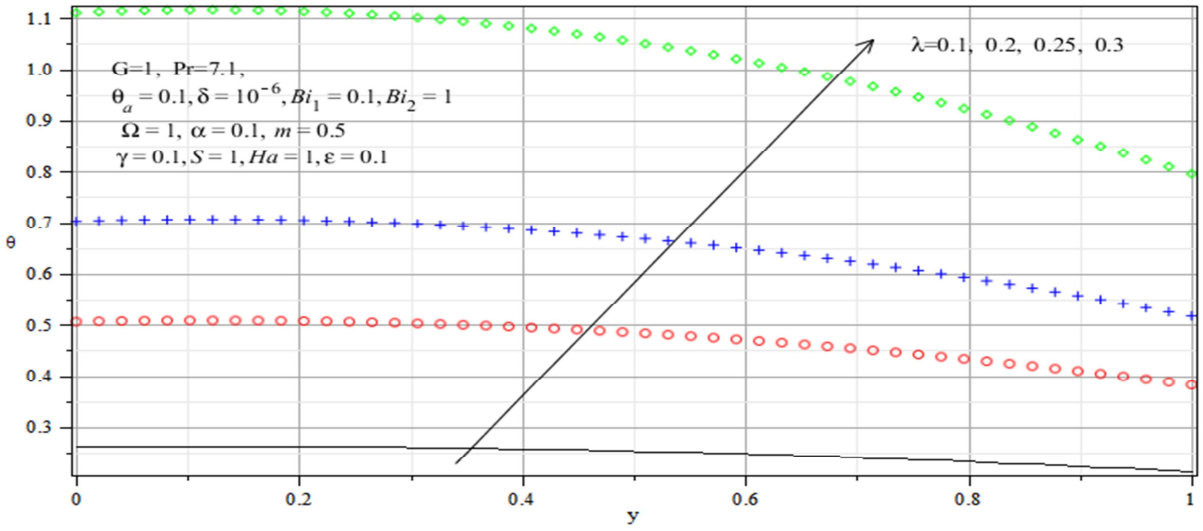

Figure 5.18: Effects of the reaction parameter (λ) on temperature.

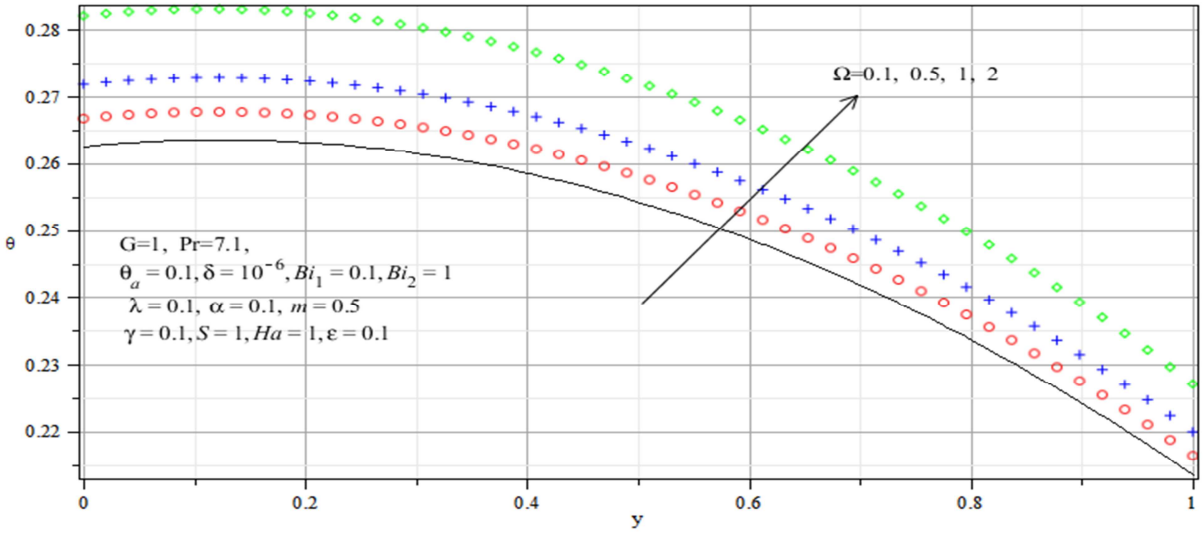

Figure 5.19: Effects of the viscous heating parameter (Ω) on temperature.

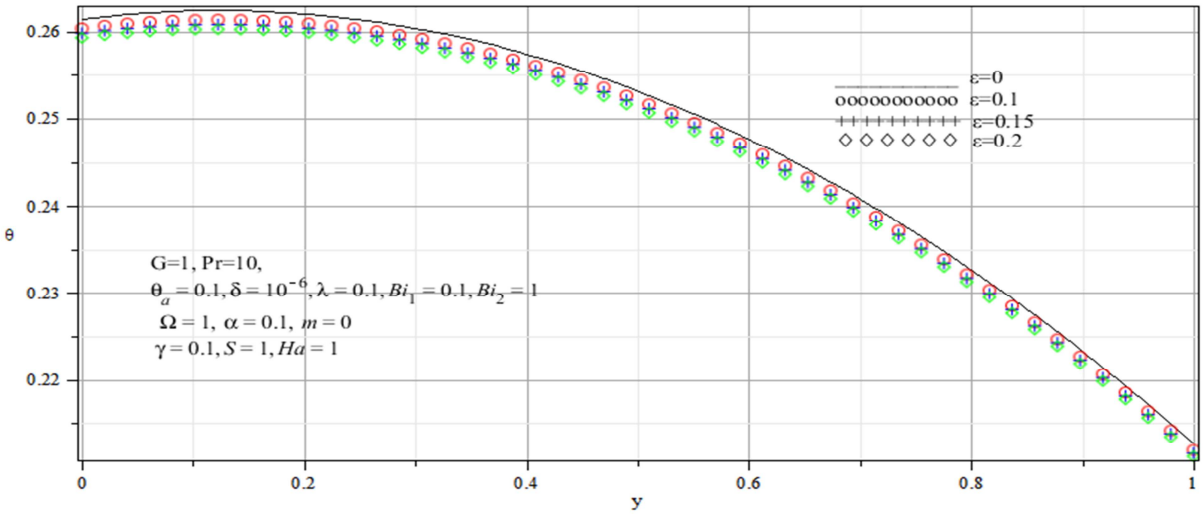

Figure 5.20: Variation of temperature with $\varepsilon : m = 0$.

Figure 5.20 ($m=0$) and Figure 5.21 ($m=-2$), sensitised and Arrhenius reactions, both display fluid temperature behaviour that is exactly opposite to that of Figure 5.15 ($m=0.5$), the bimolecular reactions. This, however, is not surprising as the temperature is expected to decrease with increasing ε when $m \le 0$. In the temperature equation, the function

$$(1+\varepsilon\theta)^m \exp\left(\frac{\theta}{1+\varepsilon\theta}\right), m \le 0$$

which represents source terms clearly decreases as ε increases. The fluid temperature thus decreases with increasing ε. As both figures show, the maximum temperature is recorded for $\varepsilon = 0$.

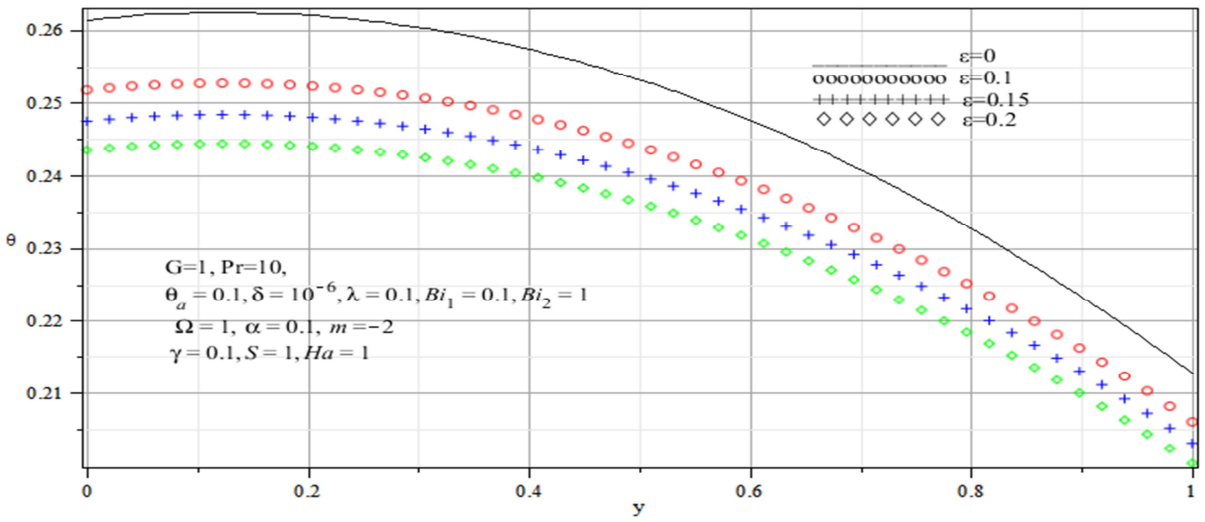

Figure 5.21: Variation of temperature with ε : $m=-2$

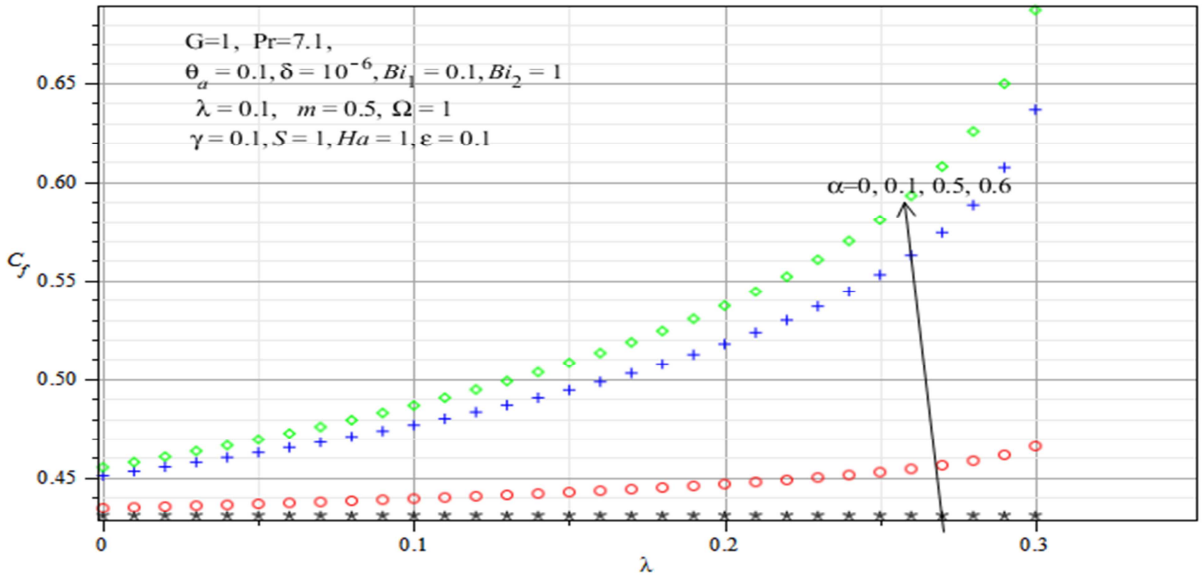

Figure 5.22: Variation with λ and α of the wall shear stress C_f .

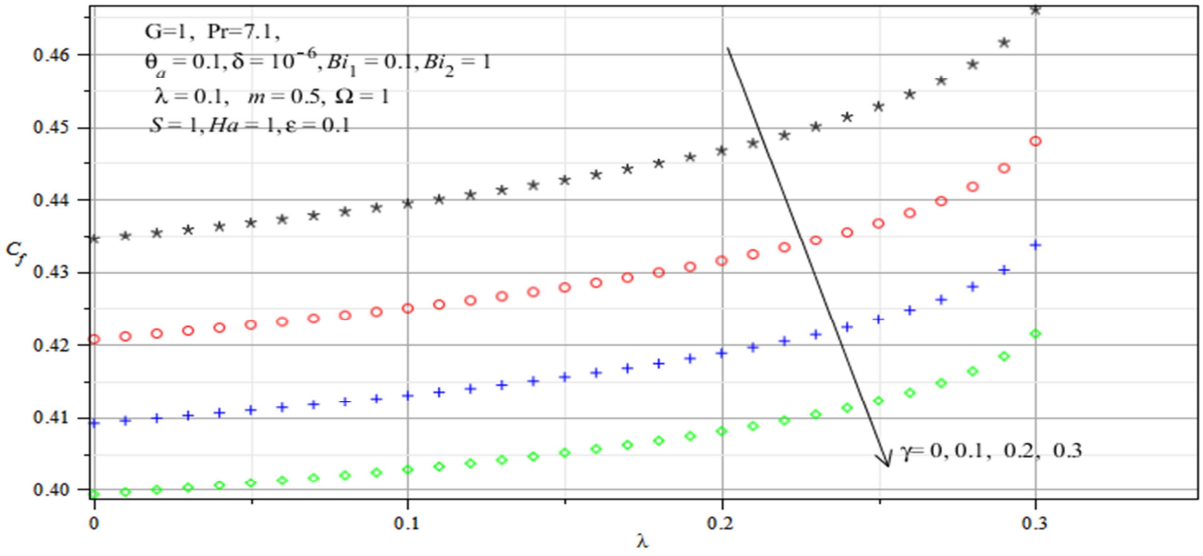

Figure 5.23: Variation with λ and γ of the wall shear stress C_f .

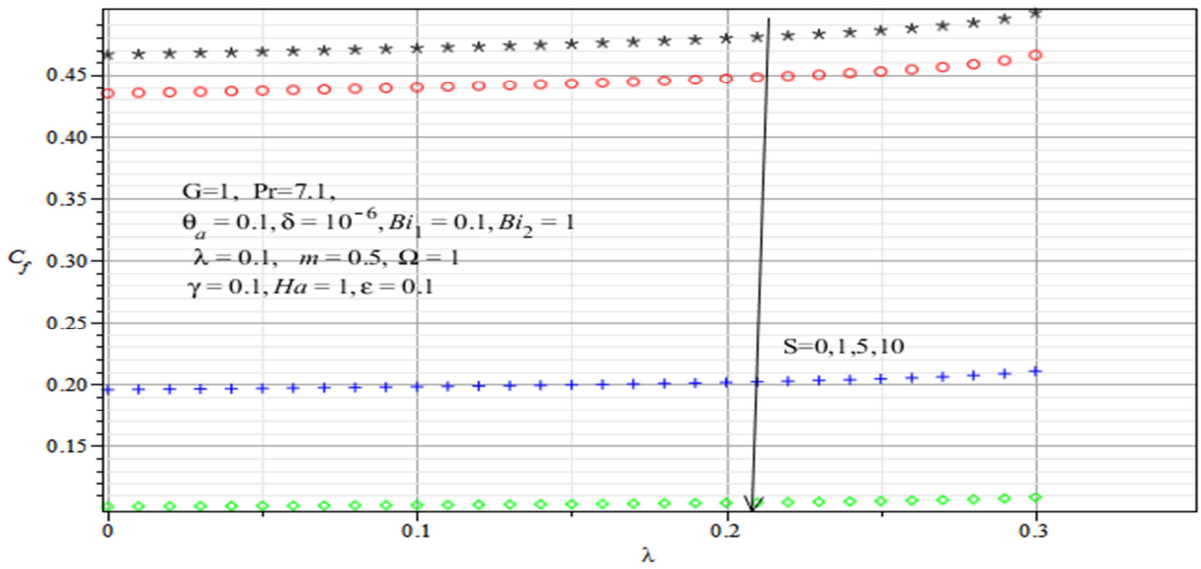

Figure 5.24: Variation with λ and S of the wall shear stress C_f .

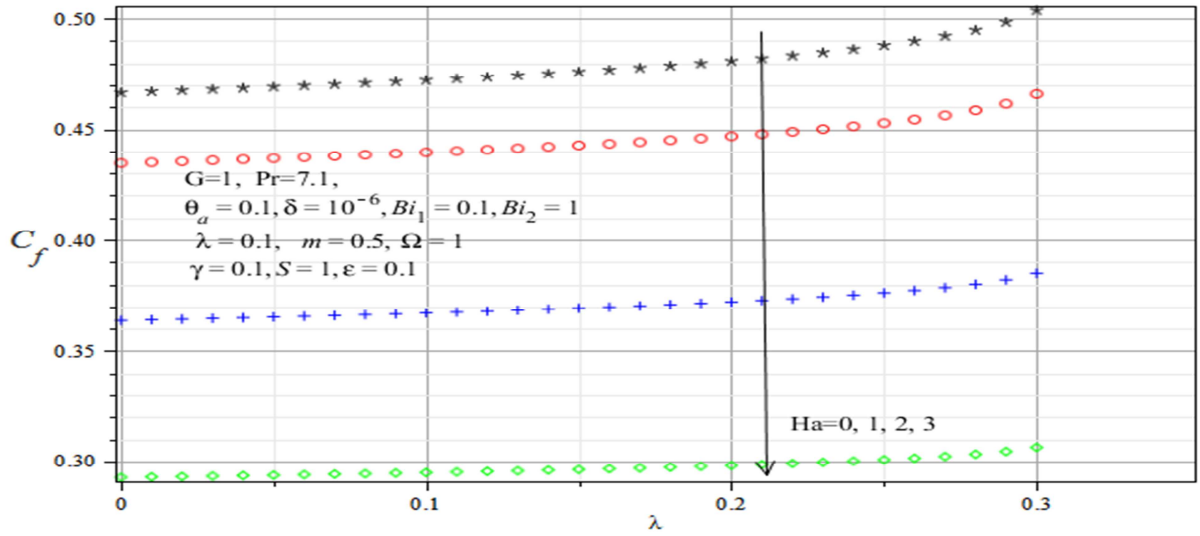

Figure 5.25: Variation with λ and Ha of the wall shear stress C_f .

5.4.2. Skin friction and Nusselt number

The physical quantities of practical and engineering primary interest are the wall shear stress (skin friction) and the wall heat transfer rate (Nusselt number). Figures 5.22 to 5.25 show the skin friction dependence on the reaction parameter λ for varying values of variable viscosity

parameter α, the non-Newtonian parameter γ, the porous medium parameter S and the Hartmann number Ha respectively. Figures 5.26 to 5.29 show the wall heat transfer rate dependence on λ for varying values of the same parameters. The figures are plotted until the values of λ are reached at which blow-up of solutions sets in. The trend that clearly stands out in the figures is that parameters that decrease the fluid velocity correspondingly decrease the wall shear stress respectively and parameters that decrease the fluid temperature correspondingly decrease the wall heat transfer. Similarly, the parameters that increase the fluid velocity and those that increase the fluid temperature also increase the skin friction and the wall heat transfer rate respectively. Table 5.1 and Table 5.2 are an attempt to clarify the trend in Figures 5.26 to 5.29 and to show that the thermal criticality values of the reaction parameter λ increase with the Hartmann number and the porous medium parameter. We also note here that $Ha = 0$ and $S = 0$ represent reactive flow with no magnetic field influence and reactive flow with no porous medium in the channel respectively.

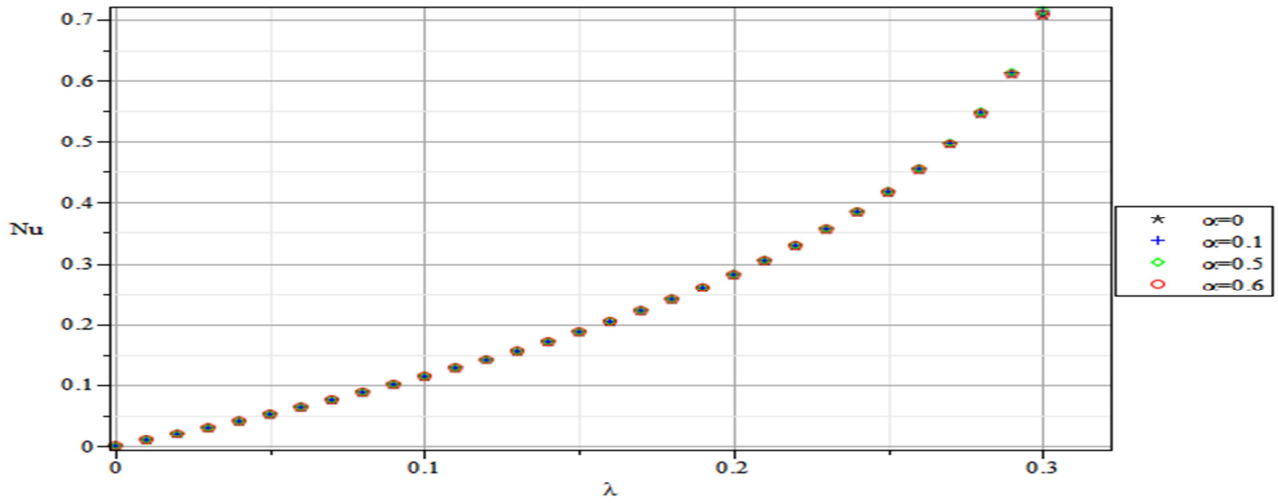

Figure 5.26: Variation with λ and α of the wall heat transfer rate Nu.

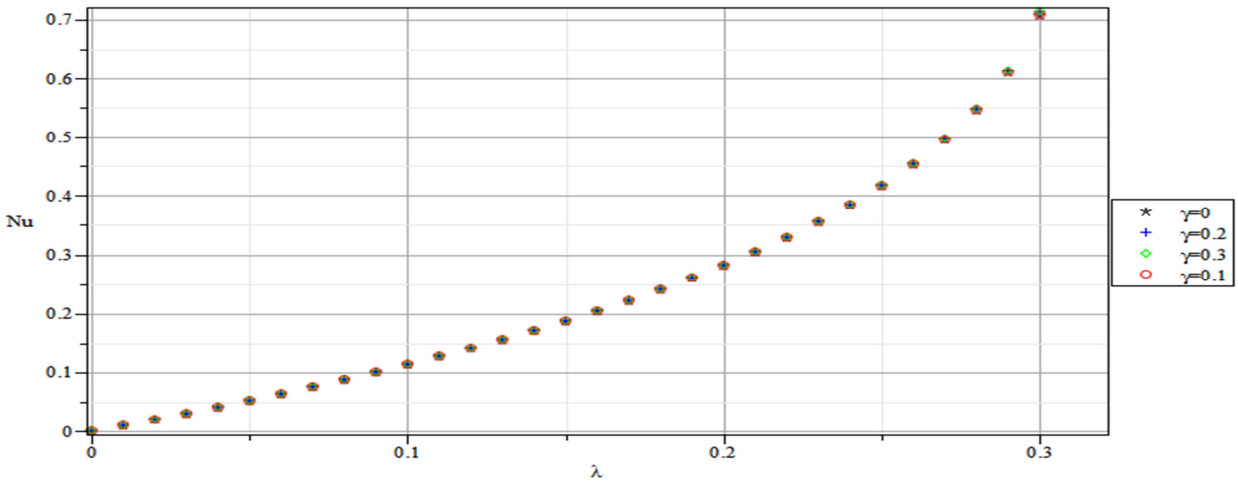

Figure 5.27: Variation with λ and γ of the wall heat transfer rate Nu .

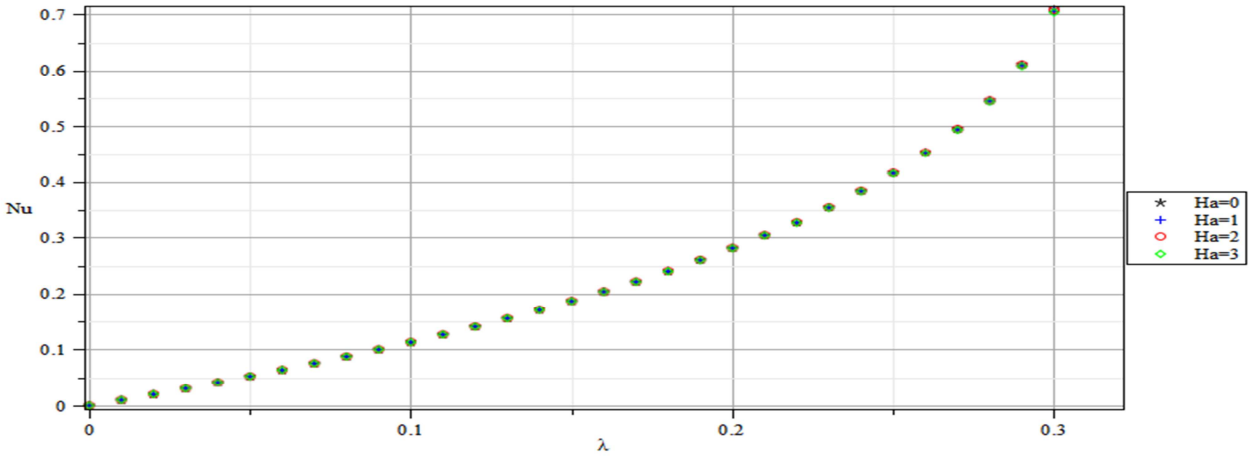

Figure 5.28: Variation with λ and Ha of the wall heat transfer rate Nu .

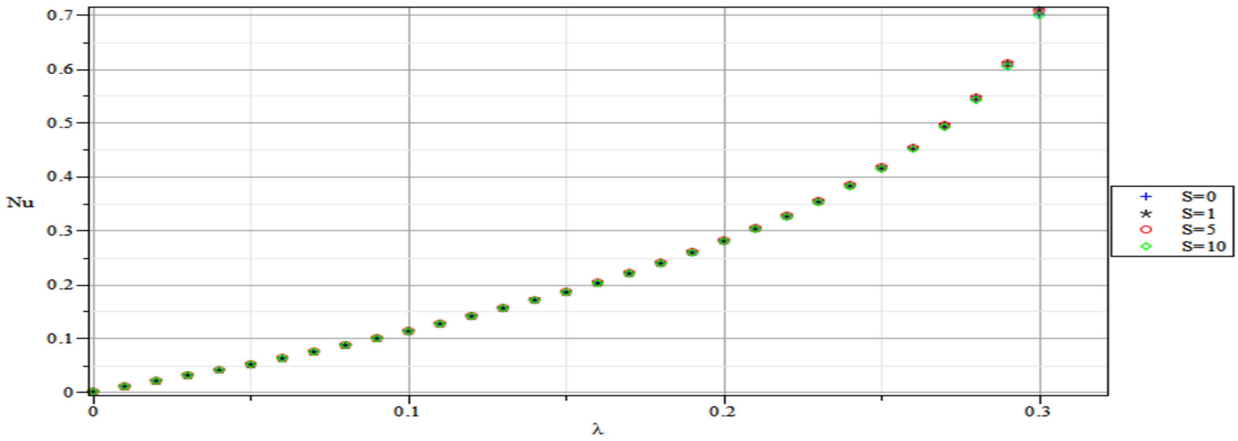

Figure 5.29: Variation with λ and S of the wall heat transfer rate Nu.

Table 5.1: Effects of magnetic field (Ha) on the thermal criticality Values of λ.

S	Ha	$Nu_{critical}$	$\lambda_{critical}$
1	0	0.911744	0.299970
1	1	0.904420	0.301990
1	2	0.894764	0.305110
1	3	0.888717	0.306580

Table 5.2. Effects of the porous medium parameter (S) on the thermal criticality values of λ.

Ha	S	$Nu_{critical}$	$\lambda_{critical}$
1	0	0.912912	0.300600
1	1	0.910081	0.300610
1	5	0.893731	0.304910
1	10	0.891999	0.306500

5.5. Conclusion

We presented a computational investigation of the transient flow of a reactive, variable viscosity, electrically conducting third-grade fluid through a porous saturated medium with asymmetrical convective boundary conditions. A transient increase in both fluid velocity and temperature with an increase in the reaction strength, viscous heating and fluid variable viscosity parameter (which decreases the viscosity) was observed. A transient decrease in both fluid velocity and temperature with the increased magnetic field, increased porous medium parameter (which decreases the porosity in the flow), increased Biot number, increased Prandtl number and increased non-Newtonian character was also observed. Due to the nature of the coupling source terms, the fluid velocity and temperature either both increase or both decrease, together. Parameters that increase the fluid velocity correspondingly increase the wall shear stress respectively and parameters that increase the fluid temperature correspondingly increase the wall heat transfer. The possible finite time blow-up of solutions means that the reaction strength must be monitored and carefully controlled in order to avoid damage to property and to save life. Blow up of solutions is reached far sooner than in the case of chapter 3 where there is no magnetic field influence.

CHAPTER SIX

CONCLUSION AND FUTURE WORK

In this thesis, we studied laminar flow of a reactive viscous non-Newtonian fluid through a channel filled with saturated porous medium. We investigated the effect of flow parameters on the velocity and temperature fields and analysed thermal effects and thermal stability criteria.

In chapter 3, the unsteady laminar flow of a reactive temperature dependent viscosity third grade fluid in a channel filled with saturated porous medium and with asymmetric convective boundary conditions was computationally investigated. It was assumed that exothermic chemical reactions take place within the flow system and that the asymmetric convective heat exchange between the flow and the ambient at the channel surfaces obeys Newton's law of cooling. We made use of a semi-implicit finite difference scheme to numerically solve the coupled nonlinear momentum and energy balance equations deriving the flow. The results were presented graphically and analysed with respect to the flow parameters. A transient increase in both fluid velocity and temperature with an increase in the reaction strength, viscous heating and fluid viscosity parameter (which decreases the viscosity) was observed. A transient decrease in both fluid velocity and temperature was observed with increase in the non-Newtonian character, the porous medium parameter (which decreases the porosity of the flow), the Prandtl and the Biot numbers. It was noticed that if the reaction strength is not carefully controlled, there is an almost sure chance of finite time blow-up of solutions. Owing to the nature of the coupling source terms, the fluid velocity and temperature were noticed to either both increase or both decrease.

Thermal effects of suction/injection on unsteady reactive variable viscosity third grade fluid flow in a channel filled with a saturated porous medium and with asymmetric convective boundary conditions was the subject of chapter 4. The effects of the flow parameters on the temperature and velocity fields, the skin friction and the wall heat transfer rate were simulated and discussed. The suction/injection Reynolds number was observed to retard the velocity field. It was also observed that the suction/injection Reynolds number, the porous medium parameter, the Prandtl number and the Biot number have a retarding effect on the temperature field. The variable viscosity parameter and the suction/injection Reynolds number increase the skin fiction while the porous medium parameter and the Prandtl number diminish it. It was also revealed

that the suction injection Reynolds number, the porous medium parameter and the Prandtl number have a diminishing effect on the rate of heat transfer at the channel walls.

In chapter 5, by way of extending the studies in chapter 3, we carried out an analysis of an unsteady hydromagnetic flow of a pressure driven, reactive, temperature dependent viscosity, electrically conducting third grade fluid. The magnetic field, like the porous medium parameter, the Prandtl number, the non-Newtonian character and the Biot number, was observed to retard both the velocity and the temperature fields. In the case of MHD flow, possibility of finite temperature blow-up increased considerably.

In all the cases that were considered, thermal stability can be achieved by knowing the effect of each flow parameter and thereby controlling it accordingly.

6.1. Further work

Future work that can be considered is to analyse similar type of flow in different geometries like cylindrical coordinates as well as considering Couette flow rather than Poiseuille flow. It will also be interesting to investigate the effect of Navier slip on the flow systems considered here. The other dimension is to consider two and three dimensional flow. Other methods of solution, like symmetry methods, will also constitute future work.

Appendix

Articles already published or submitted for publication

(1) O.D. Makinde, T. Chinyoka, L. Rundora: Unsteady flow of a reactive variable viscosity non-Newtonian fluid through a porous saturated medium with asymmetric convective boundary conditions. *Computers and Mathematics with Applications* 62 (2011) 3343 – 3352 (Published).

(2) L. Rundora, O. D. Makinde: Analysis of unsteady MHD reactive flow of non-Newtonian fluid through a porous saturated medium with asymmetric boundary conditions. *Computational & Applied Mathematics* – submitted 2012. This paper was presented at the 55th SAMS congress held at Stellenbosch University on 31 October – 2 November 2012.

(3) L. Rundora, O.D. makinde: Effects of suction/injection on unsteady reactive variable viscosity non-Newtonian fluid flow in a channel filled with porous medium and convective boundary conditions. *Journal of Petroleum Science and Engineering* – submitted 2012.

REFERENCES

[1] Abdul Hakeem, A.K., Sathiyanathan, K. 2009. *An analytic solution of an oscillatory flow through a porous medium with radiation effect* . Nonlinear Analysis: Hybrid Systems, Vol. 3, Issue 3, pp. 288-295.

[2] Akshin, N. Y., Bakhtiyarov, S., Ibragimov, R. N. 2009. *Experimental investigation of Newtonian and non-Newtonian fluid flows in porous media*. Mechanics Research Communications, Vol. 36, Issue 5, pp. 638-641.

[3] Al-Hadhrami, A.K., Elliott, L., Ingham, D.B. 2003. *A new model for viscous dissipation in porous media across a range of permeability values*. Transport in Porous Media, 53: pp. 117-122.

[4] Al-Nimr, T.M. A., Aldoss , T. K. 2004. *The effect of the macroscopic local inertial term on the non-Newtonian fluid flow in channels filled with porous medium*. International Journal of Heat and Mass Transfer, Vol. 47, Issue 1, pp. 125-133.

[5] Amaziane, A B., Jurak, M., Keko, A. Ž. 2011. *An existence result for a coupled system modeling a fully equivalent global pressure formulation for immiscible compressible two-phase flow in porous media*. Journal of Differential Equations, Vol. 250, Issue 3, pp. 1685-1718.

[6] Attia, H. A. 2005. *The effect of suction and injection on the unsteady flow between two parallel plates with variable properties*. Tamkang J. Sci. Eng., 8(1): pp. 17 – 22.

[7] Attia, H.A. 2008. *Effect of Hall current on transient hydromagnetic Couette-Poiseuille flow of a viscoelastic fluid with heat transfer*. Appl.Math.Modell., 32: pp. 375 – 388.

[8] Aziz, A. 2009. *A similarity solution for laminar thermal boundary layer over a flat plate with a convective surface boundary condition*. Communications in Nonlinear Science and Numerical Simulation, 14: pp. 1064-1068.

[9] Bakier, A.Y., Rashad, A.M., Mansour, M.A. 2009. *Group method analysis of melting effect on MHD mixed convection flow from radiate vertical plate embedded in a saturated porous media*. Communications in Nonlinear Science and Numerical Simulation, Vol. 14, Issue 5, pp. 2160-2170.

[10] Beg, O.A., Makinde, O.D. 2011. *Viscoelastic flow and species transfer in a Darcian high-permeability channel*, J. Pet. Sci. Eng., 76: pp. 93 – 99.

[11] Blanford, R.D., Thorne, K.S. 2005. *Applications of Classical Physics*. California Institute of Technology. www.pma.caltech.edu/courses/ph136 [8 November 2012]

[12] Bodmer Research Web, *Energy, Enthalpy, and the First Law of Thermodynamics*.

http://chemed.chem.purdue.edu/genchem/topicreview/bp/ch21/chemical.php [21 June 2011]

[13] Brinkman, H.C. 1947. *On the permeability of media consisting of closely packed porous particles*. Applied Scientific Research, A1: pp. 81-86.

[14] Celli, M., Rees, D.A.S., Barletta, A. 2010. *The effect of local thermal non-equilibrium on forced convection boundary layer flow from a heated surface in porous media.* International Journal of Heat and Mass Transfer, Vol. 53, Issues 17-18, pp. 3533-3539.

[15] Chai, Z., Shi, B., Lu, J., Guo, Z. 2010. *Non-Darcy flow in disordered porous media: A lattice Boltzmann Study*. Computers & Fluids, 39, pp. 2069-2077.

[16] Chamkha, A.J. 2002. *On laminar hydromagnetic mixed convection flow in a vertical channel with symmetric and asymmetric wall heating conditions*. Int. J. Heat Mass Transfer, 45: pp. 2509 – 2525.

[17] Chandra, A., Chhabra, R.P. 2012. *Effect of Prandtl Number on Natural Convection Heat Transfer from a Heated Semi-Circular Cylinder*. International Journal of Chemical and Biological Engineering 6.

[18] Chen, M., Rossen, W., Yortsos, Y. C. 2005. *The flow and displacement in porous media of fluids with yield stress.* Chemical Engineering Science, Vol. 60, Issue 15, pp. 4183-4202.

[19] Cheng, N., Hao, Z., Tan, S. K. 2008. *Comparison of quadratic and power law for nonlinear flow through porous media*. Experimental Thermal and Fluid Science, Vol. 32, Issue 8, pp. 1538-1547.

[20] Chiem, K. S., Zhao, Y. 2004. *Numerical study of steady/unsteady flow and heat transfer in porous media using a characteristics-based matrix-free implicit FV method on unstructured grids.* International Journal of Heat and Fluid Flow, Vol. 25, Issue 6, pp. 1015-1033.

[21] Chinyoka, T. 2008. *Computational dynamics of a thermally decomposable viscoelastic lubricant under shear.* Transactions of ASME, Journal of Fluids Engineering, 130(12):121201(7 pages).

[22] Chinyoka, T. 2010. *Poiseuille flow of reactive Phan-Thien-Tanner liquids in 1D channel flow*. Transactions of ASME, Journal of Heat Transfer, 132(11): 111701 (7 pages).

[23] Chinyoka, T. 2011. *Suction-injection control of shear banding in non-isothermal and exothermic channel flow of Johnson-Segalman liquids.* Transactions of ASME, Journal of Fluids Engineering 133(7): 071205 (12 pages).

[24] Chinyoka, T., Makinde, O.D. 2010. *Computational dynamics of unsteady flow of a variable viscosity reactive fluid in a porous pipe*. Mech. Res. Commun., 37: pp. 347 – 353.

[25] Cortell, R. 2007. *MHD flow and mass transfer of an electrically conducting fluid of second grade in a porous medium over a stretching sheet with chemically reactive species*. Chemical Engineering and Processing, Vol. 46, Issue 8, pp. 721-728.

[26] Das, S.S. 2009. *The effect of suction and injection on MHD three dimensional Couette flow and heat transfer through a porous medium*. J. Nav. Arch. Marine Eng, 6: pp. 41 – 51.

[27] Dholkawala, Z.F., Sarma, H.K., Kam, S.I. 2007. *Application of fractional flow theory to foams in porous media*. Journal of Petroleum Science and Engineering, Vol. 57, Issues 1-2, pp. 152-165.

[28] Dunn, J.E., Rajagopal, K.R. 1992. *Fluids of differential type: Critical review and thermodynamic analysis*. IMA Preprint Series, No: 1084.

[29] Earle, R.L. 2004. *Unit operations in food processing.* 2nd ed, The New Zealand Institute of Food Science and Technology Inc.

[30] Elert, G. 2010. *The Physics Hypertextbook*, Physics.info. http://physics.info/viscosity/ [8 November 2012].

[31] Ern, A., Mozolevski, I., Schuh, L. 2010. *Discontinuous Galerkin approximation of two-phase flows in heterogeneous porous media with discontinuous capillary pressures.* Computer methods in Applied Mechanics and Engineering, Vol. 199, Issue 23-24: pp. 1491-1501 .

[32] Fang, T. 2004. *A note on the incompressible Couette flow with porous walls*. Int. Commun. Heat Mass Transfer, 31 (1): pp. 31 – 41.

[33] Fosdick, R.L., Rajagopal, K.R. 1980. *Thermodynamics and stability of fluids of third grade.* Proceedings of The Royal Society of London A339, 351.

[34] Fourar, M., Radilla, G., Lenormand, R., Moyne, C. 2004. *On the non-linear behavior of a laminar single-phase flow through two and three-dimensional porous media.* Advances in Water Resources, Vol. 27, Issue 6, pp. 669-677.

[35] Fox, R.W., McDonald, A.T., Pritchard, P.J. 2004. *Introduction to Fluid Mechanics*. 6th edition, John Wiley & Sons, Inc, United States of America .

[36] Frank-Kamenetskii, D.A. 1969. *Diffusion and Heat Transfer in Chemical Kinetics*. Plenum Press, New York.

[37] Frank-Kamenetskii's Theory of Thermal Ignition. http://garfield.chem.elte.hu/Combustion/tutorial/frank/Default.htm [22 June 2011].

[38] Gerald, C.F., Wheatley, P.O. 1999. *Applied Numerical Analysis*. 6th edition, Addison-Wesley Longman, USA.

[39] Grillo, A., Logashenko, D., Stichel, S., Wittum, G. 2010. *Simulation of density – driven flow in fractured porous media.* Advances in Water Resources, 33: pp. 1494-1507.

[40] Hajibeygi, H., Jenny, P. 2009. *Multiscale finite-volume method for parabolic problems arising from compressible multiphase flow in porous media*. Journal of Computational Physics, Vol. 228, Issue 14, pp. 5129-5147.

[41] Hartmann, J. 1937. *Theory of laminar flow of an electrically conducting liquid in a homogeneous magnetic field*. Hg-Dynamics I, Math.Fys.Med., 15: pp. 1 – 28.

[42] Hayat, T., Abbas, Z., Pop, I., Asghar, S. 2010. *Effects of radiation and magnetic field on the mixed convection stagnation point flow over a vertical stretching sheet in a porous media*. International Journal of Heat and Mass Transfer, 53: pp. 466-474.

[43] Ideal Gas Law

http://hyperphysics.phy-astr.gsu.edu/hbase/kinetic/idegas.html [3 July 2011].

[44] Irmay, S. 1958. *On the theoretical derivation of Darcy and forchheimer formulas*. Trans. AGU., 39: pp. 702 – 707.

[45] Joseph, D.D., Kamp, A.M., Bai, R. 2002. *Modelling foamy oil flow in porous media*. International Journal of Multiphase Flow, Vol. 28, Issue 10, pp. 1659 – 1686.

[46] Khan, M., Naheed, E., Fetecau, C., Hayat, T. 2008. *Exact solutions of starting flows for second grade fluid in a porous medium*. International Journal of Non-Linear Mechanics, Vol. 43, Issue 9, pp. 868-879.

[47] Konz, M., Younes, A., Ackerer, P., Fahs, M., Huggenberger, P., Zechner, E. 2009. *Variable-density flow in heterogeneous porous media — Laboratory experiments and numerical simulations*. Journal of Contaminant Hydrology, Vol. 108, Issues 3-4, pp. 168-175.

[48] Kumaran, V., Tamizharasi, R., Vajravelu, K. 2009. *Approximate analytic solutions of stagnation point flow in a porous medium*. Communications in Nonlinear Science and Numerical Simulation, Vol. 14, Issue 6, pp. 2677-2688.

[49] Kundu, P. K., Cohen, I.M. 2004. *Fluid Mechanics*. 3rd edition, Elsevier Academic Press, UK.

[50] Liu, I.C. 2004. *Flow and heat transfer of an electrically conducting fluid of second grade over a stretching sheet subject to a transverse magnetic field*. Int. J. Heat Mass Transfer, 47: pp. 4427 – 4437.

[51] Liu, I.C. 2005. *A note on heat and mass transfer for a hydromagnetic flow over a stretching sheet*. Int. Commun. Heat Mass Transfer, 32: pp. 1075 – 1084.

[52] Liu, S., Masliyah, J. H. 1998. *On non-Newtonian fluid flow in ducts and porous media*. Chemical Engineering Science, Vol. 53, Issue 6, pp. 1175-1201.

[53] Liu, S., Masliyah, J. H. 1999. *Non-linear flows in porous media*. Journal of Non-Newtonian Fluid Mechanics, Vol. 86, Issues 1-2, pp. 229-252.

[54] Lucas, Y., Panfilov, M., Buès, M. 2007. *High velocity flow through fractured and porous media: the role of flow non-periodicity*. European Journal of Mechanics - B/Fluids, Vol. 26, Issue 2, pp. 295 - 303.

[55] Makinde, O.D. 2006. *Thermal ignition in a reactive viscous flow through a channel filled with porous medium*. Transactions of ASME, Journal of Heat Transfer, 128: pp. 601-604.

[56] Makinde, O.D. 2007. *On steady flow of a reactive variable viscosity fluid in a cylindrical pipe with an isothermal wall*. International Journal of Numerical Methods for Heat & Fluid Flow, Vol. 17 No. 2: pp. 187 – 194.

[57] Makinde, O.D. 2007. *Thermal criticality in viscous reactive flows through channels with a sliding wall: An exploitation of the Hermite-Pade approximation method*. Mathematical and Computer Modelling, 47: pp. 312 – 317.

[58] Makinde, O.D. 2007. *Thermal stability of a reactive third grade fluid in a cylindrical pipe: an exploitation of Hermite-Pade approximation technique*. Appl. Math. Comput., 189: pp. 690-697.

[59] Makinde, O.D. 2007. *Hermite-Pade approximation approach to thermal criticality for a reactive third grade liquid in a channel with isothermal walls*. Int. Commun. Heat Mass Transfer, 34 (7): pp. 870-877.

[60] Makinde, O.D. 2009. *On the Chebyshev collocation spectral approach to stability of fluid flow in a porous medium*. Int. J. Numer. Meth. Fluids, 59: pp. 791 -799.

[61] Makinde, O.D. 2009. *On MHD boundary-layer flow and mass transfer past a vertical plate in a porous medium with constant heat flux*. International Journal of Numerical Methods for Heat & Fluid Flow, Vol. 19, Nos. 3/4, pp. 546 – 554.

[62] Makinde, O.D. 2009. *Thermal stability of a reactive viscous flow through a porous-saturated channel with convective boundary conditions*. Applied Thermal engineering, 29: pp. 1773 – 1777.

[63] Makinde, O.D. 2009. *Thermal criticality for a reactive gravity driven thin film flow of a third grade fluid with adiabatic free surface down an inclined plane*. Appl. Math. Mech., 30 (3): pp. 373-380.

[64] Makinde, O.D. 1996. *Computer extension and bifurcation study by analytic continuation of porous tube flow*. J. Math.Phys.Sci., 30: pp. 1 – 24.

[65] Makinde, O.D. 2007. *Thermal stability of a reactive viscous flow through a porous saturated pipe.* Int. J. Numer. Methods Heat Fluid Flow, 17(8): pp. 836 – 844.

[66] Makinde, O.D., Aziz, A. 2010. *MHD mixed convection from a vertical plate embedded in a porous medium with a convective boundary condition*. International Journal of Thermal Sciences, 49: pp. 1813-1820.

[67] Makinde, O.D., Chinyoka, T. 2010. *Numerical investigation of transient heat transfer to hydromagnetic channel flow with radiative heat and convective cooling*. Communications in Nonlinear Science and Numerical Simulation, 15(12): pp. 3919-3930.

[68] Makinde, O.D., Chinyoka, T. 2010. *Transient analysis of pollutant dispersion in a cylindrical pipe with a nonlinear waste discharge concentration*. Computers and Mathematics with Applications, 60(3): pp. 642-652.

[69] Makinde, O.D., Chinyoka, T. 2011. *Numerical study of unsteady hydromagnetic Generalised Couette flow of a reactive third-grade fluid with asymmetric convective cooling*. Comput. Math. Appl., 61: pp. 1167 - 1179.

[70] Makinde, O.D., Chinyoka, T. 2012. *Analysis of unsteady flow of a variable viscosity reactive fluid in a slit with wall suction or injection.* J. Pet. Sci. Eng., 94 -95: pp. 1 – 11.

[71] Makinde, O.D., Maserumule, R.L. 2008. *Thermal criticality and entropy analysis for a variable viscosity Couette flow*. Phys. Scr. 78.

[72] Makinde, O.D., Mhone, P.Y. 2009. *On Temporal Stability Analysis for Hydromagnetic Flow in a Channel Filled with Saturated Porous Medium*. Flow Turbulence Combust, 83: pp. 21 – 32.

[73] Makinde, O.D., Moitsheki, R.J. 2008. *On Nonperturbative Techniques for Thermal Radiation Effect on Natural Convection past a Vertical Plate Embedded in a Saturated Porous Medium*. Mathematical Problems in Engineering.

[74] Makinde, O.D., Ogulu, A. 2008. *The Effect of Thermal Radiation on the Heat and Mass Transfer Flow of a Variable Viscosity Fluid Past a Vertical Porous Plate Permeated by a Transverse Magnetic Field*. Chemical Engineering Communications*, 195:12: pp. 1575 – 1584.*

[75] Massoudi, M., Christe, I. 1995. *Effects of variable viscosity and viscous dissipation on the flow of a third grade fluid in a pipe.* International Journal of Non-Linear Mechanics, 30: 687.

[76] Meade, D.B., Haran, B.S., White, R.E. 1996. *The shooting Technique for the Solution of Two-Point Boundary Value Problems*. Maple Tech, 3 (1): pp. 85 – 93.

[77] McDonough, J.M. 2009. *Lectures in Elementary Fluid Dynamics: Physics, Mathematics and Applications*. Department of Mechanical Engineering and Mathematics, University of Kentucky, Lexington, KY 40506 – 0503.

[78] *Natvig, F. J. R., Lie, K. A. 2008. Fast computation of multiphase flow in porous media by implicit discontinuous Galerkin schemes with optimal ordering of elements*. Journal of Computational Physics, Vol. 227, Issue 24, pp. 10108-10124.

[79] Nield, D.A. 1991. *The limitation of the Brinkman-Forchheimer equation in modeling flow in a saturated porous medium and at an interface*. International Journal of Heat and Fluid Flow, Vol. 12 Issue 3: pp. 269-272.

[80] Nield, D.A., Bejan, A. 2006. *Convection in Porous Media*. 3rd edition, Springer, New York.

[81] *Niessner, N. J., Hassanizadeh, S. M. 2009. Non-equilibrium interphase heat and mass transfer during two-phase flow in porous media—Theoretical considerations and modeling*. Advances in Water Resources, Vol. 32, Issue 12, pp. 1756-1766.

[82] Olajuwon, B.I. 2011. *Convection heat and mass transfer in a hydromagnetic flow of a second grade fluid in the presence of thermal radiation and thermal diffusion*. Int. Commun. Heat Mass Transfer, 38: pp. 377 – 382.

[83] Pal, D., Chatterjee, S. 2010. *Heat and mass transfer in MHD non-Darcian flow of a micropolar fluid over a stretching sheet embedded in a porous media with non-uniform heat source and thermal radiation*. Communications in Nonlinear Science and Numerical Simulation, Vol. 15, Issue 7, pp. 1843-1857.

[84] Parvazinia, M., Nassehi, V., Wakeman, R.J. 2005. *Multi-scale finite element modeling of laminar steady flow through highly permeable porous media*. Chemical Engineering Science, 61: pp. 586 – 596.

[85] Pascal, J. P., Pascal, H. 1997. *Non-linear effects on some unsteady non-Darcian flows through porous media*. International Journal of Non-Linear Mechanics, Vol. 32, Issue 2, pp. 361-376.

[86] Pathak, M.G., Ghiaasiaan, S.M. 2011. *Convective heat transfer and thermal dispersion during laminar pulsating flow in porous media*. International Journal of Thermal Sciences, 50: pp. 440 - 448.

[87] Prasad, K.V., Datti, P.S., Vajravelu, K. 2010. *Hydromagnetic flow and heat transfer of a non-Newtonian power law fluid over a vertical stretching sheet*. Int. J. Heat Mass Transfer, 53: pp. 879 – 888.

[88] Rajagopal, K.R. 1995. *On Boundary Conditions for Fluids of the Differential type: Navier –Stokes Equations and Related Non-linear Problems*. Plenum Press, New York, p.273.

[89] Rong, F., Guo, Z., Chai, Z., Shi, B. 2010. *A lattice Boltzmann model for axisymmetric thermal flows through porous media*. International Journal of Heat and Mass Transfer, Vol. 53, Issues 23-24, pp. 5519-5527.

[90] Sajid, M., Ahmed, I., Hayat, T., Ayub, M. 2009. *Unsteady flow and heat transfer of a second grade fluid over a stretching sheet*. Commun. Nonlinear Sci. Numer. Simul., 14: pp. 96-108.

[91] Schnack, D.D. 2009. *Lecture Notes in Physics*, Vol 780, Springer. http://www.physics.wisc.edu [21 June 2011]

[92] Seddeek, M.A., Darwish, A.A., Abdelmeguid, M.S. 2007. *Effects of chemical reaction and variable viscosity on hydromagnetic mixed convection heat and mass transfer for Hiemenz flow through porous media with radiation*. Communications in Nonlinear Science and Numerical Simulation, Vol. 12, Issue 2, pp. 195-213.

[93] Sen, M. 2005. *Notes on Finite-Difference Methods for AME 301: Differential Equations, Vibrations and Controls*. Department of Aerospace and Mechanical Engineering, University of Notre Dame, Notre Dame, IN 46556, USA.

[94] Siddiqui, A.M., Mahmood, R., Ghori, Q.K. 2006. *Thin film flow of a third grade fluid on a moving belt by He's homotopy perturbation method*. International Journal of Nonlinear Sciences and Numerical Simulation, 7(1): pp. 1-8.

[95] Smith, G.D. 1978. *Numerical solution of partial differential equations, FINITE DIFFERENCE METHODS*. Second edition, Clarendon Press.Oxford.

http://3.bp.blogspot.com [24 February 2011]

[96] Sochi, T. 2009. *Pore-scale modeling of viscoelastic flow in porous media using a BautistaeManero fluid.* International Journal of Heat and Fluid Flow, Vol. 30, Issue 6: pp. 1202-1217.

[97] Sochi, T. 2010. *Modeling the flow of yield-stress fluids in porous media*. Transport in Porous Media. doi:10.1007/s11242-010-9574-z.

[98] Sochi, T. 2010. *Non-Newtonian Flow in porous media*. Polymer, 51: pp. 5007 – 5023.

[99] Sochi, T. 2010. *Computational Techniques for Modeling Non-Newtonian Flow in Porous Media*. International Journal of Modeling, Simulation, and Scientific Computing, Vol. 1, No. 2: pp. 239-256.

[100] Som, S.K., Mondal, S.S., Dash, S.K. 2005. *Energy and energy balance in the process of pulverized coal combustion in a tubular combustor*. Journal of Heat Transfer, 127: pp. 1322-1333.

[101] Storesletten, L., Pop, I. 1996. *Free convection in vertical porous layer with walls at non-uniform temperature.* Fluid Dynam. Res., 17: pp. 107 – 119.

[102] Su, N. 2009. *N-dimensional fractional Fokker–Planck equation and its solutions for anomalous radial two-phase flow in porous media*. Applied Mathematics and Computation, Vol. 213, Issue 2, pp. 506-515.

[103] Teng, H., Zhao, T. S. 2000. *An extension of Darcy's law to non-Stokes flow in porous media*. Chemical Engineering Science, Vol. 55, Issue 14, pp. 2727-2735.

[104] Tillack, M.S., Morley, N.B. 1998. *Magnetohydrodynamics.* Standard Handbook for Electrical Engineers, 14th edition, McGraw Hill.

[105] Truesdell, C., Noll, W. 1965. *The non-linear field theories of mechanics*, in: Handbuch der Physik (Edited by S Flugge), Vol. 111/3, Springer, Berlin.

[106] Tung, V.X., Dhir, V.K. 1990. *Finite element solution of multi-dimensional two-phase flow through porous media with arbitrary heating conditions*. International Journal of Multiphase Flow, Vol. 16, Issue 6, pp. 985-1002.

[107] Tyagi, M., Jenny, P., Lunati, I., Tchelepi, H. A. 2008. *A Lagrangian, stochastic modeling framework for multi-phase flow in porous media*. Journal of Computational Physics, Vol. 227, Issue 13, pp. 6696-6714.

[108] Wang, J., *Gao*, Z., Gan., G., Wu, D. 2001. *Analytical solution of flow coefficients for a uniformly distributed porous channel*. Chem. Eng. Sci., 84 (1): pp. 1 – 6.

[109] Wendt, J.F. 2009. *Computational Fluid Dynamics*. 3rd edition, Springer-Verlag, Berlin Heidelberg.

[110] White, F.M. 2008. *Fluid Mechanics*, 6th ed. McGraw-Hill.

[111] Yang, Y., Hwang, M. 2009. *Numerical simulation of turbulent fluid flow and heat transfer characteristics in heat exchangers fitted with porous media*. International Journal of Heat and Mass Transfer, Vol. 52, Issues 13-14, pp. 2956-2965.

[112] Yiotis, A. G., Psihogios, J., Kainourgiakis, M. E., Papaioannou, A., Stubos, A. K. 2007. *A lattice Boltzmann study of viscous coupling effects in immiscible two-phase flow in porous media* . Colloids and Surfaces A: Physicochemical and Engineering Aspects, Vol. 300, Issues 1-2, 2007, pp. 35-49.

[113] Yurusoy, M., Pakdemirli, M. 2002. *Approximate analytical solutions for the flow of a third grade fluid in a pipe*. International Journal of Non-Linear Mechanics, 37: 187.

[114] Wikipedia, the free encyclopedia.

http://en.wikipedia.org/wiki/Planck_constant [14 November 2012].